UNIVERSITÀ
DEGLI STUDI
DI PADOVA

Sede Amministrativa: Università degli Studi di Padova
Dipartimento di Neuroscienze

SCUOLA DI DOTTORATO DI RICERCA IN SCIENZE MEDICHE, CLINICHE E SPERIMENTALI
INDIRIZZO NEUROSCIENZE
XXII CICLO

Normal myogenesis and increased apoptosis in myotonic dystrophy type-1 muscle cells

Direttore della Scuola: Ch.mo Prof. Antonio Tiengo
Coordinatore d'indirizzo: Ch.mo Prof. Corrado Angelini
Supervisore: Ch.mo Prof. Lodovica Vergani

Dottorando: Emanuele Loro

Summary

1. List of abbreviations

AMW	average myotube width
AS	alternative splicing
ATP	adenosine-5'-triphosphate
AUC	area under the curve
BSA	bovine serum albumine
cDM1	congenital myotonic dystrophy type 1
CK	creatine kinase
CSA	cyclosporin A
CUG-BP	CUG binding protein
Cy3	cyanine 3
Cyt-c	cytochrome c
DAPI	4',6-diamidino-2-phenylindole
DM1	myotonic dystrophy type 1
DMPK	myotonic dystrophy protein kinase
ECC	excitation contraction coupling
ER/SR	endoplasmic/sarcoplasmic reticulum
FBS	foetal bovine serum
FISH	fluorescent in situ hybridization
FURA-2-AM	FURA-2-acetoxymethyl ester
LC3	microtubule-associated protein 1 light chain 3
MBNL	muscleblind-like
PBS	phosphate buffered saline
PCD	programmed cell death
PCR	polymerase chain reaction
PTP	permeability transition pore
ROI	region of interest
ROS	reactive oxygen species
RT-PCR	real time-PCR
RyR	ryanodine receptor
SERCA	sarcoplasmic/endoplasmic reticulum calcium ATPase
SSC	saline-sodium citrate buffer
TUNEL	terminal deoxynucleotidyl transferase dUTP nick end labeling
UTR	untranslated region
Z-VAD-FMK	Z-Val-Ala-Asp-fluoromethylketon

2. Abstract:

2.1. English version

Myotonic dystrophy type 1 (DM1) is caused by $(CTG)_n$ expansion in the 3'-untranslated region of *DMPK* gene. Mutant transcripts are retained in nuclear RNA foci, which sequester RNA binding proteins thereby misregulating their functions (i.e. splicing regulation). Controversy still surrounds the pathogenesis of the DM1 muscle distress, characterized by myotonia, weakness and wasting with distal muscle atrophy.

Eight primary human cell lines from adult-onset (DM1) and congenital (cDM1) patients, $(CTG)_n$ range 90-1800, were successfully differentiated into aneural-immature and contracting-innervated-mature myotubes. Morphological, immunohistochemical, RT-PCR and Western blotting analyses of several markers of myogenesis indicated that in vitro differentiation-maturation of DM1 myotubes was comparable to age-matched controls. In all pathological muscle cells, $(CTG)_n$ expansions were confirmed by long PCR and RNA fluorescence in-situ hybridization. Moreover, the DM1 myotubes displayed the splicing alteration of insulin receptor and MBNL1 genes associated to the DM1 phenotype.

Considerable myotube loss and atrophy of 15-day-differentiated DM1 myotubes indicated activated catabolic pathways, as confirmed by the presence of apoptotic (caspase-3 activation, cytochrome c release, chromatin fragmentation) and autophagic (P62/LC3) markers. Treatment with the pancaspase inhibitor Z-VAD significantly reduced the decrease in myonuclei number and in average width in15-day-differentiated DM1 myotubes. We thus propose that the muscle wasting typical in DM1 is due to impairment of muscle mass maintenance-regeneration, through premature apoptotic-autophagic activation, rather than altered myogenesis.

Keywords: myotonic dystrophy, human primary myotubes, apoptosis, autophagy.

2.2. Italian version

La distrofia miotonica di tipo 1 (DM1) è causata dall'espansione $(CTG)_n$ nella regione trascritta ma non tradotta al 3' del gene *DMPK*. I trascritti mutati sono trattenuti in foci nucleari, i quali sequestrano diverse proteine leganti RNA spesso alterandone le funzioni (i.e. regolazione dello splicing). A livello del muscolo, i meccanismi patogenetici che portano a miotonia, debolezza e perdita di massa dei muscoli distali, non sono ad oggi chiari.

Otto linee di mioblasti primari umani, ottenuti da biopsie di pazienti affetti da DM1 nelle forme adulta e congenita (range di espansione tra 90 e 1800 CTG), sono state differenziate ed innervate con successo, ottenendo miotubi in grado i contrarre.

L'analisi morfologica e la quantificazione di diversi marker di miogenesi mediante RT-PCR e Western blotting, hanno indicato che il diferenziamento in vitro dei mioblasti primari DM1 è indistinguibile da quello ottenuto con mioblasti di controllo. In ciascuna linea DM1 è stata confermata l'espansione $(CTG)_n$ mediante long-PCR ed ibridizzazione in situ. Inoltre, nei miotubi DM1 è stato rilevata l'alterazione dello splicing del recettore per l'insulina e di MBNL1, caratteristica del fenotipo DM1.

A 15 giorni di differenziamento, una considerevole perdita di miotubi DM1 ha suggerito l'attivazione di pathways catabolici, come confermato dalla presenza di marker di apoptosi (taglio proteolitico della caspasi 3, rilascio di citocromo c dai mitocondri, frammentazione della cromatina) e di autofagia (aumento dei livelli di LC3 lipidato e di P62). Il trattamento con l'inibitore delle caspasi Z-VAD si è dimostrato efficace nell'attenuare la riduzione del numero di mionuclei e del calibro medio dei miotubi a 15 giorni di differenziamento. Proponiamo quindi che la compromissione muscolare tipica della DM1 sia dovuta, più che ad un'alterata miogenesi, a problemi nei meccanismi di mantenimento/rigenerazione, che si esplicano attraverso la prematura attivazione di apoptosi e/o autofagia

Parole chiave: distrofia miotonica, miotubi primari umani, apoptosi, autofagia.

3. Introduction

3.1. The skeletal muscle

Skeletal muscle is a form of striated muscle tissue existing under control of the somatic nervous system. It is one of three major muscle types, the others being cardiac and smooth muscle. As its name suggests, most skeletal muscle is attached to bones by bundles of collagen fibers known as tendons.

Skeletal muscle is made up of individual components known as muscle fibers (Figure 1). These fibers are formed from the fusion of developmental myoblasts. The myofibers are long, cylindrical, multinucleated units composed of actin and myosin myofibrils repeated as a sarcomere, the basic functional unit responsible for skeletal muscle's striated appearance and forming the basic machinery necessary for muscle contraction.

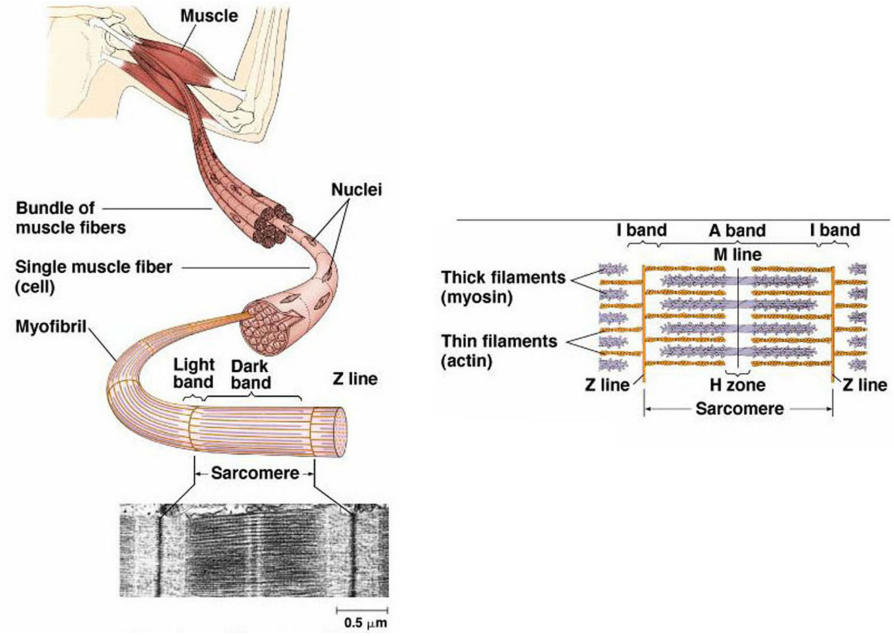

Figure 1: muscle fiber and sarcomeric organization

3.1.1 The sarcomeric unit

A sarcomere (Greek sárx = "flesh", méros = "part") is the basic unit of a muscle's cross-striated myofibril. Sarcomeres are multi-protein complexes composed of three different filament systems (Figure 2).

1. The thick filament system is composed of myosin protein which is connected from the M-line to the Z-disc by titin. It also contains myosin-binding protein C which binds at one end to the thick filament and the other to actin.
2. The thin filaments are assembled by actin monomers bound to nebulin, which also involves tropomyosin (a dimer which coils itself around the F-actin core of the thin filament).
3. Nebulin and titin give stability and structure to the sarcomere.

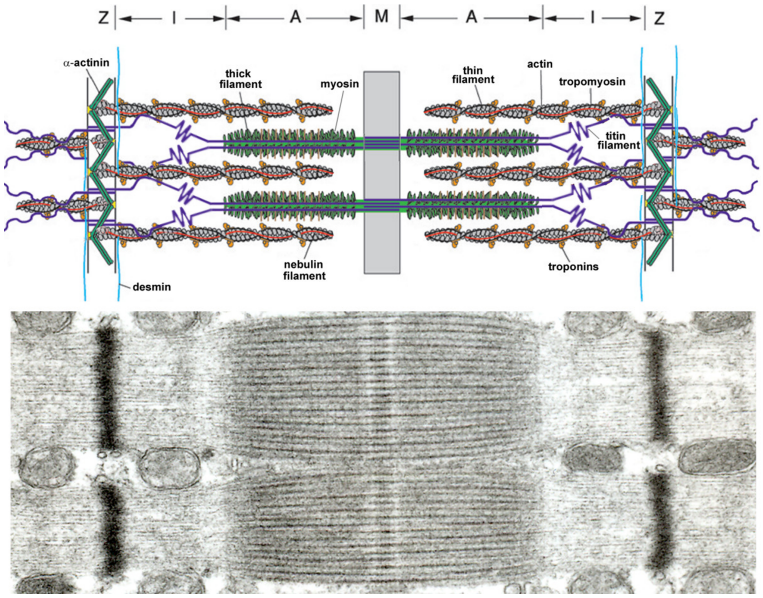

Figure 2: the sarcomeric unit

3.1.2 Physiology

Different types of muscle fibers can be distinguished according to their composition and their functional properties. Basically, type I and type II fibers differ for their contractile properties, their metabolism and the different ATPase activities (see Table 1). Type I fibers appear red due to the presence of the oxygen binding protein myoglobin. These fibers are suited for endurance and are slow to fatigue because they use oxidative metabolism to generate ATP. Type II fibers are white due to the absence of myoglobin and a reliance on glycolytic enzymes. These fibers are efficient for short bursts of speed and power and use both oxidative metabolism and anaerobic metabolism depending on the particular sub-type. These fibers are quicker to fatigue.

Table 1: main fiber types of skeletal muscle

Fibre type	Type I fibres	Type IIa fibres	Type IIx fibres	Type IIb fibres
Contraction time	Slow	Moderately fast	Fast	Very fast
Size of motor neuron	Small	Medium	Large	Very large
Resistance to fatigue	High	Fairly high	Intermediate	Low
Activity used for	Aerobic	Long-term anaerobic	Short-term anaerobic	Short-term anaerobic
Maximum duration of use	Hours	<30 minutes	<5 minutes	<1 minute
Power produced	Low	Medium	High	Very high
Mitochondrial density	High	High	Medium	Low
Capillary density	High	Intermediate	Low	Low
Oxidative capacity	High	High	Intermediate	Low
Glycolytic capacity	Low	High	High	High
Major storage fuel	Triglycerides	Creatine phosphate, glycogen	Creatine phosphate, glycogen	Creatine phosphate, glycogen
Myosin heavy chain, human genes	*MYH7*	*MYH2*	*MYH1*	*MYH4*

In addition to the actin and myosin components that constitute the sarcomere, skeletal muscle fibers also contain two other important regulatory proteins, troponin and tropomyosin, that are necessary for muscle contraction to occur. These proteins are associated with actin and cooperate to prevent its interaction with myosin. Skeletal muscle cells are excitable and are subject to depolarization by the neurotransmitter acetylcholine, released at the neuromuscular junction by motor neurons. Once a cell is sufficiently stimulated, the cell's sarcoplasmic reticulum releases ionic calcium (Ca^{2+}), which then interacts with the regulatory protein troponin. Calcium-bound troponin undergoes a conformational change that leads to the movement of tropomyosin, subsequently exposing the myosin-binding sites on actin. This allows for myosin and actin ATP-dependent cross-bridge cycling and shortening of the muscle. Muscle force is proportional to physiologic cross-sectional area (PCSA), and muscle velocity is proportional to muscle fiber length.

3.1.3 Satellite cells and muscle repair/regeneration

Satellite cells are anatomically defined as mononucleated cells located between the basal lamina and the plasmalemma of the multinucleated myofiber (1). They act as myogenic stem cells in vivo, able to supply myonuclei to growing myofibers and, importantly, also to give rise to many new satellite cells (Figure 3) (2). Because muscle is able to efficiently regenerate after repeated bouts of damage, systems must be in place to maintain a viable satellite cell pool, and it was proposed over 30 years ago that self-renewal was the primary mechanism. Self-renewal entails either a stochastic event or an asymmetrical cell division, where one daughter cell is committed to differentiation whereas the second continues to proliferate or becomes quiescent (3). The relatively recent advent of molecular markers has allowed the reliable identification of satellite cells at the light microscope level, making the classical definition of satellite cells more complex. In normal mature muscle, satellite cells are mitotically quiescent and express Pax7 (Figure 3) (4), the adhesion molecule M-cadherin (5), and saliomucin CD34 (6), among others (7). Pax3 and Pax7 factors are key upstream regulators of the early myogenic program. In fact, the ablation of these two factors in satellite cells prevents the expression of the myogenic determination gene *MyoD*. However the myogenic cascade proceeds anyway through the activation of *MyoD*'s paralogue *Myf5* which continues to be expressed and permits the activation of myogenin, one of the most important differentiation factors (1). The same factors participating in the regulation of myogenic differentiation play, through feedback mechanisms, an important role in the precise control of self-renewal process allowing the maintenance of a quiescent population of satellite cells.

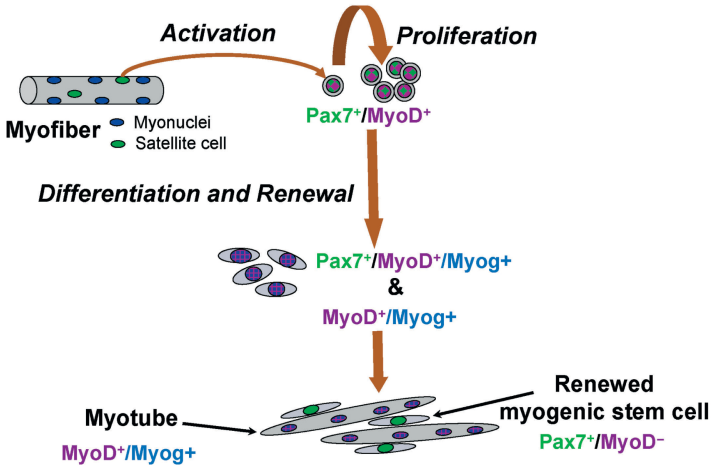

Figure 3: satellite cell activation, proliferation, differentiation, and self-renewal. The proliferating myoblast population is represented by the Pax7$^+$/MyoD$^+$ mononuclear cells. Nuclei that are MyoD$^+$/Myog$^-$ (and no longer express Pax7) are found within differentiated mononuclear cells and myotubes, whereas a minor population of Pax7$^+$/MyoD$^+$/Myog$^+$ cells represents a transitional stage within recently differentiated myoblasts; newly formed myotubes occasionally display Pax7$^+$/MyoD$^+$/Myog$^+$ nuclei as well. Renewed cells Pax7$^+$/MyoD$^-$ reentry into the satellite cell niche.

When cultured in vitro, satellite cells lose their stem cell potential and behave as myogenic primary cells. They are however able to proliferate for a limited number of passages (up to 20) conserving their myogenic potential and can be induced to differentiate by removing growth factors from the culture medium. In this way, human myogenic cells can fuse together generating polynucleated myotubes expressing the typical myogenic markers such as myogenin and myosin heavy chain. Differently from cardiomyocites, these cells however do not contract spontaneously. The most successful strategy to obtain contraction in human skeletal muscle myotubes is functional innervation with embryonic spinal cord sections (8, 9).

3.2. Myotonic Dystrophy type 1

Myotonic dystrophy (Steinert's disease, 1909) is the most prevalent form of adult muscular dystrophy with a frequency of 1 in 8000 individuals worldwide (10). The term *myotonia* indicates the slow relaxation of the muscles (especially mimic and upper-limbs muscles) after voluntary contraction or electrical stimulation, while *dystrophy* is a condition of abnormal development, often denoting the progressive deterioration of muscles. Two types of adult onset myotonic dystrophy exist. Type 1 (DM1), also called Steinert's disease (11), has a severe congenital form and a milder adult-onset form. A second form, myotonic dystrophy type 2 (DM2) is due to a different mechanism than DM1 and generally manifests with milder signs and symptoms. Affected individuals express highly heterogeneous, multisystemic symptoms including myotonia, progressive muscle weakness and wasting, cataracts, hypogonadism, frontal balding, cardiac conduction defects and ECG changes (12). The genetic defect in DM1, identified in 1992, results from the expansion of a CTG repeat in the 3' untranslated region (UTR) of dystrophia myotonica protein kinase (DMPK), a gene which maps to the chromosome 19q13.3 and encodes a serine/threonine protein kinase (13). Unaffected individuals have <38 CTG repeats, whereas expansions associated with DM1 range from 80 to >2500 repeats. Repeat lenght correlates directly with disease severity and inversely with the age of onset (14). Disease severity varies with the number of repeats: normal individuals have 5 to 35 repeats. Alleles ranging from 35 to 49 repeats have been mostly ascertained through their symptomatic offspring, which expanded into the >50-repeat range. Alleles ranging from 35 to 49 repeats are considered “premutation” alleles. Mildly affected persons have 50 to 150 repeats, and severely affected individuals have 2,000 or more copies (15) (see table 2).

Table 2: classification of disease according to the CTG expansion size.

CLASS	$(CTG)_n$ range
Premutated	35-49
E1	50-150
E2	150-1000
E3	>1000
E4	congenital, highly expanded

Amplification is frequently observed after parent-to-child transmission, but extreme amplifications are not transmitted through the male line. This mechanism explains genetic anticipation (16, 17) and the occurrence of the severe congenital form almost exclusively in the offspring of affected women (12). A parallel classification of the disease can be made upon the age of onset and the clinical progression. Based on this consideration, DM1 can be divided up into four main categories, each presenting specific clinical features and management problems: (a) congenital, (b) childhood-onset, (c) adult-onset, and (d) late-onset/asymptomatic (12).

Table 3: classification of the disease according to the age of onset and the clinical progression.

Onset	Severity	(CTG)n expansion size
late	asymptomatic	low
adult	+	50-1000
childhood	++	>1000
congenital	+++	>1000

+ mildly affected; ++ moderately affected; +++ severely affected

3.2.1 Clinical features

3.2.1.1 Diagnosis

The diagnosis of DM1 and DM2 can be difficult due to the large number of neuromuscular disorders, most of which are very rare. More than 40 neuromuscular disorders exist with close to 100 variants. As a result, patients with multiple symptoms that may be explained by a complex disorder such as DM1 or DM2 will generally be referred by their primary care physician to a neurologist for diagnosis. Depending on the presentation of symptoms, patients may be referred to a number of medical specialists including cardiologists, ophthalmologists, endocrinologists, and rheumatologists. In addition, the clinical presentation is obscured by the degree of severity or the presence of unusual phenotypes. In adult-onset DM1, symptoms typically become evident in middle life, but signs can be de-

tectable in the second decade. The diagnosis of classic adult-onset DM1 is straightforward with demonstration of progressive strength deficit in the presence of myotonia (electromyographic discharges), with frontal balding, cardiac involvement, endocrine/metabolic disfunction and cataracts. Confirmatory evidence is provided by demonstration of depressed IgG and elevated CPK in the serum. Clinical diagnosis can be difficult in mild cases, where cataracts may be the only manifestation (18).

3.2.1.2 Adult-onset Myotonic Dystrophy 1

Unlike the other muscular dystrophies, DM1 initially involves the distal muscles of the extremities and only later affects the proximal musculature. In addition, there is early involvement of the muscles of the head and neck. Involvement of the extraocular muscles produces ptosis, weakness of eyelid closure, and limitation of extraocular movements. Atrophy of masseters, sternocleidomastoids, and the temporalis muscle produces a characteristic haggard appearance. Myotonia, most frequently apparent in the tongue, forearm and hand, is rarely as severe as in myotonia congenita and tends to be less apparent as weakness progresses. At the muscle biopsy level, many of the changes are nonspecific. Most commonly there are central nuclei and ring fibers, which are not pathognomonic of DM (Figure 4).

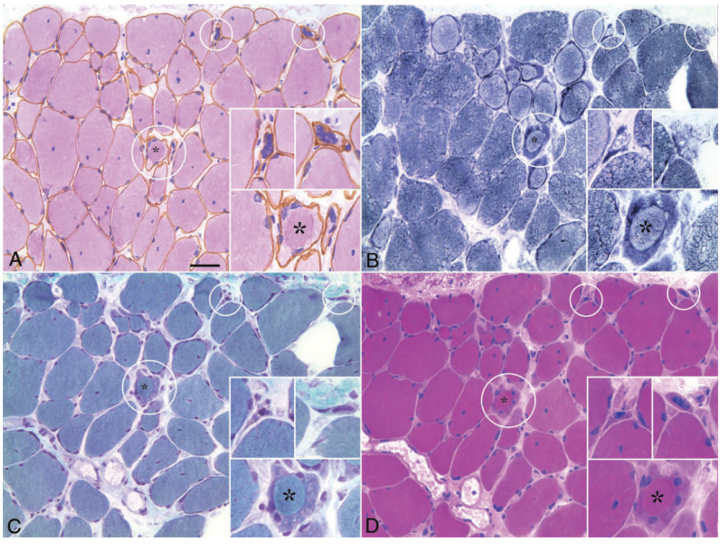

Figure 4: typical features of a myotonic dystrophy type 1 biopsy with myopathic changes. DM1 biopsies show large variability in fibre size, many internal nuclei, split fibres, ring fibres and presence of fibres with sarcoplasmic masses (one is indicated with an * and is also shown in the insets). Serial cross sections of tibialis anterior muscle biopsy stained (A) with antibodies against merosin (laminin alpha 2) and counterstained with haematoxylin–eosin, (B) with NADH-TR, (C) with Gomori trichrome, (D) with haematoxylin–eosin. Three areas are encircled and shown at a higher magnification in the insets. All three insets contain several nuclei surrounded by a merosin-stained basement membrane that can been interpreted as being nuclear clump fibres. (bar X200)

Necrosis, regeneration, and increase of collagen are never as severe as in Duchenne muscular dystrophy. Type I muscle fibers hypotrophy is common, whereas less commonly there are markedly atrophic fibers. Electron microscopy studies show sarcoplasmic masses and dilation of the terminal

cisternae of the sarcoplasmic reticulum (10). Recently, Vattemi et al. have proposed that the sarcoplasmic masses could result from the 'interruption of late myogenic differentiation' rather than the foci of abnormal regeneration and/or degeneration (19). From the molecular point of view (see page 21), nuclear aggregates of mutant mRNA and proteins (*foci*) can be identified by RNA fluorescence *in situ* hybridization (RNA-FISH), even without constituting an accepted diagnostic criterium (13, 20, 21).

I. Neurological features

There is extensive evidence for central nervous system (CNS) involvement in DM1: cognitive impairment/mental retardation, specific patterns of psychological dysfunction and personality traits, neuropatho- logical abnormalities (e.g., tau protein abnormalities), neuroimaging and neurophysiological changes, and excessive daytime sleepiness (10, 12). For some patients very disabling IQ and cognitive defects have been found to directly correlate with the size of the $(CTG)_n$ expansion and inversely with the age of onset (22, 23). Magnetic resonance imaging (MRI) of the brain showes white matter hyperintense lesions without hemispheric prevalence and cortical atrophy which do not correlate with age, disease duration, or neuropsychologic impairment (24, 25). DM1 patients often display a homogeneous personality profile characterized by avoidant, obsessive-compulsive, passive-aggressive, and schizotypic traits (26). Neurofibrillary tangles (NFT), derived from pathologic aggregation of hyperphosphorylated tau (MAPT) proteins, have also been described in the neocortex and subcortical regions (27). Biochemical characterization showed overexpression of tau protein isoforms lacking exons 2 and 3, suggesting that the DMPK mutation disrupts normal MAPT isoform expression and alters the maturation of MAPT pre-mRNA (28).

II. Cardiovascular and respiratory features

Cardiac conduction abnormalities are common in DM1 and require regular monitoring, whereas impaired myocardial function is so infrequent that routine review is not recom-mended (29). Sudden cardiac deaths are the utmost critical problem in DM1, especially because cardiac manifestation may sometimes appear before the common neuromuscular symptoms. They are mostly attributable to complete cardiac conduction block and ventricular fibrillation/tachycardia caused by cardiomyopathy. Anti-arrhythmic drugs are available for individuals with milder symptoms, while in severely affected patients the use of implantable cardiac pacemakers and cardioverter defibrillator devices is adopted.

3.2.1.3 Congenital myotonic dystrophy

Harper (1975) observed that in a small proportion of cases, myotonic dystrophy may be congenital with neonatal hypotonia, motor and mental retardation, and facial diplegia. With rare exceptions, it is

the mother who transmits the disease. Diagnosis can be difficult if the family history is not known because muscle wasting may not be apparent, and cataracts and clinical myotonia are absent, although the latter is sometimes detectable by electromyography. Respiratory difficulties are frequent and are often fatal. Those that survive the neonatal period initially follow a static course, eventually learning to walk but with significant mental retardation in 60 to 70% of cases. By age of 10 they develop myotonia and in adulthood develop the additional complications described for the adult-onset disease.

3.2.2 Molecular features

DM1 is associated with an unstable $(CTG)_n$ trinucleotide expansion located in the 3'-untranslated (3'-UTR) region of the DM protein kinase (*DMPK*) gene on chromosome 19q13.3. The mutant DMPK transcript, containing the expanded $(CUG)_n$ sequence, accumulates in discrete nuclear foci able to sequester various nuclear factors such as RNA-binding proteins or splicing regulators, causing different and highly variable downstream deleterious effects (10, 13). It has been reported that $(CTG)_n$ trinucleotide repeat length in muscle directly correlates with both frequency of severe cDM1 (30) and rate of splicing impairment typical of myotonic dystrophy (31). The first proposed pathogenic mechanism for DM1 was based on the reduction of DMPK protein caused by the triplet expansion and the *cis* and *trans* effects of the expanded sequence on neighbouring genes. In particular, chromatin condensation in the region surrounding the repeats could affect the expression of *SIX5,* whose product have been associated with sterility and testicular atrophy (32), or *DMWD*, probably responsible for brain- and testis-related symptoms (33). This explanation however could not account for the great heterogeneity of symptoms and, moreover, could not explain why, in type 2 DM, a similar phenotype could be caused by an expansion located in a completely different gene. These results indicated that protein products of the myotonic dystrophy genes do not have a major role in disease pathogenesis (13). The first cause of the pathology could then be ascribed to the mRNA produced by the *DMPK* gene rather than to the impaired protein levels. Myotonic Dystrophy became to be considered an RNA-mediated disease.

3.2.2.1 The $(CTG)_n$ repeat instability

Intergenerational expansion in DM1 was suggested to result from initial repeat, followed by somatic instability. Studies in tissues of monozygotic twin pairs indicated that this first instability event happens at very early embryonic stages, as the twins showed identical expansion patterns. Expanded DMPK alleles are already detectable in oocytes (including the germinal vesicle stage) and embryos of mothers with expanded $(CTG)_n$, who underwent in vitro fertilisation (IVF) with pre-implantation diag-

nostics for DM1 (34). One of the first proposed mechanisms involved in repeat instability at the molecular level is slippage of the replication fork during replication. Unpaired bases form loops, which result in expansions or contractions in a next round of replication, depending on whether the looped repeats are in the newly synthesised or template strand. As described in figure 5, during normal replication, helicases break the hydrogen bonds that keep the two DNA strands together, which yield the replication fork. DNA polymerase can only synthesise a new strand in a 5' to 3' direction. Hence, on one strand (leading strand) DNA polymerase reads the DNA and adds nucleotides to the nascent strand in a continuous manner. On the other strand (lagging strand) the complementary strand is synthesised in short segments (Okazaki fragments) at a time, which are later joined together by DNA ligase. Formation of secondary structures, such as hairpins can form in one of the strands. This can impair normal replication fork processing. The sequence of the strands, together with the position of the origin of replication with respect to the repeat sequence, determine which strand is more prone to form hairpins. Whether a hairpin is present in the template or nascent strand, in turn determines whether contraction or expansion results in the next round of replication.

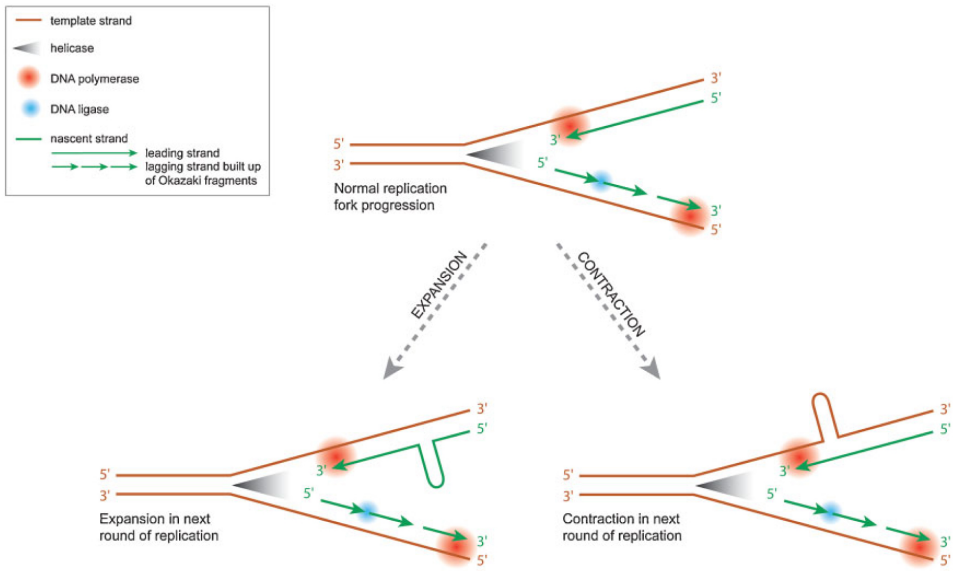

Figure 5: replication fork and repeat instability.

However, slippage alone cannot explain all aspects of repeat expansions. Many other *cis* and *trans* modifiers should act to exert the final instability of the sequence (16). Cis-acting refers to factors that are directly associated with the repeat, whereas elements that interact with the repeat can be considered trans-acting elements.

3.2.2.2 Nuclear foci

In both types of myotonic dystrophy, the RNA containing the expanded repeat forms nuclear foci (ribonuclear inclusions) in muscle cells, which can be distinguished by *in-situ* hybridization with probes specifically designed to bind the mutant mRNA (20, 21). This visual cue led to the novel theory that the ribonuclear inclusions signify a toxic gain-of-function effect mediated at the RNA level (35). Normally, newly synthesised mRNA in the nuclear compartment is transcribed in the proximity of chromosome-specific regions called nuclear speckles close to the nuclear lamina (highly enriched in poly(A)-RNA and spliceosome components such as the spliceosome assembly factor SC-35). In these domains, the mRNA undergoes splicing events and becomes ready to be exported in the cytoplasm through the nuclear pore. Recent evidences suggested that in DM1, mutant transcripts detach from the gene but no longer progress within the SC-35 domain, accumulating in multiple round foci placed at the outer boundary of SC-35 domains (36). Here, the expanded transcripts acquire a double-stranded hairpin loop structure (37) and bind many proteins with affinity for the $(CUG)_n$ sequence. In search of proteins that bind to the anomalous triplet repeat expansion, in vitro studies identified CUG-binding protein (CUG-BP1), which belongs to the CELF (CUG-BP1 and ETR-3-like factors) family of proteins (21). Also muscleblind-like proteins (MBNL1, 2, 3) were found to specifically bind expanded, but not normal size, $(CUG)_n$ repeats in a manner proportional to repeat size (38-42). These proteins act as splicing events modulators/regulators, and their sequestration have been recognised as the primary toxic action of expanded RNA.

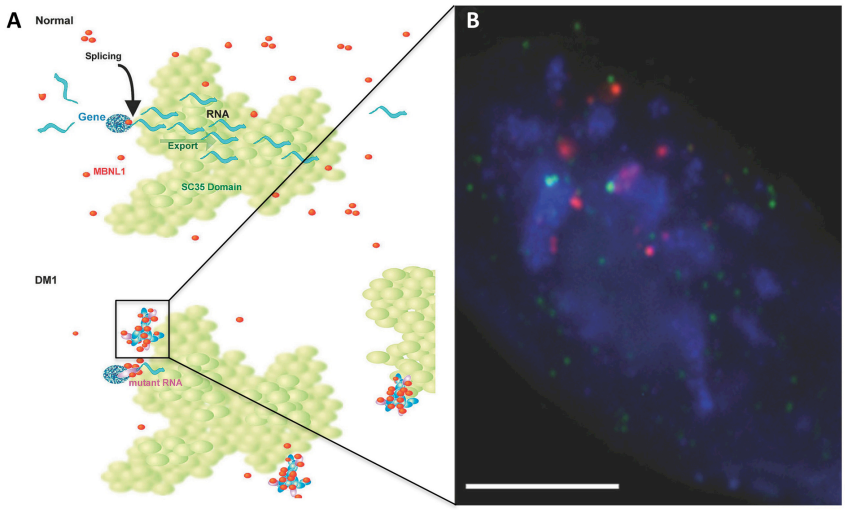

Figure 6: nuclear speckles with ribonucleoproteic foci: (A) Model of SC-35 domain function. In this model, DMPK genes are positioned at the edge of SC-35 domains. The RNAs produced from these loci are primarily spliced at the edge of the domain. These mRNAs then transit into the domain (step 1). In the interior of the domain, the bound splicing factors, such as small nuclear RNPs and serine-arginine proteins, are removed and recycle back to the domain edge. These are replaced by export factors such as tip-associated protein and Aly. The export-ready mRNAs then leave the domain (step 2) and are transported to the nuclear envelope. In DM1, the RNA is spliced, but expanded repeat sequences in the RNA are bound by MBNL1 (and perhaps other factors), forming aggregates (MRGs) that do not enter the domain and impeding export of the RNA; (B) Three-color image of SC-35 (blue) DMPK DNA (green) and CUG RNA (red) shows two gene signals associated with SC-35 domains, but only one gene is juxtaposed to the diffuse CUG RNA signal overlapping SC-35.

3.2.2.3 The spliceopathy

RNA splicing, the process in which introns are removed from a primary transcript and exons are joined together, is a critical point for regulation of gene expression. During this process, the splicing machinery makes decisions about which portions of a transcript are included in the mature mRNA. Many exons are selected consistently, but some require choice. Because of this flexibility in exon usage, a single gene can produce multiple mRNA species that differ by the inclusion or skipping of alternative exons or differences in where the boundaries of particular exons are drawn. These splicing decisions are tightly regulated, yielding a spectrum of alternative splice products that are characteristic of a particular tissue or stage of development. The outcome of alternative splicing is controlled by splicing regulatory proteins. These proteins bind to specific RNA sequences close to a regulated exon, thereby influencing the action of the splicing machinery. Modest changes in the concentration of a splicing factor can translate into large changes in the frequency of inclusion or skipping for a particular exon (43). The defect of splicing regulation, or spliceopathy, has been linked to changes in activity of two families of splicing regulators:

i Levels of CUG binding protein 1 (CUG-BP1), an RNA binding protein, are increased in DM1 muscle cells (44). A DM1-like spliceopathy is triggered in cultured cells or mice by forced overexpression of CUG-BP1 (45-48). In addition, cell degeneration in CUGexp-expressing fruit flies was aggravated by the simultaneous overexpression of human CUG-BP1 (49). Taken together, these findings support the idea that upregulation of CUG-BP1 contributes to splicing abnormalities and degenerative changes in DM1.

ii A second group of RNA binding proteins implicated in myotonic dystrophy pathogenesis are splicing factors in the muscleblind-like (MBNL) family. These proteins were initially identified by Swanson and colleagues (38) as the major CUGexp-binding proteins in the mammalian nucleus. MBNL proteins bind to CUGexp RNA in vitro with high affinity, and they also interact with CUGexp in cells, as evidenced by colocalization with RNA inclusions in DM1 muscle nuclei (50). Considerable evidence now supports the theory, originally proposed by Miller et al. (38), that sequestration of MBNL proteins is a critical step in the pathogenesis of myotonic dystrophy. The major MBNL protein expressed in skeletal muscle is MBNL1. Features of DM1, including myotonia, splicing defects, and cataracts, can be reproduced in mice by disruption of the *MBNL1* gene (51). In mouse models, the effects of $(CUG)_n$ expression or MBNL1 ablation on alternative splicing, in terms of the range of exons affected, was very similar if not identical, and highly congruent with the splicing defects observed in human DM1 (52). Thus, the spliceopathy in myotonic dystrophy is entirely consistent with depletion of MBNL1 from the nucleoplasm that has been directly visualised in DM1 muscle cells (52). Furthermore, in $(CUG)_n$-expressing muscle, the splicing defect can be reversed by overexpressing MBNL1 to levels that exceed the capacity of the repetitive RNA to sequester protein (14, 47, 53). The first indication that spliceopathy was directly involved in producing clinical signs or symptoms of

DM1 related to the insulin resistance that is characteristically found in DM1 skeletal muscle (46). $(CUG)_n$ RNA represses the inclusion of insulin receptor exon 11, resulting in a receptor protein having lower capacity for insulin signaling. Previous work also has suggested that myotonia, a core feature of myotonic dystrophy, results from the synthesis of variant ClC-1 splice isoforms that had no intrinsic channel activity (54, 55). Myotubularin-related protein 1 (MTMR1) alternative splicing have been proposed to affect myogenesys (56), while calcium homeostasis have been shown to be altered by the presence of non correct isoforms of SERCA1, RyR1, Ryr2 and SK3 (57, 58). Also CNS involvement have been proposed to be related by the misregulated splicing of Tau protein (28).

Table 4: splicing defects and related symptoms in myotonic dystrophy 1

Protein	Splicing variants	Related symptoms
Insulin receptor[1]	lower-signaling nonmuscle isoform IR-A (Δex11) substitutes the muscle specific isoform IR-B (+ex11)	Insulin resistance
Chloride channel 1[2]	muscle-specific ClCN1 Δex7a is substituted by the non muscular CLCN1+ex7a	Myotony
Cardiac T troponin[3]	embryonic cTNT+ex5 is increased compared to the adult form cTNT Δex5 in cardiac muscle	Cardiac conduction defects
MTMR1[4]	adult MTMR1-C isoform is reduced in DM1 muscle compared to control	Muscle wasting
SK3[5]	small-conductance Ca^{2+}-activated K^+ channel is still expressed in DM1 while not present in adult control muscle	Muscle weakness
SERCA1[6]	adult SERCA1a (+ex22) decrease compared to neonatal SERCA1b (Δex22)	Muscle weakness
SERCA2[6]	SERCA2d (+intron19) decreases in skeletal muscle compared to controls	Muscle weakness
RyR1[6]	less active, neonatal RyR1 ASI (Δex83) prevails in skeletal muscle compared to adult RyR ASI (+ex83)	Muscle weakness
Tau[7]	foetal brain Tau isoform (lacking ex2, 3 and 10) increases in DM1 brain compared to control	Mental retardation, memory deficit

1 Savkur et al, 2001; 2 Charlet et al, 2002, Berg et al, 2004; 3 Philips et al, 1998; 4 Buj-Bello et al, 2005; 5 Kimura et al, 2000; 6 Kimura et al, 2005; 7 Ghanem et al, 2009.

3.2.3 Disease models

3.2.3.1 Mouse models

The pathology of skeletal muscle, including both myotonic and dystrophic features, has been reproduced in different mouse models by the following different strategies (59):

I. Knock-out and overexpressor models

The first generation of mice was created in order to investigate involvement of gene products of DMPK and SIX5 in DM1 molecular pathogenesis.

Two models of *DMPK* knockout (*$DMPK^{-/-}$*) mice were independently generated by Jansen (60) and Reddy (61) by targeted replacement of the first seven exons of the *DMPK* gene by a resistance cassette, resulting in complete absence of DMPK protein. *$DMPK^{-/-}$* mice displayed only mild signs of myopathy and, in Reddy's mice, altered Ca^{2+} homeostasis and cardiac conduction abnormalities (see table 5). Other DM1 features such as myotonia, cataract and male infertility seemed to be fully absent.

A transgenic *DMPK* overexpressor mouse model was created by Jansen et al, using a genomic fragment, encoding all human DMPK exons (including $(CTG)_{11}$ repeats) and the last exon of DMWD, in transgenesis (60). No histological and ultrastructural abnormalities were observed in various tissues. Skeletal muscle physiology revealed no abnormal features, while in hearth muscle a clear but mild myopathy was detected (60).

SIX5 knock-out (*$SIX5^{-/-}$*) mice models were created independently by Klesert (62) and Sarkar (63).Both lines developed ocular cataract at higher rate than wild type animals, even if loss of SIX5 mRNA expression generally did not exceed the 50% level (62). No abnormal skeletal muscle function in *$SIX5^{-/-}$* mice was observed. It is however likely that, given the fact that cataract is also present in DM2, other mechanisms than *SIX5* (or *DMPK*) deficiency proper contribute to cataract formation in DM1 patients.

II. Mouse models with expanded $(CTG)_n$ repeats

Many attempts have been done to generate mouse models that reproduce the very high germ line mutation rate, the considerable intergenerational length changes, and the massive expansion bias see for the $(CTG)_n$ triplet repeat in DM1 families. All transgenic mouse lines displayed a varying number of repeat instability characteristics also observed in DM1 patients. Only the two models expressing long $(CUG)_n$ repeats, designated DM300 (n 300) and HSA^{LR} (n 250), showed pathological symptoms similar to those found in DM1 patients (59). Five different transgenic mice, named DMT-A-E mice (from A to E), were created by Monckton's group (64) with randomly integrated one to three

copy DNA inserts, consisting of a relatively short 3'-terminal area (exon 15) of the human *DMPK* gene spanning a $(CTG)_{162}$ repeats. Offsprings genetic analysis demonstrated repeat segregation distortion in favour of the transgene, hypermutability, sex of parent-of-origin effect and somatic instability. Gourdon's group generated different mouse lines carrying large (45 kb) human genomic DNA inserts spanning the entire DMWD-DMPK-SIX5 area and carrying repeats consisting of either 20, 55 or >300 CTG triplets (65, 66). This large insert, although randomly integrated, presumably contained all control elements necessary for correct tissue-type regulation of transcription of the human DMWD, DMPK and SIX5 genes. Typical DM1 disease features (myopathy, myotonia, muscle de- and regeneration, altered tau splice forms, mouse-line-dependent growth retardation and nuclear foci) were observed in DM300 mouse. Somatic instability was observed in both the DM55 and DM300 lineages, but by far the highest instability was observed in tissues of the DM300 mice (66). Another series of transgenic mice with $(CTG)_5$ or $(CTG)_{250}$ respectively called HSA^{SR} and HSA^{LR}, were generated by Mankodi et al. (67) and gave a strong argument in favour of the RNA dominance mechanism in DM1 pathology. The repeated sequences were inserted into the middle of the last exon of the human skeletal muscle actin gene and allowed to study the effect of expression of an untranslated expanded $(CUG)_n$ repeat in a DM1-unrelated transcript. No DM-like symptoms were detected in the HSA^{SR} mice, while HSA^{LR} mice displayed many of the characteristic skeletal muscle symptoms of DM1 patients, such as myotonia and muscle wasting, demonstrating a central, toxic role for RNA containing long $(CUG)_n$ repeats in DM1 pathology. A second generation transgenic knock-in mouse model was generated by van den Broek replacing the entire 3'-gene region by the exact cognate human segment, with either $(CTG)_{11}$ repeat or an unstable $(CTG)_{84}$ repeat. Whereas the $(CTG)_{11}$ repeat was completely stable as in the other mouse models, the $(CTG)_{84}$ slowly expanded during intergenerational segregation and showed profound somatic instability, which was progressive upon ageing, in kidney, stomach, small intestine and liver (68). Wang et al used a Cre-loxP approach including tamoxifen-inducible Cre to generate an inducible mouse model for heart-specific expression of 960 CUG RNA repeats in the context of DMPK 3′ UTR. Adult mice in which high levels of expanded CUG RNA was induced developed severe cardiomyopathy and arrhythmias resulting in 100% mortality within 2 weeks of induction. Mice from lines that expressed more than 5-fold the level of the identical mRNA lacking repeats exhibited no phenotypic or molecular changes. Repeat-expressing mice exhibited diastolic and systolic dysfunction, arrhythmias, and a full set of molecular features observed in DM1 heart tissue such as RNA foci formation, colocalization of MBNL1 with RNA foci, elevated CELF protein expression, and misregulated alternative splicing (69, 70).

Table 5: transgenic DM1 mouse models

Transgenic line	Targeting strategy	Pathology phenotype	Number of $(CTG)_n$ repeats in founder(s)	intergenerational instability (changes in repeats)	Somatic instability (change in repeats)
Knock-out and overexpressor mice					
DMPK KO[1]	replacement first 7 exons of *DMPK* gene with hygromycin cassette	mild myopathy,altered Ca2+ homeostasis	n.a.	n.a.	n.a.
DMPK KO[2]	replacement first 7 exons of *DMPK* gene with neomycin cassette	mild myopathy, reduced skeletal muscle force, cardiac conduction defects, abnormal Na+ channel gating	n.a.	n.a.	n.a.
DMPK Tg overexpressor[3]	insertion 14 kb human DM1 locus fragment, containing DMPK gene (~20 copies)	hypertrophic cardiomyopathy, enhanced neonatal mortality	11	n.d.	n.d.
Six5 KO[4]	replacement complete *Six5* gene with neomycine cassette	ocular cataract	n.a.	n.a.	n.a.
Six5 KO[5]	replacement exon 1 of *Six5* gene with beta-gal reporter	ocular cataract	n.a.	n.a.	n.a.
Expanded (CTG)n repeat mice					
DMT-A-E[6]	random insertion human genomic DMPK (CTG)162 fragment	n.d.	143–163	contractions and expansions (–7 to +7), parent-of-origin effects	in various tissues; highest in kidney (–20 to +540), age dependent
DM20, DM55, DM300[7]	random insertion 45 kb genomic fragment carrying DMWD, DMPK and SIX5, with either (CTG)20, (CTG)55 or (CTG)~360	DM300: myopathy, myotonia, altered tau splice forms, growth retardation (mouse line dependent)	55 or >300 (20 in control line)	mainly expansions, DM55 (–1 to +6), DM300 (–30 to +60), parent-of-origin effects	in various tissues; highest in kidney, pancreas, liver (–10 to + >100), age and mouse line dependent
(CTG)11, (CTG)84[8]	replacement mouse 3'-end of *Dmpk* gene by human DMPK sequence containing either (CTG)11 or (CTG)84	no overt abnormalities	84 (11 in control line)	contractions and expansions (–16 to +8), mouse strain effects	in various tissues; highest in stomach, liver, kidney, (up to +45), age and cell type dependent
HSALR HSASR[9]	random insertion genomic fragment containing human skeletal actin gene, bearing (CTG)5 or (CTG)250 in its 3'-UTR	HSALR: myotonia, myopathy, altered chloride channel splice forms, increased early mortality	~250 (5 in control line)	n.d.	n.d.
EpA960[10]	tamoxifen-inducible Cre-loxP mouse model for heart-specific expression of 960 CUG RNA repeats in the context of DMPK 3′ UTR	severe cardiomyopathy, arrhythmias, 100% mortality within 2 weeks of induction	960	n.d.	n.d.

[a] Listing of all available DM1 mouse models, including Dmpk and Six5 knock-outs, and DMPK Tg overexpressor in the upper panel, and several mouse lines carrying expanded (CTG)n repeats in the lower panel. [b] 1. (Benders et al., 1997; Jansen et al., 1996); 2. (Berul et al., 1999; Mounsey et al., 2000; Reddy et al., 1996; Reddy et al., 2002); 3. (Jansen et al., 1996); 4. (Mistry et al., 2001; Sarkar et al., 2000); 5. (Klesert et al., 2000); 6. (Fortune et al., 2000; Monckton et al., 1997; Zhang et al., 2002); 7. (Gourdon et al., 1997; Lia et al., 1998; Seznec et al., 2000; Seznec et al., 2001); 8. (van den Broek et al., 2002); 9. (Mankodi et al., 2000; Mankodi et al., 2002); 10 (Wang et al.,2007). [c] n.a. = not applicable, n.d. = not determined.

3.2.3.2 Cell models

Cell culture systems have been used effectively to investigate DM1 pathology. A number of groups have taken advantage of the disease-relevant C2C12 myoblast cell line (71-73). C2C12 myoblasts were originally isolated from injured adult mouse muscle, and provide an excellent system to study myogenesis (Blau et al., 1983; Yaffe and Saxel, 1977). Like human myogenic cells, when cultured in differentiation media that lacks growth factors, C2C12 cells enter the myogenic differentiation pathway and fuse into multinucleated myotubes. DMPK mRNA is expressed in both human myoblasts and C2C12 cells during proliferation and up-regulated during the differentiation program. Recently, C2C12 cells were used to demonstrate that hDMPK-A expression induces physiological changes like loss of mitochondrial membrane potential, increased autophagy activity, and leakage of cytochrome c from the mitochondrial intermembrane space accompanied by apoptosis (74). Human DM1 fibroblasts, converted to myogenic cells by the infection with *MyoD* amphotrophic retroviruses, were used to study the effects of mutant mRNA on the stability of CUGBP1 (75) or on the insulin receptor splicing regulation (46). Use of human DM1 primary myoblasts cultures has been rare, owing to their limited availability, to investigate Ca^{2+} homeostasis (76-78) or to verify the myogenic potential of human DM1 primary myoblasts (56, 79-85). The more research goes on with the study of myotonic dystrophy in cellular models, the more we feel the need of a model closer to human skeletal muscle. In fact, discording evidences regarding myogenesis in mouse and human models are suggesting that mouse models could not fully reflect the human ones.

3.2.4 Muscle pathology in Myotonic Dystrophy 1

At the skeletal muscle level, a prominent distal muscle weakness and atrophy at onset is observed in DM1 patients. The causes of the progressive muscle wasting that affects distal muscles before proximal muscles in the early stages of the disease are not well understood. The extent of histopathological changes, including type I fibre predominance and atrophy, increased number of central nuclei, sarcoplasmic masses, increased incidence of ring fibres and variability in fibre size, seems to be correlated with the severity of the muscle weakness rather than the severity of the myotonia (86). Satellite cells are responsible for replacing lost muscle, so dysfunction could contribute to muscle weakness and wasting in DM1. Data regarding regeneration in DM1 muscle are scarce, but it has been noted that there is a reduced regenerative response to muscle wasting in DM patients as compared to patients with other forms of muscular dystrophy.To date, many publications claimed that human muscle satellite cell function is affected in DM1 (44, 80, 87, 88), but the great majority of experiments have been performed in with murine C2C12 models (87, 89), human fibroblast-derived myogenic lines (46, 75), or human models that no longer retain the typical features of muscle progenitor cells (80, 81). Indeed, human myoblast lines were often obtained i.e. from abortive fetuses, which represent an extreme pathological condition only partially informative. Moreover,

working with cell models implies the control of the age of cell, in terms of passages in culture. Recent experiments aiming to optimise human skeletal muscle precursors *in vitro* culture showed that the expression of myogenic markers decreases even after five culture passages (90). Thus, in order to evaluate the myogenic potential of muscle derived cells, the use of 'young' cell models becomes a primary requirement. To date, the diffuse hypothesis is that in DM1, the myogenic cascade stops at MyoD/myogenin expression transition (91), leading to a block of the differentiation processes necessary for the formation of the myofibre. Moreover, an impairment of cell cycle withdrawal could also be implied leading to the inability of the satellite cell to stop proliferating and enter the differentiation program (82). The misregulated proliferation of satellite cells could then lead to their senescence, as proposed by Bigot et al. (92). Recently, Vattemi et al. (19) proposed that the sarcoplasmic masses, which are prominent features in DM1 biopsies, could result from the 'interruption of late myogenic differentiation' rather than the foci of abnormal regeneration and/or degeneration. Previously, Borg et al. (93) had suggested that the myopathic appearance of the DM1 muscle fibres was related to an abnormal and abortive regeneration. Both of these phenomena have been related to a dysfunction in the myogenic precursor cell or satellite cell compartment. Thus, a possible contribution of a cell-death mechanism could be investigate as the responsible of impaired muscle regeneration and progressive muscle wasting in myotonic dystrophy 1.

3.2.5 Therapeutic strategies

There is no cure for DM. Current treatment for DM is limited to supportive care that partially alleviates signs and symptoms of the disease but does nothing to slow or halt disease progression. The ultimate goal in development of new therapies is reversal of the disease phenotype. As the understanding of DM1 pathogenesis continues to improve, new pharmacologic approaches to treat myotonia and muscle wasting are already in early clinical trials, and therapies designed to reverse the RNA toxicity have shown promise in preclinical models by correcting spliceopathy and eliminating myotonia (14, 94, 95). The principal strategies being studied for the treatment of DM1 are:

– *Myotonia reduction:* myotonia exacerbates disability, with preferential involvement of muscles that are the weakest, such as those in the hand and forearm. Several drugs are used to treat myotonia. For example, mexiletine, an antiarrhythmic that acts on sodium channels, has been used off-label to treat myotonia in DM and in nondystrophic myotonias. In the absence of quality-controlled clinical trials, however, the safety and efficacy of antimyotonia agents in DM1 are unknown (96).

– *Reversal of muscle wasting in DM1:* IGF-1/IGFBP3: evidence suggests that wasting in DM results from a defect in muscle anabolism. For example, rates of protein synthesis are reduced and the caliber of muscle fibers progressively diminishes. Several anabolic agents already have been tested for their ability to improve muscle strength, such as dehydroepiandrosterone (DHEA) (97). Among hormones presently known to stimulate muscle anabolism, insulin-like growth factor-1

(IGF-1) has the strongest effect and its recombinant form (rhIGF-1) is being tested to increase muscle strength and function in adult patients (98).

– *Myostatin inhibition:* myostatin is a circulating protein produced and secreted by skeletal muscle that acts as a negative regulator of muscle growth and function. Reduction of myostatin activity also has disease-modifying effects in muscular dystrophy. Myostatin is not known to be overactive in DM. Nonetheless, reduction of existing myostatin activity in DM1 may have beneficial effects on protein anabolism by acting through mechanisms independent of those that cause the disease (99). Several additional approaches may be considered to reduce myostatin function in DM1, including deacetylase inhibitors, blockade of myostatin receptors, morpholino antisense oligonucleotides designed to block translation or skip exon 3 of myostatin to produce a nonfunctional protein, or viral overexpression of endogenous myostatin inhibitors (100).

– *Reduction of RNA-mediated toxicity:*

i Reversal of spliceopathy: antisense oligonucleotide-induced exon skipping. Antisense oligonucleotides (AON), designed to skip the abnormally included exon of the muscle chloride channel, exon 7a, have been developed to force the production of a full-length, fully functional chloride channel leading to the elimination of myotonia for up to 8 weeks after a single treatment. Its use as a therapy in DM patients has limitations because of its delivery and its specificity for the only myotonic features without addressing aspects of DM that result from spliceopathy of other transcripts.

ii Upregulation of MBNL1 activity: intramuscular injection with an adeno-associated virus (AAV) designed to overexpress MBNL1 protein caused the normalization of MBNL1 activity to a level sufficient to reverse myotonia and spliceopathy for up to several months after a single treatment. Another strategy to upregulate MBNL1 activity aimed to reduce its sequestration by the expanded RNA using compounds known to block MBNL1–RNA interactions by binding to structured RNA such as pentamidine and neomycin B (95) (Figure 7).

iii Downregulation of CUGBP1 activity: this strategy has been tested in new transgenic mouse models which can be treated with protein kinase C inhibitors to downregulate, or prevent upregulation, of CUGBP1 activity by reducing its phosphorylation (14) (Figure 7).

iv Neutralization or elimination of the mutant RNA: retrovirus expressing antisense RNA designed to bind and degrade the mutant DMPK allele had the intended effect of preferential reduction of mutant DMPK RNA levels. Moreover, non-viral approaches to reduce CUG_{exp} RNA include short interfering RNA (siRNA), which has demonstrated efficacy in DM1 fibroblasts. Clinical application of these strategies necessitates development of efficient means of systemic delivery of viral-mediated antisense, siRNA, or both. High specificity for degradation of the mutant allele will be re-

quired to minimize nonspecific degradation of the normal allele and subsequent reduction of DMPK protein levels.

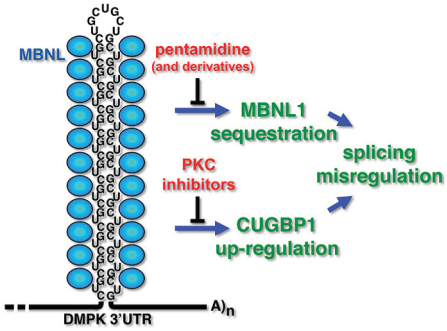

Figure 7: small molecules to combat the multiple toxic effects of CUG_{exp} RNA. CUG_{exp} RNA directly binds and sequesters MBNL1 and leads to up-regulation of CUGBP1 caused by PKC activation. The nucleic acid binding compound, pentamidine, acts as an inhibitor of MBNL1-CUG_{exp} RNA interactions. PKC inhibitors have been shown to blunt the effects of CUG_{exp} RNA in a DM1 mouse model.

3.3. Mechanisms of programmed cell death

The most widely used classification of mammalian cell death recognizes two types: apoptosis and necrosis. Autophagy, which has been proposed as a third mode of cell death, is a process in which cells generate energy and metabolites by digesting their own organelles and macromolecules. Autophagy allows a starving cell, or a cell that is deprived of growth factors, to survive. However, cells that do not receive nutrients for extended periods ultimately digest all available substrates and die (autophagy-associated cell death). Distinctions between apoptosis, necrosis, and autophagy entail differences in the mode of death and morphologic, biochemical, and molecular attributes. Programmed cell death is an important concept. Cell death is “programmed” if it is genetically controlled. Apoptosis and autophagy-associated cell death are the two fundamental types of programmed cell death. The recognition that cell death can occur by genetically controlled processes has enabled advances in unraveling the mechanisms of many diseases, and this new knowledge has facilitated the development of pharmacologic agents that initiate or inhibit programmed cell death. Moreover, there is now evidence that necrosis, traditionally considered an accidental form of cell death, can in certain instances be initiated or modulated by programmed control mechanisms (101).

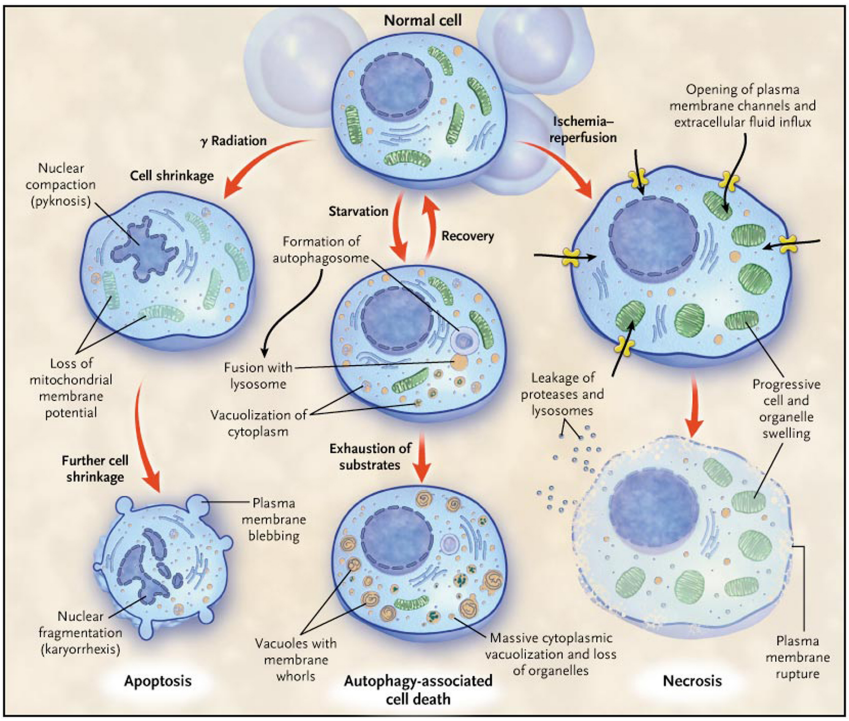

Figure 8: cell-death pathways. Among the three major pathways of cell death — apoptosis, autophagy, and necrosis — a particular mode of celldeath may predominate, depending on the injury and the type of cell.

3.3.1 Apoptosis

Apoptosis (derived from an ancient greek word that suggests 'leaves falling from a tree') is the process of programmed cell death (PCD) that may occur in multicellular organisms. By saying 'programmed', we mean that its activation is genetically controlled. Without apoptosis, 2 tons of bone marrow and lymph nodes and a 16-km intestine would probably accumulate in a human by the age of 80 (102). Programmed cell death involves a series of biochemical events leading to a characteristic cell morphology and death; in more specific terms, a series of biochemical events that lead to a variety of morphological changes, including blebbing, changes to the cell membrane such as loss of membrane asymmetry and attachment, cell shrinkage, nuclear fragmentation, chromatin condensation, and chromosomal DNA fragmentation (101) (Figure 8). Processes of disposal of cellular debris whose results do not damage the organism differentiate apoptosis from necrosis. In contrast to necrosis, which is a form of traumatic cell death that results from acute cellular injury, apoptosis, in general, confers advantages during an organism's life cycle. For example, the differentiation of fingers and toes in a developing human embryo occurs because cells between the fingers undergo apoptosis; the result is that the digits are separate. Between 50 and 70 billion cells die each day due to apoptosis in the average human adult. For an average child between the ages of 8 and 14 years, approximately 20 billion to 30 billion cells die a day. In a year, this amounts to the proliferation and subsequent destruction of a mass of cells equal to an individual's body weight. Research on apoptosis has increased substantially since the early 1990s. In addition to its importance as a biological

phenomenon, defective apoptotic processes have been implicated in an extensive variety of diseases. Excessive apoptosis causes hypotrophy, such as in ischemic damage, whereas an insufficient amount results in uncontrolled cell proliferation, such as cancer (101).

3.3.1.1 Functions

Apoptosis occurs when a cell is damaged beyond repair, infected with a virus, or undergoing stressful conditions such as starvation. Damage to DNA from ionizing radiation or toxic chemicals can also induce apoptosis via the actions of the tumor-suppressing gene p53. The "decision" for apoptosis can come from the cell itself, from the surrounding tissue, or from a cell that is part of the immune system. In these cases apoptosis functions to remove the damaged cell, preventing it from sapping further nutrients from the organism, or halting further spread of viral infection. Apoptosis also plays a role in preventing cancer. If a cell is unable to undergo apoptosis because of mutation or biochemical inhibition, it continues to divide and develop into a tumor. In the adult organism, the number of cells is kept relatively constant through cell death and division. Cells must be replaced when they malfunction or become diseased, but proliferation must be offset by cell death. This control mechanism is part of the homeostasis required by living organisms to maintain their internal states within certain limits. Homeostasis is achieved when the rate of mitosis (cell division resulting in cell multiplication) in the tissue is balanced by the rate of cell death. If this equilibrium is disturbed, one of two potentially fatal disorders occurs:

– the cells divide faster than they die, resulting in the development of a tumor.

– the cells divide slower than they die, causing cell loss.

Homeostasis involves a complex series of reactions, an ongoing process inside an organism that calls for different types of cell signaling. Any impairment can cause a disease. For example, dysregulation of signaling pathway has been implicated in several forms of cancer.

3.3.1.2 Control

The process of apoptosis is controlled by a diverse range of cell signals, which may originate either extracellularly (extrinsic inducers) or intracellularly (intrinsic inducers). Extracellular signals may include toxins, hormones, growth factors, nitric oxide or cytokines, and therefore must either cross the plasma membrane or transduce to effect a response. These signals may positively (i.e., trigger) or negatively (i.e., repress, inhibit, or dampen) affect apoptosis. A cell initiates intracellular apoptotic signalling in response to a stress, which may bring about cell suicide. The binding of nuclear receptors by glucocorticoids, heat, radiation, nutrient deprivation, viral infection, hypoxia and increased intracellular calcium concentration, for example, by damage to the membrane, can all trigger the release of intracellular apoptotic signals by a damaged cell. A number of cellular components, such as

poly ADP ribose polymerase, may also help regulate apoptosis. Before the actual process of cell death is precipitated by enzymes, apoptotic signals must cause regulatory proteins to initiate the apoptosis pathway. This step allows apoptotic signals to cause cell death, or the process to be stopped, should the cell no longer need to die. Several proteins are involved, but two main pathways of regulation have been identified: a death-receptor-mediated and a mitochondrial pathway (Figure 9). Another extrinsic pathway for initiation identified in several toxin studies is an increase in calcium concentration within a cell caused by drug activity, which also can cause apoptosis via a calcium binding protease calpain.

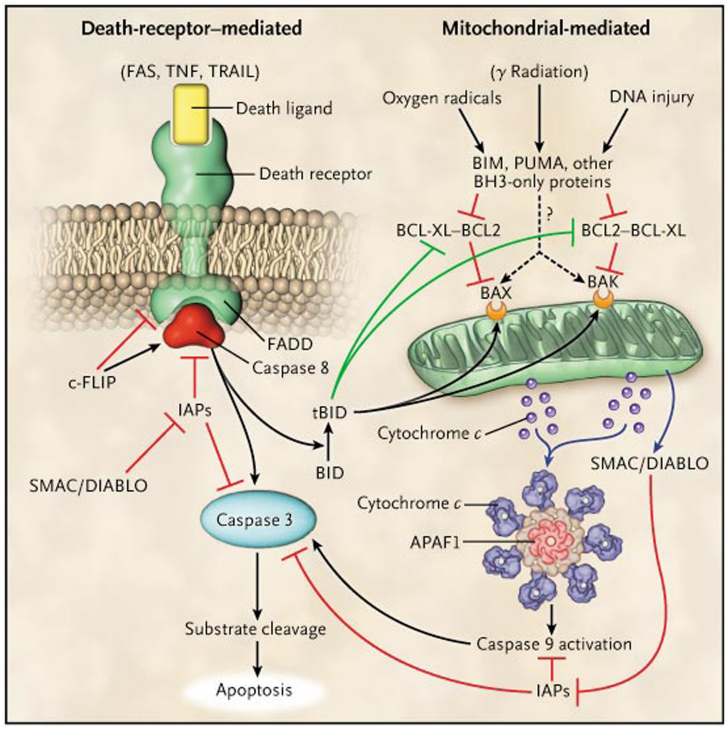

Figure 9: pathways of cellular apoptosis. There are two major pathways of apoptosis: the death-receptor pathway,which is mediated by activation of death receptors, and the BCL2-regulated mitochondrial pathway, which is mediated by noxious stimuli that ultimately lead to mitochondrial injury. Ligation of death receptors recruits the adaptor protein FAS-associated death domain (FADD). FADD in turn re- cruits caspase 8, which ultimately activates caspase 3, the key "executioner" caspase. Cellular FLICE-inhibitory protein (c-FLIP) can either inhibit or potentiate binding of FADD and caspase 8, depending on its concentration. In the intrinsic pathway, proapoptotic BH3 proteins are activated by noxious stimuli, which interact with and inhibit antiapoptotic BCL2 or BCL-XL. Thus, BAX and BAK are free to induce mitochondrial permeabilization with release of cytochrome c, which ultimately results in the activation of caspase 9 through the apoptosome. Caspase 9 then activates caspase 3. SMAC/DIABLO is also released after mitochondrial permeabilization and acts to block the action of inhibitors of apoptosis protein (IAPs), which in- hibit caspase activation. There is potential cross-talk between the two pathways, which is mediated by the truncated form of BID (tBID) that is produced by caspase 8–mediated BID cleavage; tBid acts to inhibit the BCL2–BCL-XL pathway and to activate BAX and BAK.

I. The extrinsic pathway: membrane death-receptors

Two theories of the direct initiation of apoptotic mechanisms in mammals have been suggested: the TNF-induced (tumour necrosis factor) model (103) and the Fas-Fas ligand-mediated model (104), both involving receptors of the TNF receptor (TNFR) family coupled to extrinsic signals. TNF is a cy-

tokine produced mainly by activated macrophages, and is the major extrinsic mediator of binary hipaloptic apoptosis. Most cells in the human body have two receptors for TNF: TNF-R1 and TNF-R2. The binding of TNF to TNF-R1 has been shown to initiate the pathway that leads to caspase activation via the intermediate membrane proteins TNF receptor-associated death domain (TRADD) and Fas-associated death domain protein (FADD) (105). Binding of this receptor can also indirectly lead to the activation of transcription factors involved in cell survival and inflammatory responses. The link between TNF and apoptosis shows why an abnormal production of TNF plays a fundamental role in several human diseases, especially in autoimmune diseases. The Fas receptor (also known as Apo-1 or CD95) binds the Fas ligand (FasL), a transmembrane protein part of the TNF family (104). The interaction between Fas and FasL results in the formation of the death-inducing signaling complex (DISC), which contains the FADD, caspase-8 and caspase-10. In some types of cells (type I), processed caspase-8 directly activates other members of the caspase family, and triggers the execution of apoptosis of the cell. In other types of cells (type II), the Fas-DISC starts a feedback loop that spirals into increasing release of pro-apoptotic factors from mitochondria and the amplified activation of caspase-8. Following TNF-R1 and Fas activation in mammalian cells a balance between pro-apoptotic (BAX, BID, BAK, or BAD) and anti-apoptotic (Bcl-Xl and Bcl-2) members of the Bcl-2 family is established (101). This balance is the proportion of pro-apoptotic homodimers that form in the outer-membrane of the mitochondrion. The pro-apoptotic homodimers are required to make the mitochondrial membrane permeable for the release of caspase activators such as cytochrome c and SMAC. Control of pro-apoptotic proteins under normal cell conditions of non-apoptotic cells is incompletely understood, but it has been found that a mitochondrial outer-membrane protein, VDAC2, interacts with BAK to keep this potentially-lethal apoptotic effector under control. When the death signal is received, products of the activation cascade displace VDAC2 and BAK is able to be activated. There also exists a caspase-independent apoptotic pathway that is mediated by AIF (apoptosis-inducing factor) (106).

II. The intrinsic pathway: the mitochondrion

The mitochondria are essential to multicellular life. Without them, a cell ceases to respire aerobically and quickly dies, a fact exploited by some apoptotic pathways. Apoptotic proteins that target mitochondria affect them in different ways. They may cause mitochondrial swelling through the formation of membrane pores, or they may increase the permeability of the mitochondrial membrane and cause apoptotic effectors to leak out (101). There is also a growing body of evidence indicating that nitric oxide (NO) is able to induce apoptosis by helping to dissipate the membrane potential of mitochondria and therefore make it more permeable (107). Mitochondrial proteins known as SMACs (second mitochondria-derived activator of caspases) are released into the cytosol following an increase in permeability. SMAC binds to inhibitor of apoptosis proteins (IAPs) and deactivates them, preventing the IAPs from arresting the apoptotic process and therefore allowing apoptosis to pro-

ceed. IAP also normally suppresses the activity of a group of cysteine proteases called caspases (108), which carry out the degradation of the cell, therefore the actual degradation enzymes can be seen to be indirectly regulated by mitochondrial permeability. Cytochrome c is also released from mitochondria due to formation of a channel, MAC, in the outer mitochondrial membrane (109), and serves a regulatory function as it precedes morphological change associated with apoptosis (101, 110). Once cytochrome c is released it binds with Apaf-1 and ATP, which then bind to pro-caspase-9 to create a protein complex known as an apoptosome. The apoptosome cleaves the pro-caspase to its active form of caspase-9, which in turn activates the effector caspase-3 (110). MAC is itself subject to regulation by various proteins, such as those encoded by the mammalian Bcl-2 family of anti-apoptotic genes (109). Bcl-2 proteins are able to promote or inhibit apoptosis either by direct action on MAC or indirectly through other proteins. It is important to note that the actions of some Bcl-2 proteins are able to halt apoptosis even if cytochrome c has been released by the mitochondria.

3.3.1.3 Execution

Many pathways and signals lead to apoptosis, but there is only one mechanism that actually causes the death of a cell. After a cell receives stimulus, it undergoes organized degradation of cellular organelles by activated proteolytic caspases. A cell undergoing apoptosis shows a characteristic morphology (Figure 8):

– Cell shrinkage and rounding are shown because of the breakdown of the proteinaceous cytoskeleton by caspases;

– The cytoplasm appears dense, and the organelles appear tightly packed;

– Chromatin undergoes condensation into compact patches against the nuclear envelope in a process known as pyknosis, a hallmark of apoptosis;

– The nuclear envelope becomes discontinuous and the DNA inside is fragmented (karyorrhexis). The nucleus breaks into several discrete chromatin bodies or nucleosomal units due to the degradation of DNA;

– The cell membrane shows irregular blebs;

– The cell breaks apart into apoptotic bodies, which are then phagocytosed.

Apoptosis progresses quickly and its products are quickly removed, making it difficult to detect or visualize. During karyorrhexis, endonuclease activation leaves short DNA fragments, regularly spaced in size.

3.3.1.4 Removal of dead cells

The removal of dead cells by neighboring phagocytic cells has been termed efferocytosis. Dying cells that undergo the final stages of apoptosis display phagocytotic molecules, such as phosphatidylserine, on their cell surface (111). Phosphatidylserine is normally found on the cytosolic surface of the plasma membrane, but is redistributed during apoptosis to the extracellular surface by a hypothetical protein known as scramblase. These molecules mark the cell for phagocytosis by cells possessing the appropriate receptors, such as macrophages (112). Upon recognition, the phagocyte reorganizes its cytoskeleton for engulfment of the cell. The removal of dying cells by phagocytes occurs in an orderly manner without eliciting an inflammatory response.

3.3.2 Autophagy

The word “autophagy,” which is derived from the Greek to eat (“phagy”) oneself (“auto”), was first used for structures that were observed on electron microscopy and that consisted of single- or double-membrane lysosomal-derived vesicles containing cytoplasmic particles, including organelles, in various stages of disintegration. We now understand that autophagy is the process by which cells recycle their own non-essential, redundant, or damaged organelles and macromolecular components (113). It is an adaptive response to sublethal stress, such as nutrient deprivation, that supplies the cell with metabolites it can use for fuel. Autophagy also has a role in the suppression of tumor growth, deletion of toxic misfolded proteins, elimination of intracellular microorganisms, and antigen presentation (114). Electron microscopy is the best way to visualise autophagosomes, the hallmark of autophagy. These structures fuse with lysosomes, where acid hydrolases catabolize the ingested material into metabolic substrates. The typical whorls in autophagic vacuoles are remnants of membranes. A complex set of autophagy-related proteins regulates the formation of autophagosomes (115). Among these is a complex consisting of class III phosphatidylinositol-3-kinase (PI3K) and beclin-1 (BECN1), a member of the BCL2 family with a BH3-only domain. There is additional control by mTOR (the mammalian target of rapamycin), a serine–threonine protein kinase that integrates input from cellular nutrients, growth factors, and cellular redox state to inhibit autophagosome formation (115).

3.3.2.1 Types of autophagy

Three forms of autophagy have been defined on the basis of how lysosomes receive material for degradation (115):

– Macroautophagy (Figure 10) is the sequestration of organelles and long-lived proteins in a double-membrane vesicle, called an autophagosome or autophagic vacuole (AV), inside the cell. Autophagosomes form from the elongation of small membrane structures known as autophagosome pre-

cursors. The formation of autophagosomes is initiated by class III phosphoinositide 3-kinase (PI3K) and autophagy-related gene (Atg) 6 (also known as Beclin-1). In addition, two further systems are involved, composed of the ubiquitin-like protein Atg8 (known as LC3 in mammalian cells) and the Atg4 protease on the one hand and the Atg12-Atg5-Atg16 complex on the other (116). Two proteins, Alfy and P62 (also known as SQSTM1), have been suggested for the targeting of proteins to autophagosomes (117, 118). Alfy has been found in proximity to autophagic membranes and colocalizing with protein aggregates under conditions of starvation and proteasome inhibition, which are known to upregulate macroautophagy (118, 119). Similarly, P62 (SQSTM1) has been found to localize to protein aggregates, is degraded by macroautophagy, and could be coimmunoprecipitated with Atg8 (LC3) (117). Both proteins were suggested to target protein aggregates to autophagosomes, in the case of P62 (SQSTM1) by binding to Atg8 (LC3). The outer membrane of the autophagosome fuses in the cytoplasm with a lysosome to form an autolysosome or autophagolysosome where their contents are degraded via acidic lysosomal hydrolases.

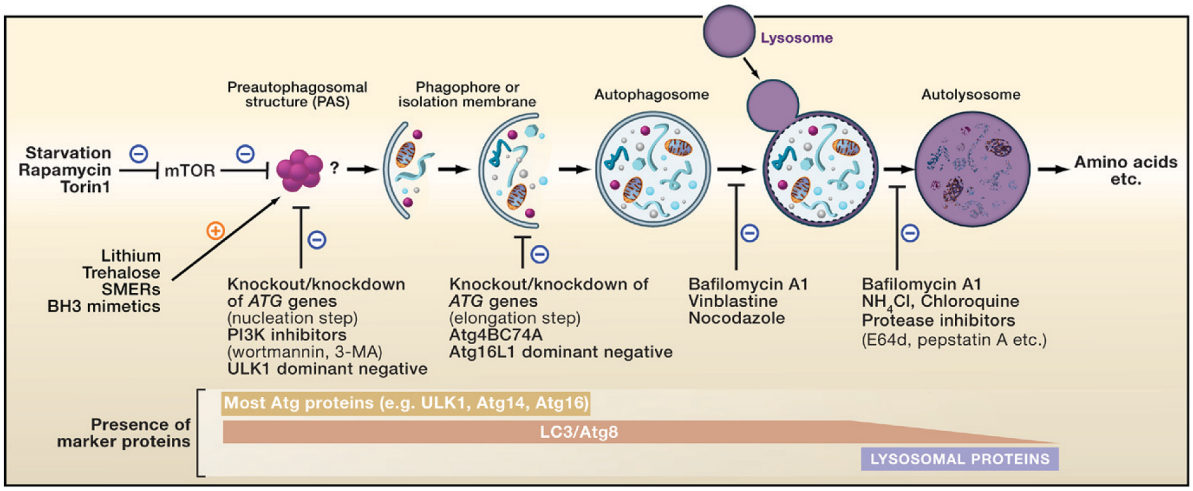

Figure 10: the process of macroautophagy. A portion of cytoplasm, including organelles, is enclosed by a phagophore or isolation membrane to form an autophagosome. The outer membrane of the autophagosome subsequently fuses with the lysosome, and the internal material is degraded in the autolysosome. A partial list of treatments and reagents that modulate autophagy are indicated. Notably, lithium may also inhibit autophagy through mTOR activation. Atg proteins that have thus far been identified on isolation membranes include ULK1/2, Atg5, Beclin 1, LC3, Atg12, Atg13, Atg14, Atg16L1, FIP200, and Atg101.

– Microautophagy, on the other hand, happens when lysosomes directly engulf cytoplasm by invaginating, protrusion, and/or septation of the lysosomal limiting membrane.

– In Chaperone-mediated autophagy, or CMA, only those proteins that have a consensus peptide sequence get recognized by the binding of a hsc70-containing chaperone/co-chaperone complex. This CMA substrate/chaperone complex then moves to the lysosomes, where the CMA receptor lysosome-associated membrane protein type-2A (LAMP-2A) recognizes it; the protein is unfolded and translocated across the lysosome membrane assisted by the lysosomal hsc70 on the other side (120). CMA differs from macroautophagy and microautophagy in what substrates are translo-

cated across the lysosome membrane on a one-by-one basis, whereas in the macroautophagy and microautophagy the substrates are engulfed or sequestered in-bulk and because CMA is very selective in what it degrades and can degrade only certain proteins and not organelles (114, 121).

3.3.2.2 Functions

I. Nutrient starvation

During nutrient starvation, increased levels of autophagy lead to the breakdown of non-vital components and the release of nutrients, ensuring that vital processes can continue (113, 122, 123). Atg7 has been implicated in nutrient-mediated autophagy, as mice studies have shown that in Atg7-deficient mice starvation-induced autophagy was impaired (124) and profound muscle atrophy and age-dependent decrease in force were detectable (125).

II. Infection

Autophagy plays a role in the destruction of some bacteria within the cell. Intracellular pathogens such as Mycobacterium tuberculosis persist within cells and block the normal actions taken by the cell to rid itself of it. Stimulating autophagy in infected cells overcomes the block and helps to rid the cell of pathogens (126). In addition to "simple" breakdown of pathogens, it has also been shown that at least in some cell types (plasmacytoid dendritic cells) autophagy plays a role in detection of virus by the so-called pattern recognition receptors (PRR), which are part of the innate immune system (116).

III. Repair mechanism

Autophagy degrades damaged organelles, cell membranes and proteins, and the failure of autophagy is thought to be one of the main reasons for the accumulation of cell damage and ageing (127).

IV. Programmed cell death

The role of autophagy in cell death is controversial (128). Despite agreement that autophagy is an adaptive response, there is no agreement that unbridled autophagy can deplete organelles and critical proteins to the point of caspase-independent cell death without signs of apoptosis. Although there are numerical increases in autophagosomes in some dying cells, it is unclear whether these structures facilitate cell death or are a feature of a cell that can no longer compensate by sacrificing vital components, a process that has been referred to as autophagy-associated cell death rather

than autophagy-induced cell death. The genetic deletion of key autophagic genes accelerates rather than inhibits cell death, which emphasizes the predominant survival role of autophagy (125).

3.3.3 Necrosis

Necrosis (from the Greek “nekros,” for corpse) is best defined by light or electron microscopic detection of cell and organelle swelling or rupture of surface membranes with spillage of intracellular contents (129). The term “oncosis” (Greek for swelling) is preferred by some investigators, and “oncotic necrosis” has also been used. The compromise of organellar membranes allows proteolytic enzymes to escape from lysosomes, enter the cytosol, and cause cell demolition. Necrosis usually results from metabolic failure that has coincided with rapid depletion of ATP; it classically occurs in ischemia. Necrosis is usually considered an accidental (i.e., nonprogrammed) form of cell death that occurs in response to acute hypoxic or ischemic injury, such as myocardial infarction and stroke. It occurs spontaneously in neoplasms when cell proliferation outpaces angiogenesis. The exposure of cells to supraphysiologic conditions (e.g., mechanical force, heat, cold, and membrane-permeabilizing toxins) also precipitates necrosis (101). Necrosis typically begins with cell swelling, chromatin digestion, disruption of the plasma membrane and organelle membranes (101). Late necrosis is characterized by extensive DNA hydrolysis, vacuolation of the endoplasmic reticulum, organelle breakdown, and cell lysis (129). The release of intracellular content after plasma membrane rupture is the cause of inflammation in necrosis.

3.3.3.1 Causes

There is now evidence that necrosis, traditionally considered an accidental form of cell death, can in certain instances be initiated or modulated by programmed control mechanisms. Cellular necrosis can be induced by a number of external sources, including injury, infection, cancer, infarction, poisons, and inflammation (129). The sudden failure of one part of the cell triggers a cascade of events. In addition to the lack of chemical signals to the immune system, cells undergoing necrosis can release harmful chemicals into the surrounding tissue. In particular, damage to the lysosome membrane can trigger release of the contained enzymes, destroying other parts of the cell. Worse, when these enzymes are released from the non-dead cell, they can trigger a chain reaction of further cell death (101).

3.3.3.2 Mediators of Process

Reactive oxygen species, calcium ions, poly–ADP–ribose polymerase (PARP), calcium-activated non-lysosomal proteases (calpains), and cathepsins mediate necrosis (101). PARP is a DNA-repair enzyme that can deplete cellular ATP stores when it catalyzes the repair of multiple DNA strand breaks that occur in cell injury. In apoptosis, PARP undergoes rapid cleavage and inactivation (de-

tection of cleaved PARP is a diagnostic test for apoptosis), so stores of ATP are preserved. ATP is necessary for numerous effector processes in apoptosis, whereas exhaustion of ATP shifts the cell from apoptosis to necrosis. Increase of intracellular calcium ions, a central feature of necrosis, activates proteases that degrade critical proteins. Intriguingly, the source and amount of increased calcium ions may induce different types of cell death: the influx of calcium ions across the plasma membrane triggers necrosis, whereas the release of calcium ions from the endoplasmic reticulum more readily induces apoptosis (130).

3.3.3.3 Regulation

Accumulating evidence indicates that necrosis is more ordered than was originally thought. When cells die from necrosis, damage-associated molecular-pattern (DAMP) molecules, such as high-mobility group box 1 (HMGB1) protein, enter the circulation and activate innate immune cells (131). Thus, the first cells that die from trauma or infection may function as sentinels, alerting the host to the need for defensive or reparative responses. In addition, necrosis can be initiated by the activation of selected cell-surface receptors. For example, high concentrations of TNF induce hepatocyte necrosis. The identification of an intracellular serpin (protease inhibitor) that prevents necrosis caused by multiple noxious stimuli indicates that necrosis can be regulated, programmed, and driven by a peptidase stress-response pathway (101).

3.3.3.4 Cross-talk between cell-death mechanisms

The type and intensity of noxious signals, ATP concentration, cell type, and other factors determine how cell death occurs (132, 133). The blockade of a particular pathway of cell death may not prevent the destruction of the cell but may instead recruit an alternative path (Figure 11a), i.e. the *Atg7*$^{-/-}$ mice, in which autophagy was inhibited, showed an increased susceptibility to apoptosis (125). In several conditions, autophagy constitutes a stress adaptation that avoids cell death (and de facto suppresses apoptosis) (Figure 11c), whereas in other cellular settings, autophagy constitutes an alternative pathway to cellular demise that is called autophagic cell death (or type II cell death) (Figure 11b). In general terms, it appears that similar stimuli can induce either apoptosis or autophagy. Whereas a mixed phenotype of autophagy and apoptosis can sometimes be detected in response to these common stimuli, in many other instances, autophagy and apoptosis develop in a mutually exclusive manner, perhaps as a result of variable thresholds for both processes, or as a result of a cellular 'decision' between the two responses that may be linked to a mutual inhibition of the two phenomena (132). Cross-inhibitory interactions between apoptosis and autophagy may cause polarization between the two processes. During nutrient deprivation the default pathway would be autophagy, which creates a metabolic state with high (or increased) ATP that is anti-apoptotic. Successful removal of the damaged organelles followed by repair and adaptation would allow for surviv-

al, while failure to restore homeostasis would result in delayed apoptosis. By contrast, the default pathway that is triggered by other signals such as DNA damage or death-receptor activation would be immediate apoptosis, which occurs in a rapid, self-amplifying process, precluding simultaneous autophagic responses (132, 134). Furthermore, cells may be more susceptible to apoptosis if autophagy is inhibited (125) or, on the contrary, undergo autophagy or worse necrosis in presence of apoptosis inhibition (Figure 11d).

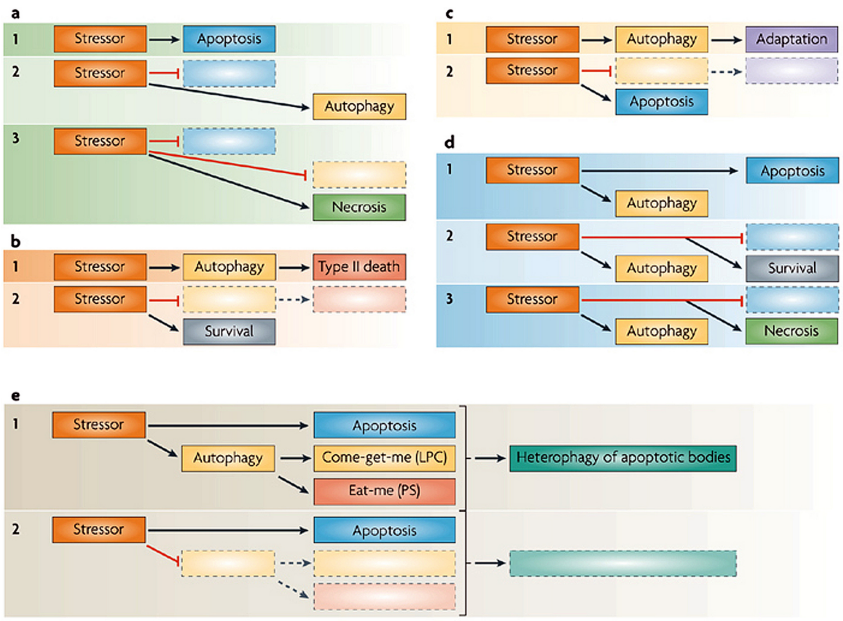

Figure 11: scenarios for the interaction between apoptosis and autophagy. a) A particular set of insults induces apoptosis (part 1), which, if inhibited, can switch to autophagy. At least in some cellular settings, serves as a defence mechanism that prevents or retards necrosis (parts 2,3). b) Some conditions can trigger a lethalautophagic response that is responsible for cell death, for example, in naïve cells (parts 1,2) or in cells in which the apoptotic pathways have been interrupted. c) Another set of stimuli (or perhaps simply a lower dose of insults) provokes a protective autophagic response (part 1), which is required for adaptation of the cell and the avoidance of apoptosis (part 2). d) Frequently, lethal conditions trigger an autophagic response that, independently of the autophagic response, is followed by apoptosis (part 1). In this case, inhibition of apoptosis causes either cell survival (part 2) or necrosis (part 3). In this scenario, the order of events (autophagy, then apoptosis) is chronological, not hierarchical, meaning that inhibition of autophagy does not prevent apoptosis. e) Autophagy can be indispensable for sustaining the high ATP levels that are required for cells to emit signals to phagocytic cells that engulf the apoptotic bodies (part 1). Inhibition of autophagy does not affect apoptotic cell death, yet it abolishes the heterophagic removal of apoptotic material (part 2). LPC, lysophosphatidylcholine; PS, phosphatidylserine.

Nuclear factor κB, ATG5, ATP, and PARP probably function as molecular switches that determine whether a cell undergoes apoptosis, necrosis, or autophagy. Protein p53 also modulates autophagy and other responses to cell stress. Recent work indicates that basal p53 activity suppresses autophagy, whereas the activation of p53 by certain stimuli induces autophagy and the activation of p53 by different stimuli results in the engagement of apoptosis, mediated by PUMA and NOXA.

3.3.3.5 Experimental detection of cell-death

I. Apoptosis and necrosis

During apoptosis cells undergo certain morphological changes which can be detected by electron microscopy. Next to this classic detection method, apoptosis can be detected by different methods/ principles (135) of which important ones are listed below:

- *Annexin V:* this molecule binds phosphatidylserine, a lipid which translocates from the inner to the outer leaflet of the plasma membrane during early stages of apoptosis. Since necrotic cells may have holes in the membrane which cause false positive signals, annexin V is used in conjunction with a DNA binding dye (i.e. propidium iodide) to distinguish apoptotic (single staining) from necrotic (double staining) cells.
- *Caspase activation:* some caspases (i.e. 2, 8, 10) initiate apoptosis, others (i.e. 3, 6, 7) are downstream effectors. Most caspase assays either rely on cleavage of a specific substrate or on the binding of an irreversible inhibitor. Other assays are based on the caspase specific cleavage of target proteins such as PARP or cytokeratin-18. Assays may detect early to late stages of apoptosis.
- *ssDNA:* large stretches of single stranded DNA (ssDNA) occur in heat denatured cells from mid to late stages of apoptosis. The ssDNA can be detected by a specific antibody.
- *Mitochondrial membrane potential:* mitochondrial dysfunction occurs early in apoptosis and is accompanied by a decreased membrane potential. Potential assays test the mitochondria`s ability to concentrate a dye (i.e. TMRM) using its proton gradient.
- *Cytochrome c release:* during apoptosis the outer mitochondrial membrane ruptures while both membranes fail during necrosis. The detection of released cytochrome c is specific for early to late stages of apoptosis if cells to be analyzed kept an intact inner membrane.
- *TUNEL:* at a late stage of apoptosis, caspase-activated endonucleases cause double-stranded DNA breaks. The TUNEL (terminal deoxy-nucleotidyltransferase [TdT] dUTP nick end labelling) assay marks those breakpoints with TdT and tagged (e.g. biotinylated) nucleotides, which are then read using enzyme-tagged or fluorescently labelled antibodies. TUNEL indicates DNA cleavage from any form of cell death and necrotic cells may also be labelled.

II. Autophagy

There are no absolute criteria for determining the autophagic status that apply to every situation. This is because some assays are inappropriate, problematic or may not work at all in particular cells, tissues or organisms. An important point is that autophagy is a dynamic, multi-step process that can be modulated at several steps, both positively and negatively. In this respect, the autophagic path-

way is not different from other cellular pathways. An accumulation of autophagosomes, could, for example, reflect either increased autophagosome formation due to increases in autophagic activity, or to reduced turnover of autophagosomes. In some cases, autophagy-associated cell death is due to reduced autophagic flux, due to the inhibition of the fusion of autophagosomes with lysosomes or to loss of the degradative functions of lysosomes. Therefore, the use of autophagy markers such as LC3-II needs to be complemented by knowledge of overall autophagic flux to permit a correct interpretation of the results (136, 137). Three different strategies can be exploited to detect autophagy induction:

– *Monitoring phagophore and autophagosome formation by steady state methods*: these methods do not allow a determination of whether the process goes to completion. The use of electron microscopy is a valid and important method both for the qualitative and quantitative analysis of changes in various autophagic structures, even if it could be affected by the large potential for sampling artefact. The complex PE (phosphatidylethanolamine)-LC3-II is the only protein marker that is reliably associated with completed autophagosomes, and can be detected by western blotting (distinguishing the inactive LC3-I form and the active lipidated PE-LC3-II form), or by fluorescence microscopy (measured as an increase in punctate LC3 signals). Other experimental strategies could aim to measure the TOR and Atg1 kinase activity, or the transcriptional regulation of certain autophagy related genes.

– *Flux measurements:* autophagy includes not just the increased synthesis or lipidation of Atg8/LC3, or an increase in the formation of autophagosomes, but most importantly flux. Therefore, autophagic substrates need to be monitored to verify that they have reached this organelle, and, when appropriate, degraded. To achieve such informations, radioactive amino acids incorporation can be used to monitor the autophagic protein degradation; the turnover of LC3-II can be estimated by measuring its accumulation following the addition of protease inhibitors or lysosomal blockers. The P62 protein serves as a link between LC3 and ubiquitinated substrates. P62 becomes incorporated into the completed autophagosome and is degraded in autolysosomes. Inhibition of autophagy correlates with increased levels of P62, suggesting that steady state levels of this protein reflect the autophagic status. Autophagic activity can also be monitored by the sequestration of an autophagic cargo from the soluble (cytosol) to the insoluble (sedimentable) cell fraction (which includes autophagic compartments).

– *Other methods warranting special cautions:* acidotropyc dyes such as acridine orange and Lyso Tracker Red can be used to follow autophagy, but they often are not specific for autophagic organelles. Many chemical inhibitors/inducers of autophagy are available, but often they are not entirely specific, and thus it is preferable to analyse specific loss/gain of function *Atg* mutants.

4. Methods

4.1. Clinical data

After informed consent, biopsies of vastus lateralis were obtained from five healthy donors (2 females and 3 males, age range 2-55 years), and from eight unrelated DM1-patients [3 E2 < 450 $(CTG)_n$, 3 E3 >1000 $(CTG)_n$ and 2 congenital E4]. DM1 patients were diagnosed at the Department of Neurology, University of Padua, Italy (Table 6). The diagnosis of DM was based on clinical, electromyographic (high frequency repetitive discharges), ophthalmologic and cardiac investigations. The degree of muscle impairment was assessed using muscular disability grading (Muscular Disability Rating Scale, MDRS), based on a five-point scale as previously described (138): grade 1, no clinical impairment; grade 2, minimal signs of clinical impairment; grade 3, distal weakness; grade 4, mild or moderate proximal weakness; grade 5, severe proximal weakness (confined to wheelchair for short or long distances). In addition to MDRS rating of muscle impairment, we also assessed cognitive impairment, cataract, cardiac involvement, endocrine dysfunctions and motor impairment (Table 6).

Table 6: clinical information of studied DM1 patients

Patient	Sex	Onset/Age at biopsy	MDRS	Cardiac involvement		Serum CK (IU/L)	Cataract	$(CTG)_n$ in blood
				CD	CM			
E2₁	M	25/ 49	3	LAH	none	236	cataract	160
E2₂	F	33/33	0	none	none	114	none	450
E2₃	F	37/ 39	1	none	ND	224	none	90-200
E3₁	M	11/55	3	PM	FHK	normal	ND	1800
E3₂	F	4/29	3	none	none	618	none	1300
E3₃	M	3/15	2	LAH	none	874	initial	1450
E4₁	M	0/15 days	3	none	none	-	none	1600
E4₂	M	0/14	4	none	none	ND	ND	1700

CD, cardiac conduction; CM, cardiac morphology; FHK, focal hypokinesis; LAH, left anterior hemiblock; ND, not done; PM, pacemaker.

4.2. Cell cultures

Primary myoblasts were obtained as previously described (83). Cells were cultured with Ham's F14 medium (Euroclone) plus 20% FBS (Gibco) and 10 µg/mL insulin (Sigma). When a 70% confluence was reached, differentiation was triggered by lowering FBS to 2%. Samples were collected at 0, 4, 10 and 15 days of differentiation using techniques specific to the various different analyses. Z-VAD-FMK 50 µM (ALEXIS Biochemicals) treatment was performed for 5 days (from 10 to 15 days of differentiation), with daily change of medium.

Functional innervation was obtained by co-culturing differentiating myoblasts with13-day-old Sprangue-Dawley rat embryo spinal cord maintaining dorsal root ganglia, as previously described (9, 83).

4.3. Morphological analysis and immunofluorescence

Bright-field images of myotubes were collected using a Zeiss IM35 microscope equipped with a standard camera. Differentiation was quantified considering the average number of nuclei per myotube in 100X images of at least 100 myotubes for each cell line. Myotubes average width at 10 and 15 days of differentiation was measured using ImageJ software. For each parameter, at least 100 myotubes per class were considered. Similar parameters were measured in a separate set of experiments with and without Z-VAD treatment: 100 and 50 myotubes from untreated-treated controls and DM1, respectively, were considered. Immunofluorescence was performed in fixed myotubes, permeabilized with 0.2% Triton X-100 and incubated for 30 min with 0.5% BSA and 10% horse serum in PBS. Primary specific antibodies were diluted in PBS plus 2% BSA and incubated for 1 hour at room temperature (slow Myosin Heavy Chain (MHC), diluted 1:400, gift from Prof. Schiaffino) or overnight at 4°C (LC3, diluted 1:100, Cell Signaling). Secondary Alexa488 or Cy3-conjugated antibodies (Invitrogen-Molecular Probes) were incubated for 1 hour. Samples, mounted in Vectashield mounting medium with DAPI (4'-6-diamidino-2-phenylindole) (Vector Laboratories), were observed with an Olympus BX60 fluorescence microscope (20X magnification). Quantitative analysis of at least 30 LC3 stained myotubes per sample was performed using commercial software by creating specific regions of interest (ROIs) corresponding to single myotubes, and counting the amount of LC3-positive vesicles. Data were expressed as number of LC3-positive vesicles/μm^2.

4.4. RNA fluorescence in situ hybridization (RNA-FISH)

Myoblasts and 4-, 10-, 15-day myotubes grown on coverslips were fixed in 4% paraformaldehyde, 10% acetic acid in PBS for 15 min at 4°C and permeabilized in 0.2% Triton X-100 in PBS for 5 min at room temperature. RNA-FISH was performed as described (31). Samples were pre-hybridized

with 2X SSC (300 mM NaCl, 30 mM sodium citrate, pH7)/50% formamide and hybridized at 37°C for 4 hours in a moist dark chamber with 30 ng/ml TxRed-$(CAG)_{10}$ oligonucleotide probe in 40% formamide, 10% dextran sulfate in 2X SSC. Stained myotubes were washed twice in 2X SSC for 10 min RT, then mounted in Vectashield (Vector) with 0.1 mg/ml DAPI (4'-6-diamidino-2-phenylindole) (Vector, Laboratories, Inc, Burlingame, California, USA) and observed with Leica TCSP5 confocal microscope collecting 10 µm z-stacks.

4.5. Molecular analysis of $(CTG)_n$ expansion

Genomic DNA was extracted from blood, muscle tissue and muscle cells at 0, 4, 10 days of differentiation using a salting-out procedure (139). $(CTG)_n$ repeat expansion sizes were determined by a combination of long-PCR method developed by Bonifazi et al. (140) and Southern blot analysis. Expanded fragments were sized by measuring the bands of highest intensity, presumably corresponding to the most representative alleles.

4.6. RNA analysis

Total RNA was isolated from myoblasts and 4- and 10-days myotubes using Trizol® reagent (Sigma). 1 µg of total RNA was reverse-transcribed to cDNA using the SuperScript® III First-Strand Synthesis System for RT-PCR (Invitrogen). The expression levels of *CK-M* (muscle specific creatine kinase) and *MYOG* (myogenin) genes, compared to the expression of the housekeeping gene β*2-microglobulin*, were measured by Sybrgreen RT-PCR with ABI PRISM7000 sequence detection system. The following specific primers were used: *CK-M*, F, 5'-CAAGGAACTCTTTGACCCCA-3', R, 5'-CCACAGAGAGCTTCTCCACC-3', *myogenin*, F, 5'-AAGAGAAGCACCCTGCTCAA-3', R, 5'-CAGATGATCCCCTGGGTTG-3', β*2-microglobulin*, F 5'-ATGAGTATGCCTGCCGTGTGA-3', R, 5'-GGCATCTTCAAACCTCCATG-3'. *Atrogin* (Hs00369709_m1) and *Murf1* (Hs00822397_m1) gene expression was determined by a multiplex TaqMan QRT-PCR reaction using a VIC™ labeled human β-*actin* (Hs99999903_m1) specific probe as housekeeping. Genes of interest were all FAM™ labeled. The PCR splicing assays for *IR* and *MBNL1* genes were performed as previously described (31). Total PCR products, obtained within the linear range of amplification, were electrophoresed on 3.5% agarose gel. Quantitative analysis of the amplified products was performed using ethidium bromide staining. The integrated optical density of each band and the fraction of fetal transcript vs. total transcript were quantified by densitometry using commercial software.

4.7. ROS production assay

The rate of H_2O_2 production in living cells was determined using the oxidation in the extracellular medium of 20 mM fluorogenic indicator Amplex red in the presence of 1 unit/ml horseradish peroxidase (POD) and was expressed as A.U./min/mg prot. 30,000 myoblasts were seeded in triplicate in 12-well culture plates and differentiated. The assay was conducted with 4-, 10- and 15-day myotubes. Fluorescence was recorded on a microplate reader (Ascent Fluoroscan FL2.5 – Labsystem) (Ex: 530 nm; Em: 585 nm), in presence of 10 mM apocynin (40-hydroxy-30-methoxyacetophenone) in order to inhibit H_2O_2 production by plasma membrane NADPH-oxidase.

4.8. TUNEL and cytochrome c release detection

Apoptosis in 0-, 4-, 10- and 15-day myotubes was performed using the terminal deoxynucleotidyltransferase-mediated dUTP nick end labeling (TUNEL) method. DNA fragmentation by endogenous endonucleases is a key feature of programmed cell death and also occurs in certain stages of necrosis. The terminal deoxynucleotidyl transferase-mediated dUTP nick-end labeling (TUNEL) method is characterized by higher sensitivity than most other cyto(histo)chemical approaches and has long been considered to be the gold standard to detect apoptosis in situ. However, TUNEL false positivity may result from necrotic cell death (at least in some cases), as well as from inappropriate processing of samples, which may occur – for example – during sectioning (135). Cells were fixed in 4% formaldehyde, permeabilized with 0.2% Triton X-100 and processed for TUNEL analysis (TUNEL System - Promega). Visualization of all nuclei was performed with Vectashield mounting medium with 0.1 µg/ml DAPI.

Cytochrome c release from mitochondria occurs in response to pro-apoptotic stimuli. This release of cytochrome c in turn activates caspase 9, a cysteine protease. Caspase 9 can then go on to activate caspase 3 and caspase 7, which are responsible for destroying the cell from within. The release of cyt-c can be studied by immunofluorescence methods, measuring its colocalization with mitochondria, usually marked with specific antibodies such as anti-TOM20. Cytochrome c/TOM20 colocalization was performed on 15-day differentiated myotubes using a balanced mix of anti-cytochrome c (BD Pharmingen, diluted 1:100) and anti-TOM20 (Santa Cruz, diluted 1:200) antibodies. At least 10 myotubes per cell line were analyzed using Leica TCSP5 confocal microscope and the correlation parameter R was calculated using ImageJ software.

4.9. Western blotting

Myotubes were collected after 10 and 15 days of differentiation. For muscle samples, 10 µm cryosections were used. Total protein extracts were prepared as previously described (141) and electrophoresed in 7.5-17.5% T30C4 SDS-PAGE gels or 4-12% NuPAGE precast gels (Invitrogen). Proteins

were blotted into nitrocellulose membrane or 0.45 μm PVDF (Invitrogen) and probed with specific antibodies against myogenin (diluted 1:500, Hybridoma bank), P-AKT (Ser473) (diluted 1:1000, Cell Signaling), total AKT (diluted 1:1000, Cell Signaling), cleaved caspase 3 (diluted 1:1000, Cell Signaling), P62 (diluted 1:6000, Progen), LC3 (diluted 1:400, NanoTools). After incubation with specific secondary HRP-conjugated antibodies, recognized bands were visualized by chemiluminescence (GE HealthCare). Integrated optical density of each band was calculated with commercial software and normalized compared to actin amounts.

4.10. Statistical analysis

Statistical analysis was performed only where 3 or more experimental values were available. Quantitative data were presented as means ± SE. In the case of normal distribution of values, confirmed by Shapiro's test, statistical comparisons were performed using the Student's t test. With non-Gaussian distributions, non-parametric Kruskal-Wallis and Wilcoxon tests were applied. TUNEL data were analyzed with the non-parametric two way ANOVA test. In every analysis values of $P<0.05$ were considered significant.

5. Results

5.1. Differentiation of DM1 myoblasts is normal

Morphological, molecular and immunological analysis were performed during the first 15 days of differentiation in primary skeletal muscle cell culture lines derived from eight DM1 patients (six adult-onset DM1, two cDM1 - Table 6, page 47), with blood $(CTG)_n$ repeats within the DMPK gene ranging from 90-1800 and from five age-matched controls. Muscle terminal differentiation was induced by a shift to a medium containing a low concentration of mitogens. Normal and DM1 cells grew at the same rate and went through the same number (2-7) of passages, to exclude the effect of age-in-culture on the expression of myogenic factors. Since our culture procedure established a mixture of fibroblasts and myoblasts, in all the cell lines the percentage of desmin-positive myoblast population was calculated and found to exceed 80%. In fact, the expression of desmin is peculiar of myoblasts, while it is not present in fibroblasts. To compare the myogenic capacity of myoblasts from normal and DM1 patients we examined morphological aspects (Figure 12) at 4 and 10 days of differentiation (stages T4 and T10). A representative set of images in Figure 12A shows that the differentiation capacity was unaffected by the presence of the $(CTG)_n$ expansion. Slow myosin heavy chain (MHC), is a contractile protein expressed in adult skeletal muscle and can be used as a marker of myogenic differentiation. MHC detection was performed by immunofluorescence in all the control and pathological cell lines. Ribonuclear foci detection (arrows in Figure 12B) by FISH proved the pathological origin of analysed myotubes in DM1 samples.

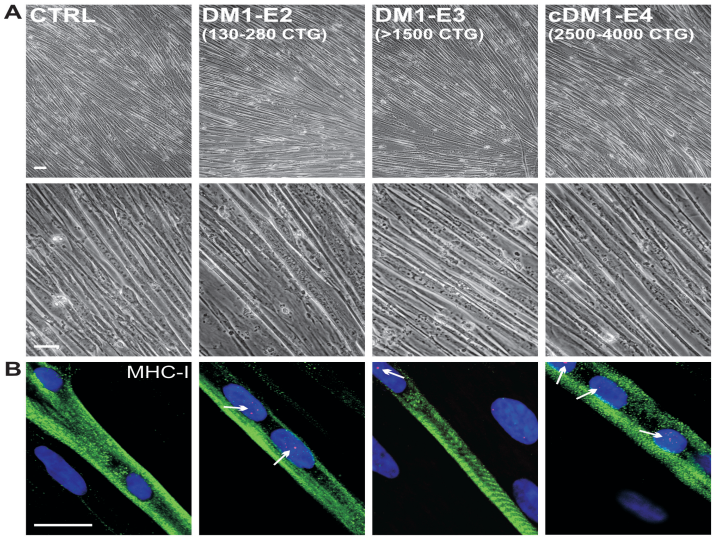

Figure 12: normal myogenic potential of DM1 myoblasts - morphological analysis. (A) Representative pictures of 10-day-differentiated myotubes from control and DM1 patients. DM1 lines generated multinucleated myotubes similar to controls. Expansion (CTG)n range in myotubes : DM1-E2: 130-280; DM1-E3: > 1500, cDM1-E4: congenital form, 2500-4000. Scale bars 30 µm. (B) No differences of slow-MHC expression were detected in fixed 10-day-differentiated myotubes from control and DM1 patients. Nuclear *DMPK* mRNA foci (arrows) were labeled by $(CAG)_{10}$ probe fluorescence *in situ* hybridization. Sarcomeric organization is well defined in DM1 myotubes. Scale bar 25 µm.

The levels of myogenin were estimated by a combination of RT-PCR and Western assays (Figures 13A, B_1 and B_2) while the level of muscle-specific creatine kinase (CK-M) was quantified by RT-PCR (Figure 13C). We found that in the T4- and T10-differentiated DM1 myotubes, all the tested parameters were similar to controls.

All the DM1 cell lines were then subjected to fusion assays. Again, the myogenic potential, expressed as number of syncytial nuclei per myotube, was similar to controls (Figure 13D).

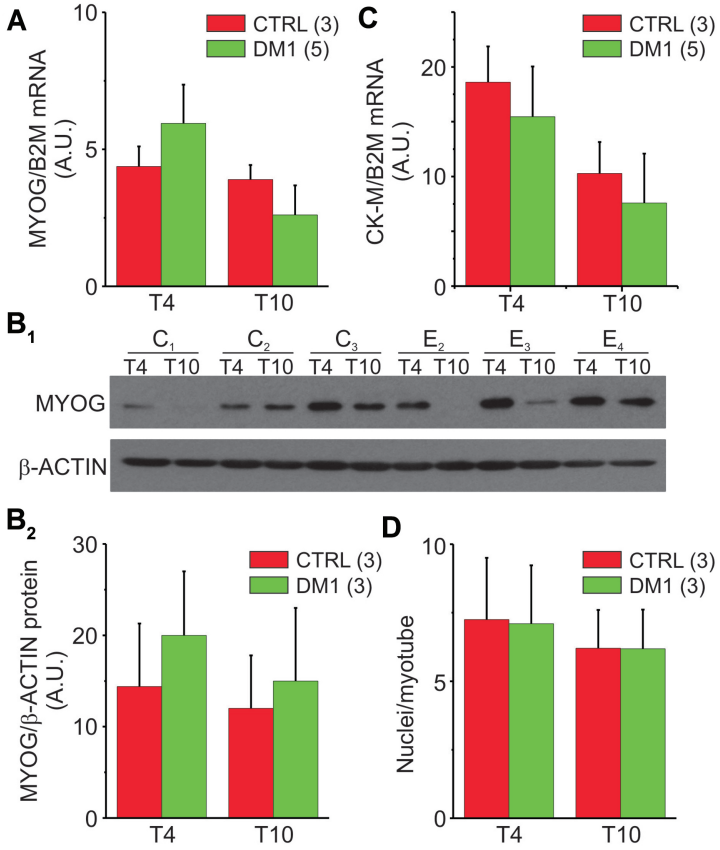

Figure 13: normal myogenic potential of DM1 myoblasts - molecular markers. (A-B) In 4- to 10-day-differentiated myotubes (T4-T10) from five DM1 and three controls, the RNA (A) and the protein presence (B_1-B_2) of myogenin were similar. DM1-$E2_1$, DM1-$E3_2$, and cDM1-$E4_1$ patients were tested in myogenin blot. The values of myogenin mRNA and protein amount are given as arbitrary units (AU) of ratio with β_2-microglobulin housekeeping gene or with β-actin, respectively. The data are expressed as mean ± SE of three different experiments of RT-PCR (carried out in triplicate) and a single WB analysis. (C) Analogous expression levels of muscle specific creatine kinase (CK-M) in T4-T10 myotubes from five DM1 and three control subjects. The values of CK-M mRNA are given in arbitrary units (AU) of ratio with β_2-microglobulin housekeeping gene. The data are expressed as mean ± SE of three different experiments of RT-PCR done in triplicate (D) Similar average number of syncytial nuclei in T4-T10 of three DM1 and three control myotubes, expressed as mean ± SE. The analysis was performed on at least 100 myotubes for each line.

Moreover, to check the maturation capacity of DM1 muscle cells, primary DM1 myotubes were innervated with sections of rat embryo spinal cord. This kind of procedure allows further muscle maturation to be achieved, thanks to the diffusion of axons from the gangliar roots (9, 83). All the innervated DM1 myotubes acquired the ability to depolarise and contract as controls (Figure 14). Taken

together these data suggest that our DM1 human primary myoblasts did not present any impairment in the early steps of myogenesis, behaving as controls until 10 days of differentiation.

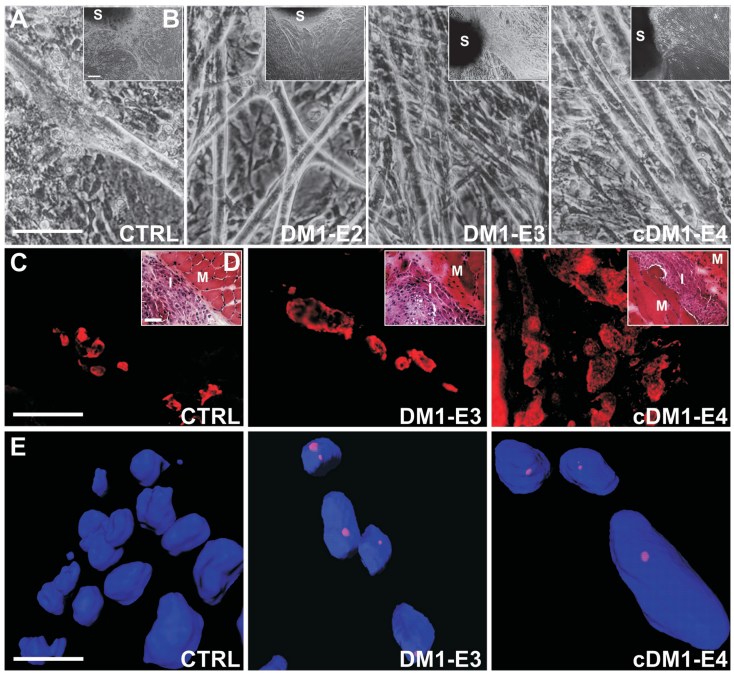

Figure 14: innervated DM1 myotubes. (A-B) Representative bright field images of innervated myotubes from control and DM1 patients. (A) high magnification. Scale bar 100 µm; (B) low magnification, showing the piece of rat spinal cord. S=Spinal cord (Scale bar 100 µm; (C) Representative images of positive immunohistochemical staining anti fetal myosin of transverse sections of innervated myotubes from control and DM1 patients, showing a normal maturation in all samples. (D) Hematoxilin eosin staining of myotubes, collected and included between two mouse muscle sections. The obtained sandwich was frozen and cut into 10 µm sections suitable for the analysis. M= mouse muscle; I= innervated human myotubes. Scale bar 100 µm; (E) Three-dimensional representative FISH images of innervated myotubes from control and DM1 patients with foci. Scale bar 10 µm.

5.2. Pathological hallmarks in DM1 muscle cells

To exclude the possible selection of healthy differentiating cells, our cultured DM1 myotubes were characterised for the presence of the main molecular hallmarks of the DM1 disease:

– the $(CTG)_n$ expansion

– the presence of ribonucleic foci

– the splicing misregulation of two genes representative of the DM1 spliceopathy, the insulin receptor (IR) and muscleblind-like 1 (MBNL1).

5.2.1 The $(CTG)_n$ expansion

$(CTG)_n$ expansion, monitored by long-PCR, was held stable throughout differentiation in each DM1 line and was similar to or even higher than that found in the parental adult muscle (Fig. 2A).

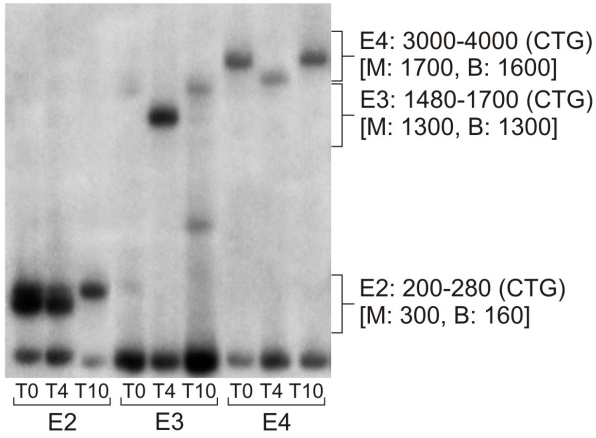

Figure 15: $(CTG)_n$ expansion analysis in DM1 cells during differentiation. Abnormal $(CTG)_n$ expansion was detected in undifferentiated (T0), T4 and T10 DM1-E2, -E3 and -E4 myotubes by long PCR technique. The $(CTG)_n$ repeats were maintained constant throughout the DM1 muscle culture. In brackets: the $(CTG)_n$ expansion present in the corresponding adult muscle (M) and blood (B) of the same patient.

5.2.2 Nuclear foci

In all DM1 myotubes, expanded DMPK transcripts accumulating in the nucleus together with nuclear proteins with affinity for the expanded CUG sequence, generated aggregates easily detectable by FISH (20), confirming the presence of DMPK pathological transcripts in all the studied muscle cells. The same ribonucleic aggregates were detected in the corresponding frozen muscle section of patients from which cells derived (Figure 16).

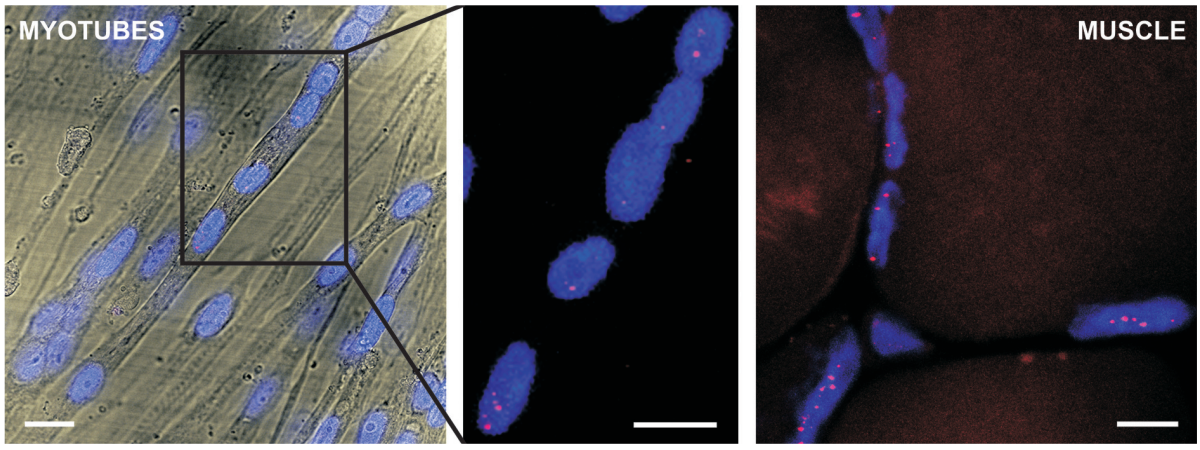

Figure 16: representative images of nuclear foci detection in DM1 fixed myotubes or muscle sections, obtained by FISH with a TexasRed labeled $(CAG)_{10}$ probe. All DM1 cells showed the presence of nuclear foci. Scale bar 25 µm.

5.2.3 Splicing alterations

Abnormal regulation of alternative splicing of various genes, including insulin receptor and MBNL1 (IR-A and MBNL1ex7 being their foetal isoforms), prevail in affected adult DM1 muscle in relation to the $(CTG)_n$ expansion (31). It has been associated with the development of classical symptoms of DM1 such as insulin resistance and muscle wasting. However, a strong correlation is not always present between the symptoms and the molecular defects they should belong to; in fact the patients considered for this study did not suffer from diabetes even if a clear insulin receptor splicing unbalance was present. To assess the in trans effect of the CUG repetition on the splicing regulation in DM1 differentiating myoblasts, we analysed the expression of IR and MBNL1 gene isoforms at different times of differentiation (stages T0, T4 and T10) and compared it with the patterns of the corresponding patients (M). RT-PCR amplification showed that in DM1 cells the ratios of the IR-A/TOT (Figure 17A) and MBNLex7/TOT (Figure 17B) increased in correlation with the $(CTG)_n$ length and were significantly higher compared to controls especially in the E3 (IR-A $p<0.05$, MBNL1 $p<0.01$) and E4 samples (IR-A $p<0.01$; MBNL1 $p<0.001$). Differentiation progress did not influence the unbalance of splicing, which maintained constant during the maturation into myotubes.

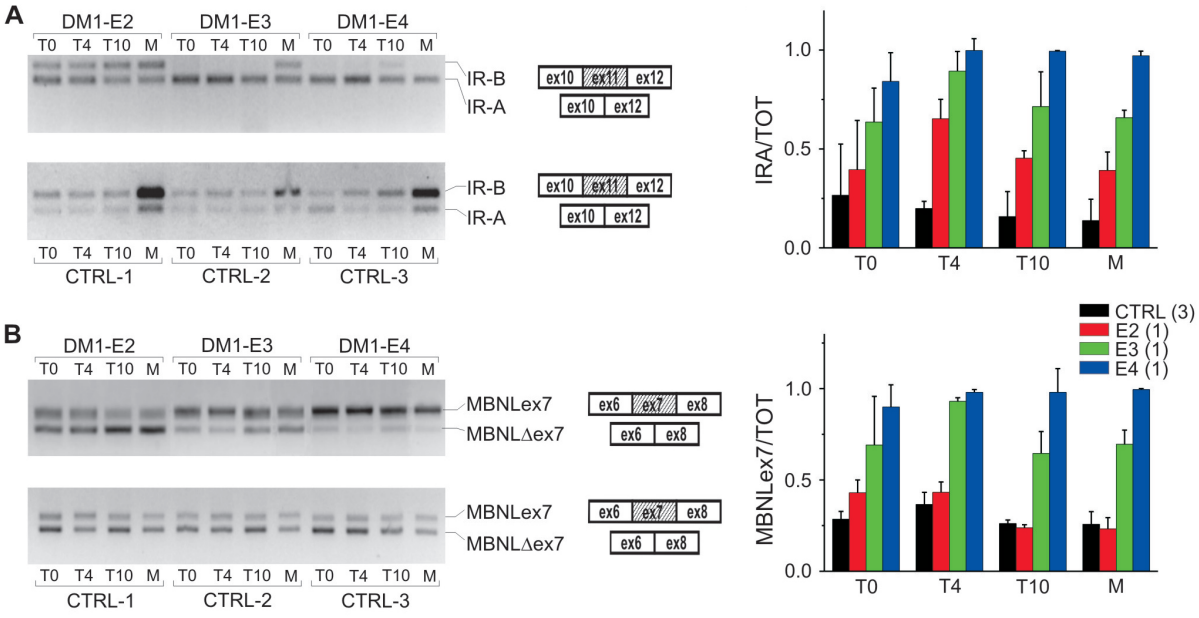

Figure 17: panels showing the RT-PCR splicing assay of *IR* (A) and *MBNL1* (B) in T0-T4-T10 DM1-$E2_1$, -$E3_2$, and -$E4_1$ and three normal myotubes and in the corresponding parental muscle biopsies. Exons analyzed for each gene are shown. The diagrams represent the ratio of aberrant isoform to total transcript in DM1 and control samples given as median values.

5.3. Catabolic pathways in DM1 muscle cells

These results were accompanied by the observation that DM1 myotube population drastically decreased after 12-15 days of differentiation compared to controls (Figure 18A), and that average width of DM1 myotubes with $(CTG)_n$ expansion was statistically reduced by 30% compared to controls ($p<0.01$) (Figure 18C). Several studies demonstrated that muscle atrophy is accompanied by a reduction in mean number of myonuclei per fibre. Consistently, we found a statistically significant reduction in the number of nuclei/myotube in DM1 lines, by 16% compared to controls (Figure 18B) (142). Together, these results suggested the activation of catabolic pathways in our muscle cells of DM1 patients.

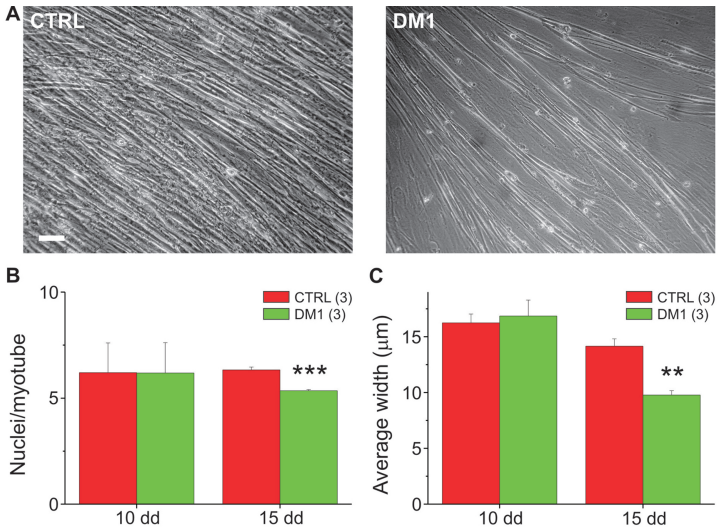

Figure 18: reduction of DM1 myotube population after 15 days of differentiation.(A) Representative bright field images of control and cDM1-$E4_1$ myotube population after 15 days of differentiation. Scale bar 100 µm. (B) Average number of nuclei per myotube at 10-15 days of differentiation. The nuclei/myotubes values were obtained considering at least 100 myotubes/cell line and are expressed as mean±SE. In 15-day-old DM1 myotubes, the syncytial nuclei number was significantly reduced compared to controls (*** $p<0.001$). (C) Average myotube width (AMW), measured in at least 100 myotubes/cell line with commercial software, is expressed as mean ± SE. Pathological lines after 15 days of differentiation shown a significant decreased AMW (**$p<0.01$). Analisys was carried out on DM1-$E2_1$, DM1-$E3_2$, and cDM1-$E4_1$ patients and three controls.

To characterise the signalling involved in DM1 myotubes loss, we investigated:

i. the expression of atrophy-related genes;

ii. the presence of oxidative stress;

iii. the activation of apoptotic systems;

iv. the activation of autophagic systems.

Expression of Atrogin1 and Murf1, the two critical atrophy-related muscle-specific ubiquitin-ligases, did not differ from controls (Figure 19). This finding suggests a minor contribution, at this time point, of ubiquitin-proteasome system to myotube loss.

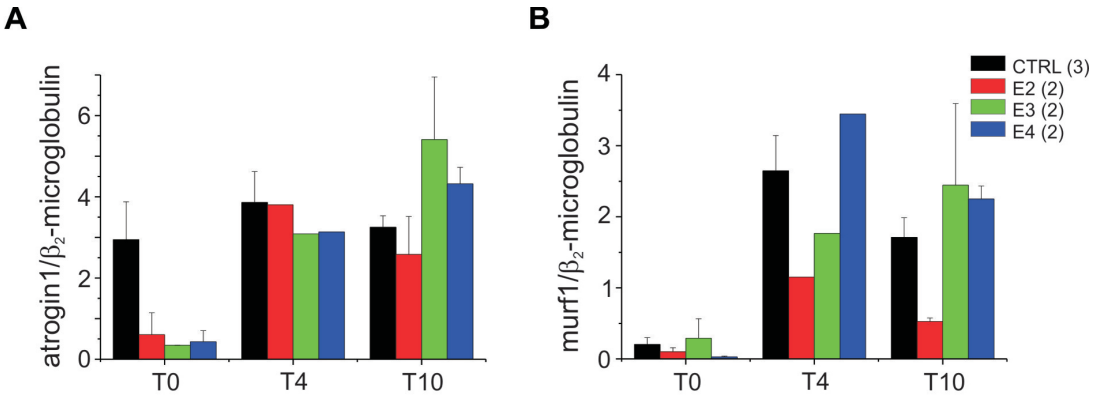

Figure 19: RT-PCR quantification of the expression of atrophy-related genes atrogin1 (A) and murf1 (B) was performed with undifferentiated (T0) and T4, T10 differentiated cultures. No significant differences were detected between control and DM1.

ROS production, tested in myotubes from 4 to 15 days of differentiation, did not show noticeable differences compared to controls at 4-10 days of differentiation (Figure 20). However, 15-day-differentiated DM1-E2 and cDM1-E4 myotubes significantly produced more H_2O_2 than controls. This finding suggests that dysfunctional mitochondria or conditions that generate ROS persist in DM1-E2 and E4 myotubes and can therefore contribute to myotube wasting.

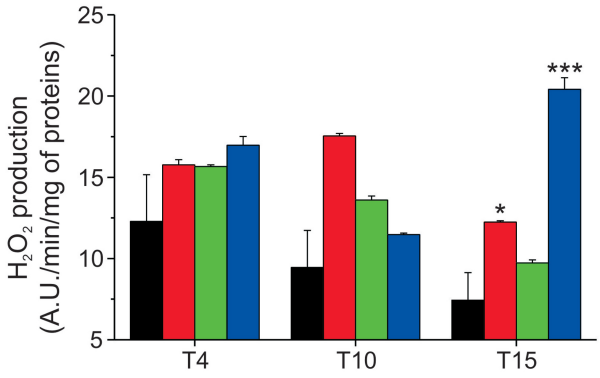

Figure 20: H_2O_2 release by 4 to 15-day-differentiated DM1 myotubes. The H_2O_2 release in the culture medium by differentiated myotubes was measured by Amplex red method. ROS production was found to be increased in apoptotic. DM1-$E2_1$, and cDM1-$E4_1$ myotubes compared to three controls. The values, expressed as arbitrary units/minute/mg of proteins (AU/min/mg), are the mean ± SE of two experiments in triplicate (*$p<0.05$; ***$p<0.001$).

We next monitored the presence of apoptosis by studying chromatin fragmentation by TUNEL, release of cytochrome c from mitochondria and caspase-3 cleavage (Figure 21). All these approaches confirmed a higher amount of apoptosis in DM1 myotubes when compared to controls. Especially TUNEL assay revealed a constant elevated presence of apoptotic nuclei in all DM1 myotubes during the differentiation: in particular T10-T15 DM1-$E2_1$, -$E2_2$ and cDM1-$E4_1$, -$E4_2$ samples had approxim-

ately 10-15 times more apoptotic myonuclei than control samples (Figure 21A_1-A_2). Consistently, cytochrome c release (Figure 21B_1-B_2) and activation of caspase-3 (Figure 21C_1-C_2) were clearly increased in myotubes from the same lines of DM1-E2 and E4, while DM1-E3 lines showed reduced apoptotic values which were, however, higher than controls. Interestingly pAKT, a pro-survival factor, is increased by 50% only in DM1-E3 cells but not in DM1-E2 and cDM1-E4 lines (Figure 21D_1-D_2) (143).

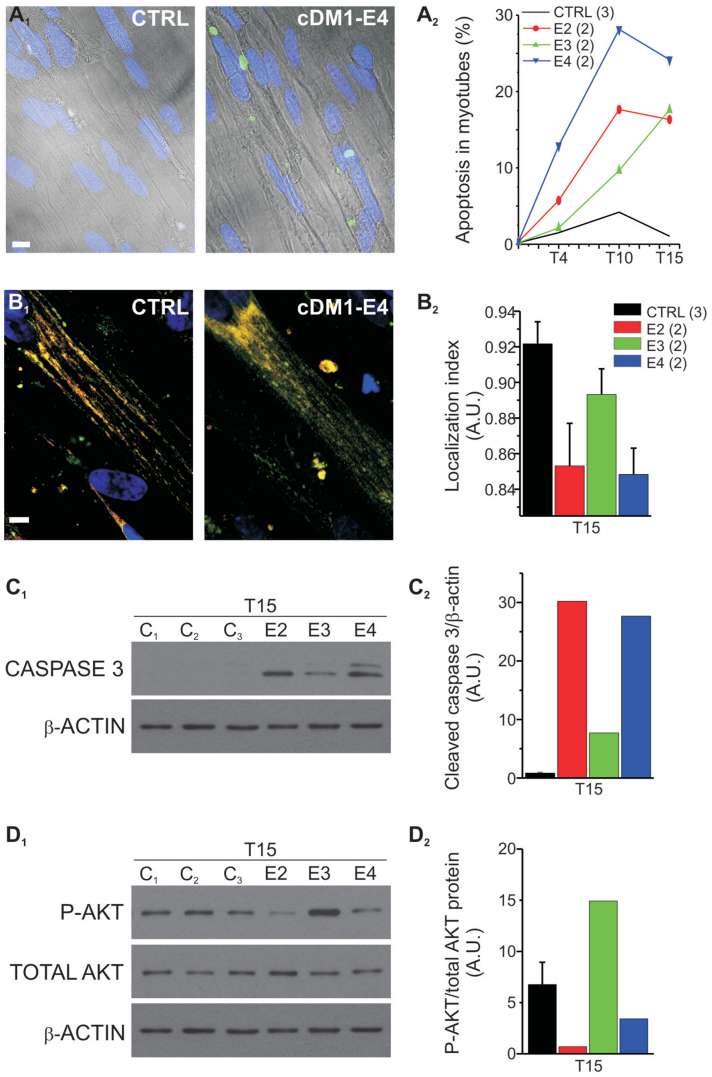

Figure 21: (A_1) Representative images of TUNEL reaction in normal and cDM1- $E4_2$ myotubes. Scale bar 20 μm. (A_2) Undifferentiated (T0), T4, T10 and T15 DM1-$E2_1$, -$E2_2$, -$E3_2$, -$E3_3$ and cDM1-$E4_1$, -$E4_2$ and three control myotubes were scored for apoptotic nuclei positive to TUNEL staining. The data are expressed as percentage of TUNEL-positive nuclei-apoptotic myotubes to total myotubes, counted in ca 150 myotubes/cell line. Frequency of apoptosis in pathological myotubes was found to be significantly increased compare to control for $p<0.001$ by non-parametric two-way ANOVA analysis. (B_1) Representative images of cytochrome c release in cDM1-$E4_2$. (B_2) Localization index of cytochrome c in fixed myotubes from the same control and DM1 patient lines. During apoptosis cytochrome c leaks from mitochondria to cytosol. The colocalization of cytochrome c stain (green) and mitochondrial marker TOM 20 (red) was near one in normal myotubes and significantly decreased in DM1-E2, -E4 myotubes ($p<0.05$) but not in DM1-E3 lines. Values were obtained in 10 myotubes/cell line. (Scale bars 10 μm). (C_1) Western blot analysis for activated caspase-3 proved positive only in pathological DM1-$E2_1$, -$E3_2$ and -$E4_1$ myotubes, not in normal myotubes. (C_2) The diagram represents the values of activated caspase-3 compare to a β-actin, obtained by integrated optical density quantification. (D_1) Western blot analysis for pAKT and AKT in 15-day-differentiated DM1-$E2_1$, -$E3_2$ and -$E4_1$ and three control myotubes. (D_2) pAKT amount given as ratio to total AKT.

To establish the relevance of apoptotic process, 10-day DM1 myotubes were treated for 5 days with 50 µM Z-VAD, a pancaspase inhibitor. Members of the caspase gene family (cysteine proteases with aspartate specificity) exhibit catalytic and substrate-recognition motifs that have been highly conserved (144). These characteristic amino acid sequences allow caspases to interact with both positive and negative regulators of their activity and have been exploited for the development of peptides that successfully compete for caspase binding. It is possible to generate reversible or irreversible inhibitors of caspase activation by coupling caspase-specific peptides to certain aldehyde, nitrile or ketone compounds. Fluoromethyl ketone (FMK)-derivatized peptides act as effective irreversible inhibitors with no added cytotoxic effects. The treatment produced a visual decrease of atrophic DM1 myotubes (Figure 22A), a significant 23% increase in number of myonuclei (Figure 22B) and a 26% rise of average myotube width (AMW) (Figure 22C) in DM1-E2 and DM1-E4 myotubes compared to the untreated. Overall, these data provided evidence that apoptosis actively contributed to the observed catabolic pathways.

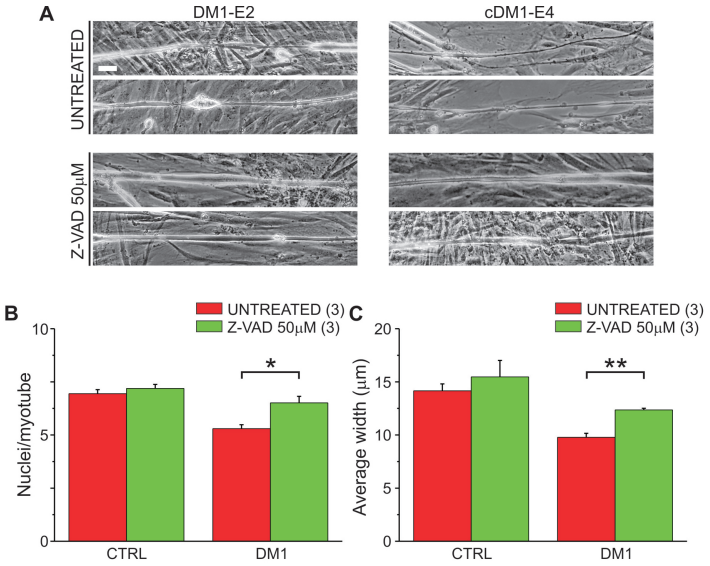

Figure 22: Z-VAD treatment in 10- to 15-day-differentiated DM1 myotubes.The pancaspase inhibitor Z-VAD caused a visual impression of increased trophicity in the DM1-treated myotubes. (A) Representative images of DM1-$E2_1$ and $E4_2$ myotubes with and without Z-VAD treatment. Scale bar 25 µm. A consistent, statistically significant increase was found in: (B) Myonuclei (*$p<0.02$); (C) AMW (**$p<0.01$) in DM1-treated myotubes compared with the untreated. The number of single lines studied is given in brackets.

The alter ego of apoptosis is the autophagic system, which is the vehicle for delivering proteins and organelles to the lysosome (114). The modern view considers autophagy as a pro-survival system that keeps the cell clear of toxic proteins and damaged organelles. However, excessive autophagy contributes to protein breakdown and muscle atrophy in skeletal muscle (145, 146) and to cell death in mononucleated cells. In view of this relationship with apoptosis and muscle loss, we studied the level of autophagy activation in control and DM1 myotubes. LC3-positive vesicles, a marker of activ-

ated autophagy (114), were significantly increased in DM1-E2, -E3 and -E4 myotubes at T15 compared to controls; the quantification is represented in the graph as number of LC3-positive vesicles/ μm^2 (Figures 23A_1-A_2). Instead, P62 showed no substantial changes among the various groups (Figures 23B_1-B_2). It is interesting to note that the DM1-E3 lines (which showed the lowest levels of apoptosis -Figure 21- and no ROS production -Figure 20) present the highest levels of autophagy, giving rise to a similar apoptosis effect, i.e. degeneration of 15-day myotubes.

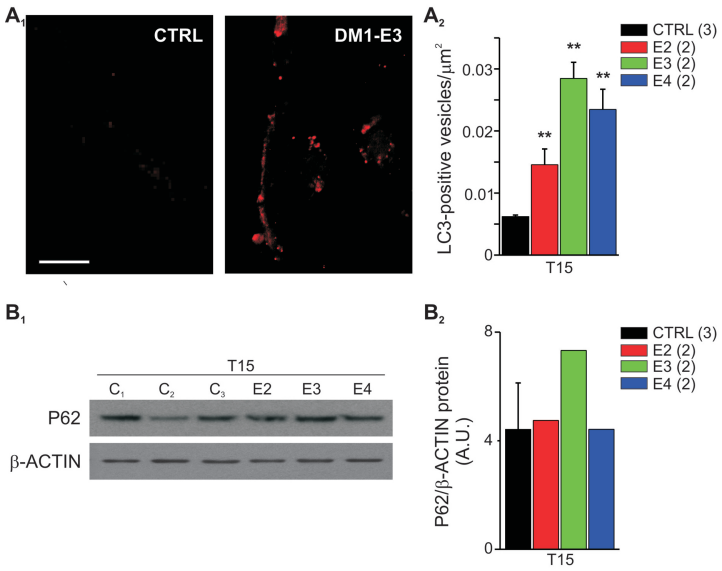

Figure 23: autophagy and proliferative response in differentiated DM1 myotubes. The clusterization of LC3 was measured as autophagic marker in T15 myotubes from three controls and six DM1 by immunofluorescence. (A_1) Representative images of LC3 positive vesicles in control and DM1-E32 myotubes. Scale bar 25 µm. (A_2) The diagram represents mean ± SE of the data obtained by scoring 10 images/cell line as described in Materials and Methods and indicates a significant increase of clustered LC3 in DM1-$E2_1$, -$E2_2$, -$E3_2$, -$E3_3$ and cDM1-$E4_1$, -$E4_2$ myotubes compared to controls (**p<0.01). (B) The protein level of P62 was revealed by Western blot analysis and quantified by densitometry in three controls and DM1-$E2_2$, -$E3_3$ and cDM1-$E4_2$ The bar graph represents the P62/ β-actin ratio.

5.3.1 Biopsies show differential activation of apoptosis and autophagy in human skeletal muscle

To further confirm the role of autophagy and apoptosis in muscle loss of DM1 patients we studied human muscle biopsies from which satellite cells were extracted for the in vitro experiments. TUNEL positive nuclei were detected in DM1-E2 and -E3 (Figures 24 A_1-A_2) while autophagy, revealed by LC3 lipidation, was strongly induced in DM1-E3 and –E4 (Figures 24 B_1-B_2). Analysis on P62 expression revealed an accumulation of the protein in DM1-E3 (Figures 24 C_1-C_2), which suggest an alteration of autophagy flux. In conclusion, adult myofibers confirmed the findings of fully differentiated myotubes supporting a possible pathogenetic role of apoptosis and autophagy in DM1 muscle wasting.

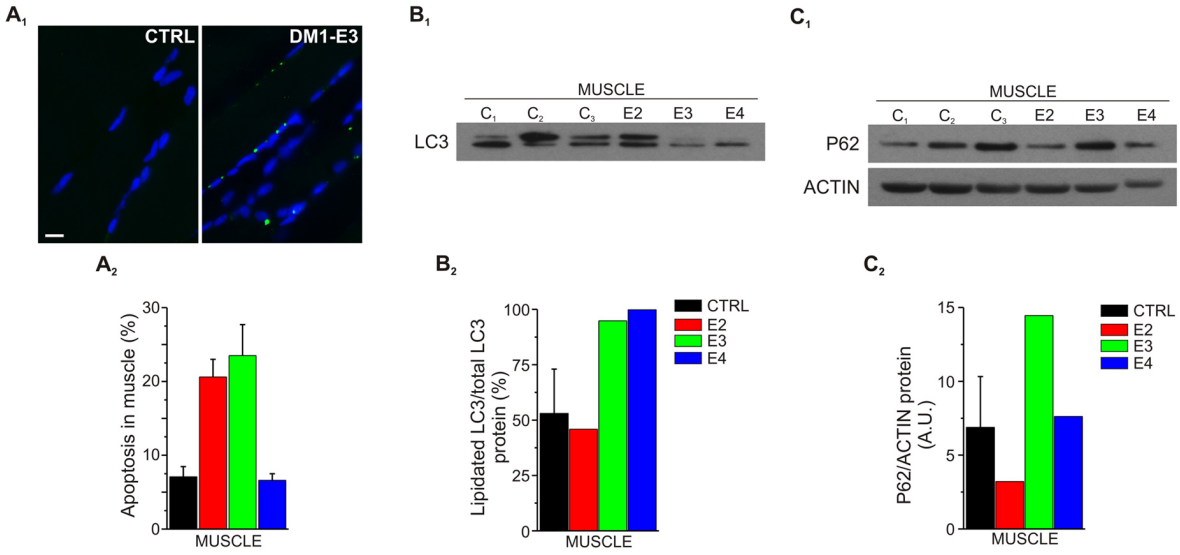

Figure 24: apoptotic and autophagic features in parental DM1 muscle biopsies. (A_1) Representative images of TUNEL reaction in normal and DM1-E3 muscle. (A_2) Quantification of TUNEL positive nuclei in DM1-E2, -E3, -E4 and control skeletal muscles. The data are expressed as percentage of TUNEL-positive nuclei to total nuclei. Scale bar 25 µm. (B_1) Immunoblot detection of lipidated LC3 in adult muscle biopsies from controls (C) and DM1-E2, -E3, -E4; (C_2) Quantification of lipidated LC3 expressed as ratio to unlipidated LC3. (C_1) P62 protein level revealed by Western blot analysis and quantified by densitometry (C_2) The bar graph represents the ratio of P62 to actin.

6. Discussion

6.1. Myogenic potency in DM1

The present study clearly demonstrates that primary muscular satellite cells from DM1 patients with either congenital or adult form have normal fusion, differentiation and maturation capacity. When we studied the myogenic capacity we found that number of syncytial nuclei, the expression level of myogenic markers (CK-M, myogenin and MHC) and the contractile capability after innervation were similar to controls and unaffected by the number of $(CTG)_n$ repeats. $(CTG)_n$ expansion was confirmed at RNA level by the presence of ribonuclear foci, the pathological hallmark of DM1, which was always found in undifferentiated (Figure 15), differentiated and innervated DM1 muscle cells. In vivo, the retention into ribonuclear foci of the expanded DMPK transcript is associated to the misregulation of alternative splicing. This in trans effect on the alternative splicing of many RNAs, which does not result in the production of mutant protein but leads to expression of spliced products inappropriate for a particular tissue, is the major molecular defect identified in DM1 (10, 13). We provide evidence that splicing unbalance is present in undifferentiated and differentiated DM1 muscle cells. Moreover, similarly to what is observed *in vivo* (31), also *in vitro* there is a correlation between the extend of the $(CTG)_n$ repeat size and the degree of abnormal splicing. Differentiation capacity of primary human DM1 muscle cells is controversial. Normally differentiated human myotubes were reported in calcium homeostasis studies from a large cohort of 15 adult DM1 patients (76-78) and recently in five DM2 patients (79). Moreover in vitro successfully innervated muscle fibers from 17 adult DM1 patients were used for studies of electrophysiological properties of DM1 mature myotubes (83) and developmental regulation of DMPK (84, 85). In contrast, other reports claim an impaired myogenesis (80, 82) or a delayed maturation of primary myotubes from three cDM1 and few adult DM1-DM2 patients (56, 81). In addition a large number of publications describe myogenic alterations in mouse muscle models (72, 73) or in primary DM1 fibroblasts converted in myoblasts by MyoD transfection (46, 75). The delayed muscle development has been proposed as being determined by dysfunction of the signaling pathway that includes MyoD, Myf5, MRF4, factors responsible for the commitment of muscle stem cells to the myogenic lineage, and myogenin and MFR4, factors involved in the expression of the terminal muscle phenotype. It was found that the levels of the commitment factor MyoD were reduced both in C2C12 cells expressing mutant DMPK 3'-UTR RNA and in DM1 patient myoblasts (78, 82). However, this reduction of MyoD protein levels was not accompanied by a decrease in its homologue Myf5. Moreover, Timchenko et al. (82) proposed that myoblasts from one DM1 and one DM2 patients failed to undergo differentiation because of an impairment of the p21/CDK4/Rb/E2F pathway usually essential for the withdrawal from cell cycle. A recent publication proposed (147) that the ectopic expression of cyclin D3 corrects differentiation in

DM1 myoblasts by increasing the CUGBP1-eIF2 interaction necessary for activation of the myogenic program and the correct expression of myogenic markers such as myogenin. The discordance between our results showing a normal DM1 primary myoblast differentiation and the reported alteration in the myogenic process of DM1 myoblasts might be accounted for by the different models used (i.e. myoblasts from human adult vs. fibroblasts converted into myoblasts and mouse model) or by a difference in the morphological and clinical severity of the disease (i.e. myoblasts from human cDM1 patients that survived after the neonatal period vs. myoblasts from aborted cDM1 fetuses) or by a difference in the number of passages of cultured cells, which may also influence myogenesis (148) because of the recently reported implication of the p16 premature senescence of DM1 myoblasts (86, 92).

6.2. Catabolic pathways and a novel pathogenetic mechanism

During differentiation, myoblasts undergo sequential events, ending with fusion into syncytial cells, a cell type more resistant to sublethal damage than proliferating myoblasts, which go on to generate muscle fibers. However, in many degenerative and metabolic diseases, muscle fibers die with no marked inflammatory response: this could probably be due to apoptosis (149). Therefore the study of myotubes in vitro is a good model for predicting if apoptosis is active at least in developing myofibers. Apoptosis in primary myotubes was evident in merosin, dystrophin and dystrophin-associated protein-deficient cell lines (150, 151). Recently Ullrich congenital dystrophy, caused by collagen-VI mutations, presented an increased occurrence of spontaneous apoptosis (152). At 15 days of culture we observed a statistically significant decrease in the number of myonuclei in DM1 patients and concomitant evidences of atrophy. It has been reported that ubiquitin-proteasome, autophagy-lysosome and caspase-3/9 activation contributes, albeit to a different extent to muscle loss. Indeed, we found an increase of apoptosis and autophagy even though no induction of atrophy related genes, atrogin-1 and MuRF1, was observed in any of the 15-day-differentiated DM1 myotubes; however, it could not be excluded that these ubiquitin-ligases might contribute to myotube atrophy between 10 and 15 days. It is interesting to note that the reduced incidence of apoptosis in DM1-E3 cells matches with a concomitant significant increase of autophagy and of AKT activation. This trend can be explained in terms of the well known inverse relationship found between the pro-cell death system, apoptosis, and the pro-survival system, autophagy (114). In our DM1 myotubes, apoptosis occurred after differentiation and not in undifferentiated myoblasts. The role of apoptosis was confirmed by Z-VAD treatment, which significantly recovered the number of myonuclei and AMW, so identifying apoptosis as a potential candidate for therapeutic approaches (Figure 22). A novel pathogenetic mechanism is emerging from our findings. It is important to underline that activation of autophagy matches with the $(CTG)_n$ expansion, autophagy being highly activated in samples with high numbers of $(CTG)_n$ (Figure 23). This correlation is consistent with the hypothesis that autophagy is in-

duced to clear toxic proteins and organelles, in order to maintain cell viability. Thus autophagy may act as a pro-survival system, which can also reduce muscle mass as a result of its proteolytic activity. Increasing the number of $(CTG)_n$ triplets can affect the expression of critical factors for protein-folding processes, response to protein unfolding/misfolding, and many other cellular components including proteins involved in Ca^{2+} homeostasis. Thus autophagy failure or exhaustion can lead to accumulation of toxic proteins, which can interfere with organelle (mitochondria) function and with cellular signaling leading to myofiber degeneration. It should be noted that we found an increase of H_2O_2 production in 15-day-differentiated DM1-E2 and cDM1-E4 myotubes, which showed higher level of apoptosis and lower level of autophagy. Since one of the main sources of ROS is dysfunctional mitochondria, the presence of H_2O_2 suggests a failure in the removal system for altered mitochondria. The persistence of abnormal mitochondria would induce the release of pro-apoptotic factors. Therefore a failure or overload of autophagy induces accumulation of death-signaling components, which triggers apoptosis and myofiber degeneration. This hypothesis is in line with the established fact that autophagy and apoptosis are mutually exclusive and not synergistic (132). In conclusion, this is the first study focused on the differentiation of myoblasts from patients with adult classical DM1 and cDM1 that survived at the perinatal crisis, and allows us to formulate a new hypothesis to explain the progressive DM1 muscular pathogenesis. We propose that apoptosis-autophagy is the key event, probably coupled to oxidative stress and misregulation of calcium homeostasis, which may also be linked to premature senescence of satellite cells.

7. Supplementary experiments

7.1. Rationale

Our data show that the muscle wasting typical in DM1 is due to the impairment of muscle mass maintenance-regeneration, through premature programmed cell-death activation after 10-15 days of differentiation.

Intracellular Ca^{2+} has been implicated as an important regulator of both cell proliferation and apoptosis. Defects in its homeostasis have been associated with many pathological conditions such as Duchenne's increased death of cardiomyocites (153). In particular conditions, changes in the distribution of Ca^{2+} from the ER to the mitochondria can result in an abnormal build up of Ca^{2+} in the mitochondrial matrix resulting in the formation of a permeability transition pore (PTP), collapse of the mitochondrial membrane potential and the release of pro-apoptotic factors (e.g. cytochrome c and an apoptosis-inducing factor) (154). The regulation of intracellular Ca^{2+} homeostasis in skeletal muscle cells depends mainly on two sarcoplasmic reticulum (SR) proteins: ryanodine receptor 1 (RyR1) and sarcoplasmic/endoplasmic reticulum Ca^{2+}-ATPase (SERCA). . As a consequence of SERCA's activity, the resting cytosolic free Ca^{2+} is maintained three to four orders of magnitude lower than the intra-SR/ER Ca^{2+} concentration. During a normal skeletal muscle contraction/relaxation cycle, Ca^{2+} is released from SR into the cytoplasm through RyR1, in response to plasma membrane depolarization. The RyR1 mechanical interaction with voltage-gated calcium channels is responsible for the Ca^{2+} efflux [excitation-contraction (EC) coupling] (155) which induces muscle contraction. In order to allow relaxation, Ca^{2+} is subsequently pumped back into the lumen of SR by the SERCA, by a process coupled to ATP hydrolysis (156).

Ca^{2+} is subsequently pumped back into the lumen of SR by SERCA to allow relaxation. Many publications during the last 20 years focused on the effects of the $(CTG)_n$ expansion on the splicing (58, 157), expression (57, 77) and functionality (77, 78, 158) of SERCA and RyR1. The fetal isoforms of both transporters are increased in DM1 muscle, causing a documented alteration of the calcium balance. Benders et al showed that in DM1 cells there is an increase cytosolic Ca^{2+} concentration probably due to a reduced expression of SERCA1 and to an increased activation of voltage-gated Ca^{2+} channels, which are usually inactive in resting control cells (76-78). Moreover, Kimura et al analysed the effects of alternative splicing on the functionality of RyR and SERCA1, showing that the foetal splicing RyR ASI(-) has a decreased affinity for $^{[3H]}$ryanodine but similar Ca^{2+} dependency, and decreased channel activity in single-channel recording when compared with wild-type RyR1 (58). Moreover, in a following publication, they showed that depolarisation-dependent Ca^{2+} release was enhanced by >50% in myotubes expressing RyR1 ASI(–) compared with RyR1 ASI(+), although

DHPR L-type currents and SR Ca^{2+} content were unaltered, while RyR1 ASI(–) channel function was depressed (158). In the hypothesis that such impairment could lead to the activation of programmed cell death, we built up a set of preliminary experiments with primary DM1-E3 myotube cultures (obtained following the protocol described at page 48).

7.2. Alternative splicing of RyR1 and SERCA1

First, we analyzed the splicing alteration pattern of RyR1 and SERCA1 in myoblasts and myotubes at 10 days (when programmed cell-death started) and 15 days (when the majority of myotubes dies) of differentiation. The adopted PCR protocol was similar to the one used for the detection of insulin receptor and MBNL1 alternative splicing. The primer sequences used are described in table 7.

Table 7: primer sequences for analysis of the alternative splicing of calcium transporters.

Primer	Sequence	T_m
RYRasI F	5' gacaacaaaagcaaaatggc3'	57°C
RYRasI R	5' cttggtgcgttcctggtc3'	57°C
RYRasIIF	5' ttgagagacagaacaaggc3'	56°C
RYRasIIR	5' ggtcttgtgtgaattcatca3'	56°C
Serca1ex22F	5' atcttcaagctccgggccc3'	62°C
Serca1ex22R	5' cagctctgcctgaagatgtg3'	62°C

There are three genes encoding RyR in mammals. RyR1 and RyR2 are expressed in skeletal muscle and heart muscle, respectively. Although RyR3 is not predominant, it is detected in immature skeletal muscles and decreases markedly at later stages of development. The expression of RyR1 splice variants is regulated both developmentally and in a tissue-specific manner. Futatsugi et al. (157) described several splice variants of the skeletal muscle RyR1. The variant ASI(-), which lacks ASI (exon 70, residues 3481–3485), constitutes 100% of RyR1 expressed in mouse embryonic skeletal muscle and 30% of those in adult muscle. Consistent with these results, Kimura et al. (58) found that the ASI(+) isoform was dominantly expressed in normally developed human muscles and ASI(-) predominated in cultured myotubes. In contrast, ASI(-) was significantly increased in DM1 adult muscle when compared with control.

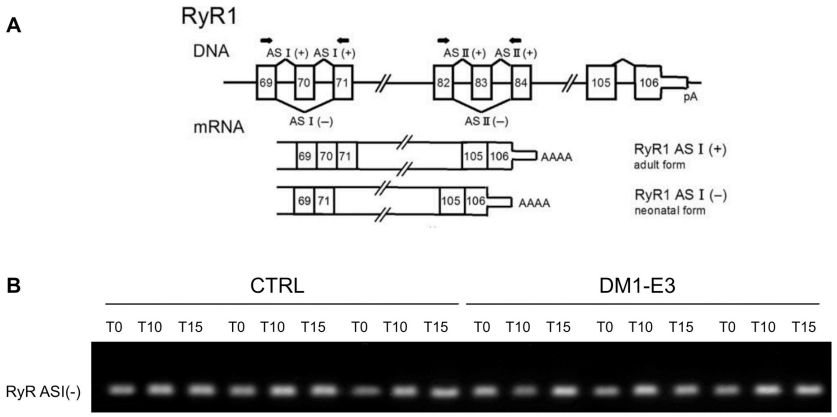

Figure 25: RyR1 alternative splicing 1 (ASI). (A) schematic representation of RyR1 gene and its splicing isoforms RyR1 ASI(+) and RyR1 ASI(-). (B) PCR detection of RyR ASI splicing in control (CTRL) and DM1-E3 myoblasts (T0) and myotubes (T10, T15). Only the fetal isoform was detectable both in control and pathological cultures.

The adult splicing isoform RyR ASI(+) was not detectable in primary myoblasts/myotubes from both controls and DM1 samples (Figure 25), indicating that the adult form ASI(+) is only expressed in adult muscle (as previously shown by (58)). Another variant, ASII(-), which lacks ASII (exon 83, residues 3865–3870), is transiently expressed in skeletal muscle after birth and constitutes 10% of RyR1 in adults. In mice, the splicing change in ASII takes place earlier than that in ASI and the ASII(+) isoform is dominantly expressed even in human myotubes (58).

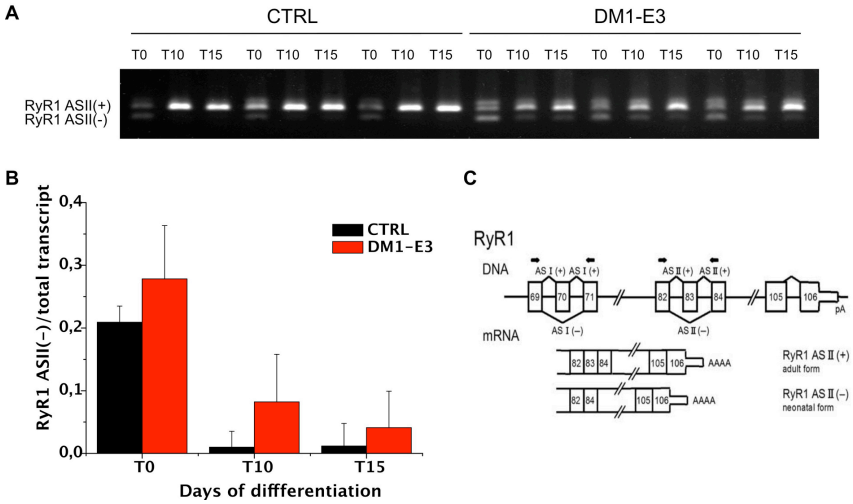

Figure 26: RyR1 alternative splicing 2 (ASII). (A) PCR detection of fetal ASII(-) and ASII(+) isoforms. Bands were separated in a3% agarose electrophoresis gel. (B) Bar chart of fetal/total splicing isoforms, obtained by densitometric analysis of each band. (C) schematic representation of the ASII splicing isoforms of RyR1.

During differentiation, the amount of the fetal isoform RyR1 ASII(-) decreased in both controls and pathologic samples indicating a gradual maturation of myotubes. However, the presence of the

ASII(-) isoform maintained elevated in pathological myoblasts/myotubes compared to controls (Figure 26).

SERCAs are also encoded by three homologous genes: SERCA1, SERCA2 and SERCA3. Transcripts from these genes undergo alternative splicing in a developmentally regulated and tissue-specific manner, giving rise to isoforms that differ in their C-terminal region. SERCA1a (adult form) and 1b (neonatal form) are mainly expressed in fast-twitch (type 2) skeletal muscle and SERCA2a is expressed in slow-twitch (type 1) skeletal and cardiac muscles, whereas SERCA2b expression is widespread. SERCA3 is expressed in several non-muscle tissues at variable levels, co-localizing with SERCA2b. We performed the same protocols used for RyR1 to test the impaired balance of SERCA1 splicing in differentiating muscle cultures from control and DM1-E3 lines (Figure 27).

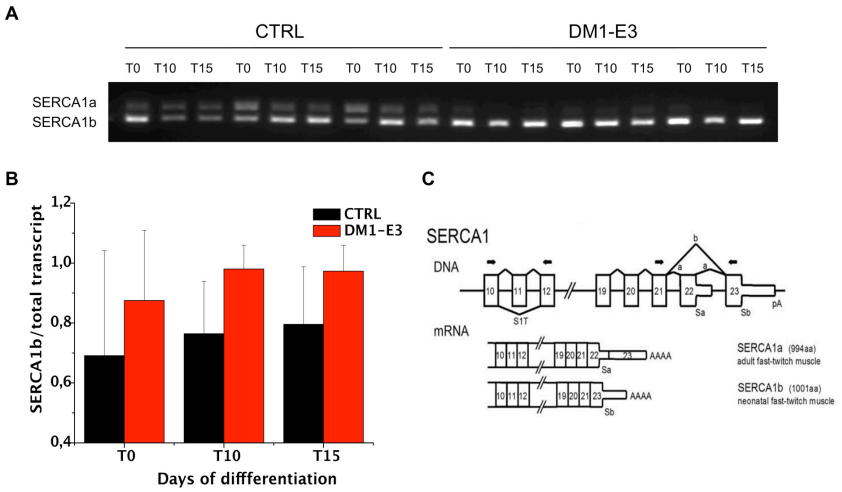

Figure 27: SERCA1 alternative splicing. (A) PCR detection of fetal SERCA1b and adult SERCA1a isoforms. Bands were separated in a 3% agarose electrophoresis gel. (B) Bar chart of fetal/total splicing isoforms, obtained by densitometric analysis of each band. (C) schematic representation of the ASII splicing isoforms of RyR1.

As shown in Figure 27, the amount of fetal/total transcript for SERCA maintained constant during differentiation, showing the preponderance of the fetal isoform in DM1-E3 samples compared to controls.

7.3. Analysis of Ca^{2+} balance

After having verified that the splicing of RyR1 and SERCA1 is affected by the $(CTG)_n$ expansion, we set up a series of experiments aiming to verify the functionality of calcium homeostasis in our cell model. We therefore used the ratiometric fluorescent probe FURA2-AM to monitor the release/uptake of Ca^{2+} in 10-15 days differentiated myotubes. When myotubes are stimulated either by maintained depolarization with KCl, myoplasmic Ca^{2+} levels initially rise and then decay as a consequence

of declining release from the sarcoplasmic reticulum (SR) and the uptake operated by the SERCA pumps (155). The inhibition of SERCA activity, therefore, allows to deplete the SR having a measure of the amount of calcium stored. Control and DM1-E3 myoblasts were seeded in 24 mm glasses and differentiated as previously described (see page 48). After 10/15 days of differentiation myotubes were washed with HBSS and loaded with the membrane permeable fluorescent probe FURA2-AM 5 μM for 30 minutes at 37°C. When added to cells, FURA-2AM crosses cell membranes and once inside the cell, the acetoxymethyl groups are removed by cellular esterases. Removal of the acetoxymethyl esters regenerates "FURA-2", the pentacarboxylate calcium indicator. Measurement of Ca^{+2}-induced fluorescence at both 340 nm and 380 nm allows for calculation of calcium concentrations based 340/380 ratios. The use of the ratio automatically cancels out certain variables such as local differences in FURA-2 concentration or cell thickness that would otherwise lead to artifacts when attempting to image calcium concentrations in cells. The excess of probe was washed with HBSS and each sample was then analysed in presence of external calcium with an Olympus IX81 inverted fluorescence microscope according to the protocol reported by BarretoChang et al. (159). Membrane depolarisation was obtained by the addition of 120 mM KCl and monitoring the change of fluorescence. For each sample more myotubes were considered. The traces obtained for each myotube were analysed singularly with commercial software to determine the peak height of Ca^{2+} release, the area under the curve (AUC), the kinetic of re-uptake by the SERCA, and the time necessary to restore the physiological cytoplasmic concentration.

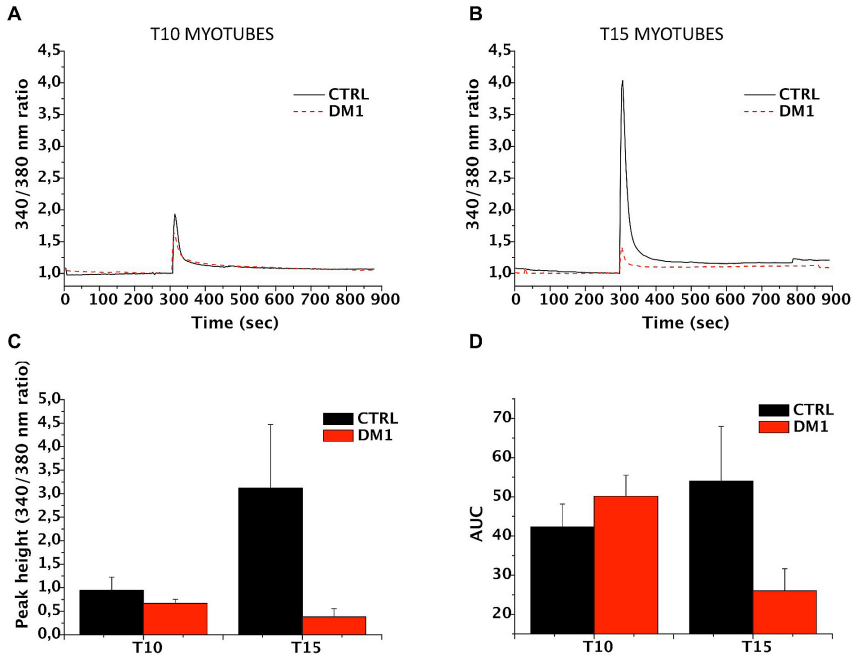

Figure 28: KCl-induced Ca^{2+} release in control and DM1-E3 myotubes at 10 (A) and 15 (B) days of differentiation. Controls n_{10}=10; n_{15}=10. DM1 n_{10}=13; n_{15}=6. Traces represent the average values of multiple experiments. Data are expressed as mean±standard error. (C) Bar chart representing the average peak of the calcium release induced by KCl in control and DM1 myotubes. (D) Bar chart representing the average area under the curve (AUC) calculated from traces A and B. Data are expressed as mean±standard error.

Figure 28 shows the response to depolarisation of control and DM1-E3 myotubes at different stages of maturation. In control lines the three fold increased response (from 0,94±0,28 to 3,12±1,34) to KCl was in line with the progression of differentiation. On the contrary, the recorded signal in DM1 myotubes (from 0,67±0,08 to 0,38±0,17) did not increase during differentiation. These data correlate with the molecular evidences of a splicing imbalance toward the neonatal isoforms of calcium transporters, especially RyR1. The mathematical analysis of traces allowed to calculate the kinetic parameters of calcium release/uptake in normal and DM1 myotubes (Table 8).

Taken together these data suggest an impairment of Ca^{2+} release following depolarising stimuli. These effect could be due to the reduced functionality of neonatal isoforms of RyR which are more represented in DM1 cultures compared to controls. Moreover, a reduced efflux of calcium from organelles, and in particular from sarcoplasmic reticulum, could be due to a reduced storage. To verify this possibility, we performed the same FURA analysis using the SERCA inhibitor 2,5-di-(t-butyl)-hydroquinone 50 µM instead of KCl. By inhibiting the uptake of calcium operated by the SERCA, we allowed the physiological leakage of ions from the SR to deplete the stores. The analysis of these traces could be suggestive of the total amount of Ca^{2+} in the reticulum. We assumed an almost null contribution of the external calcium uptake by the L-type membrane channels, which in myotubes function only as external Ca^{2+} sensors, stimulating its release from the ER without importing it from the extracellular environment (160).

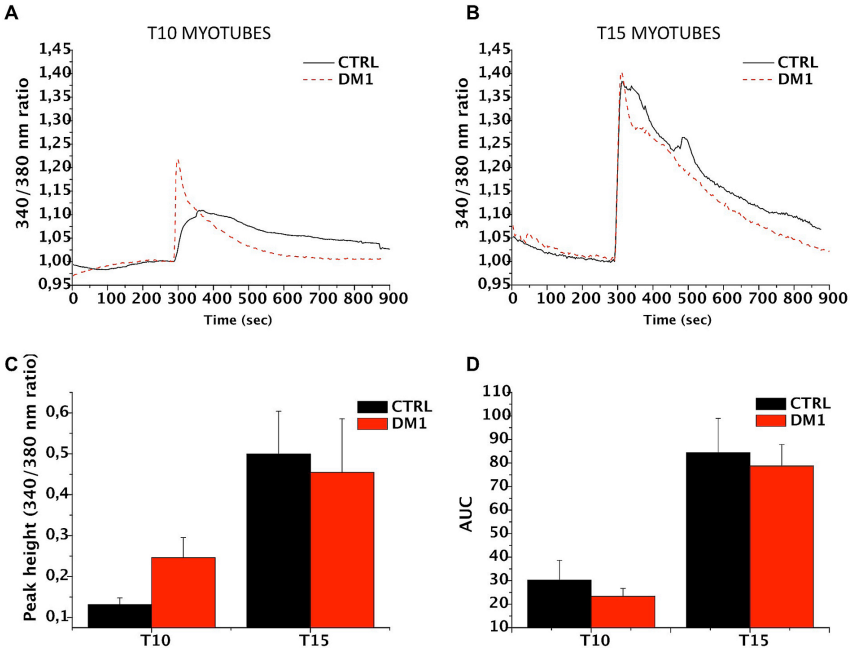

Figure 29: depletion of SR Ca^{2+} stores by t-butyl inhibition of SERCA pump in control and DM1-E3 myotubes at 10 (A) or 15 (B) days of differentiation. Controls n10=13; n15=9. DM1 n10=17; n15=8. Traces represent the average values of multiple experiments. (C) Bar chart representing the average peak of the calcium release induced by t-butyl in control and DM1 myotubes. (D) Bar chart representing the average area under the curve (AUC) calculated from traces A and B. Data are expressed as mean±standard error.

The inhibition of SERCA allowed us to estimate the amount of Ca^{2+} stored in the ER of control and DM1 myotubes by integrating the peaks and calculating the area under the curve (AUC). As shown in Figure 29 and in Table 8, AUC was only slightly reduced in pathologic samples compared to controls, suggesting that calcium stores in DM1 myotubes are similar to those of healthy samples.

Table 8: mathematical analysis of KCl-induced Ca^{2+} release in control and DM1-E3 myotubes

	T10 myotubes		**T15 myotubes**	
	control	**DM1-E3**	**control**	**DM1-E3**
120 mM KCl				
n	10	13	10	6
Peak	0,94±0,28	0,67±0,08	3,12±1,34	0,38±0,17
AUC	42,29±5,86	50,13±5,42	53,98±13,96	26,04±5,60
T_C	135,49±0,16	133,50±0,61	135,82±0,38	132,93±0,52
Slope	-0,095±0,02	-0,05±0,02	-0,075±0,02	-0,08±0,04
50 µM t-butyl				
n	13	17	9	8
Peak	0,13±0,02	0,25±0,05	0,50±0,10	0,45±0,13
AUC	30,23±8,29	23,41±3,29	84,41±14,59	78,79±9,02

Taken together, these data suggest that the amount of Ca^{2+} available for ECC in DM1 myotubes is normal, but the functionality of channels normally controlling the release/uptake from cellular compartments results impaired. Different possibilities raise from our observations: first, as already documented, the increased presence of neonatal forms of RyR1 with reduced activity could be responsible for the limited release of Ca^{2+} after depolarisation (Table 8). The re-uptake kinetics by SERCA, which can be described by the slope of the descending phase of curves in Figure 28, resulted not modified by the pathology, indicating a normal functionality of calcium re-uptake. However, to be sure about the amounts of stored calcium in ER, experiments without external Ca^{2+} may become important. In fact, even if in normal myotubes, the contribution of membrane uptake can be negligible, some previous evidences in mouse skeletal muscle fibres, suggested that the depletion of Ca^{2+} in the sarcoplasmic reticulum could stimulate Ca^{2+} entry, thus invalidating the estimation of Ca^{2+} storage by t-butyl. Moreover, we don't know if the $(CTG)_n$ expansion could also influence the splicing of membrane channels leading to the expression of neonatal isoforms which, like in myoblasts, could pump Ca^{2+} inside the myotube.

7.4. Analysis of mitochondrial contribute to apoptosis

Our work showed how apoptotic activation in DM1 myotubes was associated with both caspases activation and cytochrome c release from mitochondria. In the hypothesis that mitochondrial activation of apoptosis goes through an induced Ca^{2+} influx, we performed TUNEL assay in 15 days myotubes treated with 1μM cyclosporin (CSA). CSA inhibits the opening of the mitochondrial transition pore (PTP) which is believed to mediate calcium entry and cytc release. In other pathologies such as Duchenne (161) or Ullrich (152, 162) muscular dystrophy, an overload of mitochondrial calcium leads to apoptotic death and the treatment with CSA revealed effective.

Each primary myoblast line was seeded on two culture glasses as described at page 50. After 10 days of differentiation, myotubes were treated with 1 μM CSA with daily change of medium. At day 15 myotubes were fixed and TUNEL reaction was performed.

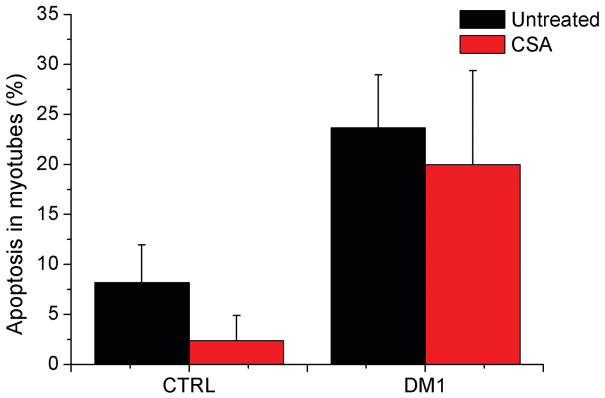

Figure 30: TUNEL detection of apoptosis in control (n=3) and DM1-E3 (n=3) myotubes at 15 days of differentiation. Samples were treated for 5 days with 1 μM CSA with daily change of medium. Results are expressed as mean±standard error of the mean.

The inhibition of the PTP lead to a slight and non specific reduction of apoptosis both in control and DM1 myotubes, indicating that mitochondrial calcium overload is not the primary cause of apoptosis in DM1 myotubes, but probably is a consequence of a general defective homeostasis of the whole cell.

7.5. Final considerations and future work

The contribution of programmed cell death to the muscle wasting in myotonic dystrophy 1 is clear, and poses new questions about the development of the pathology and the consequent therapeutic strategies. Moreover, a linkage with calcium homeostasis, fundamental in every living organism, seems to be reasonable. Calcium overload is involved in the pathogenesis of many muscle diseases and in some cases it constitutes a primary target for the development of specific therapies. Our preliminary data about calcium storage and delivery in primary myotubes suggest a different kind of imbalance. Our evidences suggest a reduced mobilisation of calcium from organelles in which neonatal isoforms of channels and transporters are predominant. Reduced amounts of accessible calcium could lead to apoptosis in an indirect way, maybe causing stress of the endoplasmic reticulum, which is known to be linked to apoptosis. Thus, our future work will aim to better characterise calcium homeostasis in affected primary muscle cultures, also looking for the typical ER stress markers, and to try different strategies to correct this impairment. The selective overexpression of mature isoforms of RyR1 and SERCA could improve calcium balance and allow to understand how this intervention could relief the pathological condition. Other strategies may be directed to restore the corrected splicing functions by increasing the amount of available MBNL1 by its overexpression, or by pushing toward the generation of correctly spliced mRNA. Exon skipping may be the primary method to achieve this condition, already representing one of the most promising therapeutical approaches to treat Duchenne and Becker muscular dystrophies (163). In example, antisense oligonucleotides (AOS) could be designed to induce the exclusion of exon 6 in MBNL1, normalising its splicing functionality. This approach could allow to induce the expression of normal isoforms of many involved proteins such as RyR1, SERCA or the same MBNL1.

8. Bibliography

1. Buckingham M. Skeletal muscle progenitor cells and the role of Pax genes. C R Biol. 2007;330:530-3.

2. Collins CA, Olsen I, Zammit PS, Heslop L, Petrie A, Partridge TA, Morgan JE. Stem cell function, self-renewal, and behavioral heterogeneity of cells from the adult muscle satellite cell niche. Cell. 2005;122:289-301.

3. Zammit PS, Partridge TA, Yablonka-Reuveni Z. The skeletal muscle satellite cell: the stem cell that came in from the cold. J Histochem Cytochem. 2006;54:1177-91.

4. Seale P, Sabourin LA, Girgis-Gabardo A, Mansouri A, Gruss P, Rudnicki MA. Pax7 is required for the specification of myogenic satellite cells. Cell. 2000;102:777-86.

5. Irintchev A, Zeschnigk M, Starzinski-Powitz A, Wernig A. Expression pattern of M-cadherin in normal, denervated, and regenerating mouse muscles. Dev Dyn. 1994;199:326-37.

6. Beauchamp JR, Heslop L, Yu DS, Tajbakhsh S, Kelly RG, Wernig A, et al. Expression of CD34 and Myf5 defines the majority of quiescent adult skeletal muscle satellite cells. J Cell Biol. 2000;151:1221-34.

7. Chargé SB, Rudnicki MA. Cellular and molecular regulation of muscle regeneration. Physiol Rev. 2004;84:209-38.

8. Martinuzzi A, Askanas V, Kobayashi T, Engel WK, Di Mauro S. Expression of muscle-gene-specific isozymes of phosphorylase and creatine kinase in innervated cultured human muscle. J Cell Biol. 1986;103:1423-9.

9. Kobayashi T, Askanas V, Engel WK. Human muscle cultured in monolayer and cocultured with fetal rat spinal cord: importance of dorsal root ganglia for achieving successful functional innervation. J Neurosci. 1987;7:3131-41.

10. Harper PS. Myotonic dystrophy. London: Saunders; 2001.

11. Wagner A, Steinberg H. Hans Steinert (1875-1911). J Neurol. 2008;255:1607-8.

12. Machuca-Tzili L, Brook D, Hilton-Jones D. Clinical and molecular aspects of the myotonic dystrophies: a review. Muscle Nerve. 2005;32:1-18.

13. Wheeler TM, Thornton CA. Myotonic dystrophy: RNA-mediated muscle disease. Curr Opin Neurol. 2007;20:572-6.

14. Cooper TA. Chemical reversal of the RNA gain of function in myotonic dystrophy. Proc Natl Acad Sci U S A. 2009;106:18433-4.

15. New nomenclature and DNA testing guidelines for myotonic dystrophy type 1 (DM1). The International Myotonic Dystrophy Consortium (IDMC). Neurology. 2000;54:1218-21.

16. Brouwer JR, Willemsen R, Oostra BA. Microsatellite repeat instability and neurological disease. BioEssays. 2009;31:71-83.

17. Gomes-Pereira M, Monckton DG. Chemical modifiers of unstable expanded simple sequence repeats: what goes up, could come down. Mutat Res. 2006;598:15-34.

18. Bundey S, Carter CO, Soothill JF. Early recognition of heterozygotes for the gene for dystrophia myotonica. J Neurol Neurosurg Psychiatry. 1970;33:279-93.

19. Vattemi G, Tomelleri G, Filosto M, Savio C, Rizzuto N, Tonin P. Expression of late myogenic differentiation markers in sarcoplasmic masses of patients with myotonic dystrophy. Neuropathol Appl Neurobiol. 2005;31:45-52.

20. Taneja KL, McCurrach M, Schalling M, Housman D, Singer RH. Foci of trinucleotide repeat transcripts in nuclei of myotonic dystrophy cells and tissues. J Cell Biol. 1995;128:995-1002.

21. Cho DH, Tapscott SJ. Myotonic dystrophy: emerging mechanisms for DM1 and DM2. Biochim Biophys Acta. 2007;1772:195-204.

22. Turnpenny P, Clark C, Kelly K. Intelligence quotient profile in myotonic dystrophy, intergenerational deficit, and correlation with CTG amplification. J Med Genet. 1994;31:300-5.

23. Damian MS, Bachmann G, Koch MC, Schilling G, Stöppler S, Dorndorf W. Brain disease and molecular analysis in myotonic dystrophy. Neuroreport. 1994;5:2549-52.

24. Censori B, Provinciali L, Danni M, Chiaramoni L, Maricotti M, Foschi N, et al. Brain involvement in myotonic dystrophy: MRI features and their relationship to clinical and cognitive conditions. Acta Neurol Scand. 1994;90:211-7.

25. Meola G, Sansone V. Cerebral involvement in myotonic dystrophies. Muscle Nerve. 2007;36:294-306.

26. Delaporte C. Personality patterns in patients with myotonic dystrophy. Arch Neurol. 1998;55:635-40.

27. Sergeant N, Sablonnière B, Schraen-Maschke S, Ghestem A, Maurage CA, Wattez A, et al. Dysregulation of human brain microtubule-associated tau mRNA maturation in myotonic dystrophy type 1. Hum Mol Genet. 2001;10:2143-55.

28. Ghanem D, Tran H, Dhaenens CM, Schraen-Maschke S, Sablonnière B, Buée L, et al. Altered splicing of Tau in DM1 is different from the foetal splicing process. FEBS Lett. 2009;583:675-9.

29. Harper PS, Van Engelen BGM, Eymard B, Wilcox DE. Myotonic dystrophy: present management, future therapy. Oxford University Press, Oxford; 2004.

30. Tsilfidis C, MacKenzie AE, Mettler G, Barceló J, Korneluk RG. Correlation between CTG trinucleotide repeat length and frequency of severe congenital myotonic dystrophy. Nat Genet. 1992;1:192-5.

31. Botta A, Rinaldi F, Catalli C, Vergani L, Bonifazi E, Romeo V, et al. The CTG repeat expansion size correlates with the splicing defects observed in muscles from myotonic dystrophy type 1 patients. J Med Genet. 2008;45:639-46.

32. Sarkar PS, Paul S, Han J, Reddy S. Six5 is required for spermatogenic cell survival and spermiogenesis. Hum Mol Genet. 2004;13:1421-31.

33. Westerlaken JH, Van der Zee CE, Peters W, Wieringa B. The DMWD protein from the myotonic dystrophy (DM1) gene region is developmentally regulated and is present most prominently in synapse-dense brain areas. Brain Res. 2003;971:116-27.

34. Jansen G, Willems P, Coerwinkel M, Nillesen W, Smeets H, Vits L, et al. Gonosomal mosaicism in myotonic dystrophy patients: involvement of mitotic events in (CTG)n repeat variation and selection against extreme expansion in sperm. Am J Hum Genet. 1994;54:575-85.

35. Davis BM, McCurrach ME, Taneja KL, Singer RH, Housman DE. Expansion of a CUG trinucleotide repeat in the 3' untranslated region of myotonic dystrophy protein kinase transcripts results in nuclear retention of transcripts. Proc Natl Acad Sci U S A. 1997;94:7388-93.

36. Smith KP, Byron M, Johnson C, Xing Y, Lawrence JB. Defining early steps in mRNA transport: mutant mRNA in myotonic dystrophy type I is blocked at entry into SC-35 domains. J Cell Biol. 2007;178:951-64.

37. Jasinska A, Michlewski G, de Mezer M, Sobczak K, Kozlowski P, Napierala M, Krzyzosiak WJ. Structures of trinucleotide repeats in human transcripts and their functional implications. Nucleic Acids Res. 2003;31:5463-8.

38. Miller JW, Urbinati CR, Teng-Umnuay P, Stenberg MG, Byrne BJ, Thornton CA, Swanson MS. Recruitment of human muscleblind proteins to (CUG)(n) expansions associated with myotonic dystrophy. EMBO J. 2000;19:4439-48.

39. Fardaei M, Larkin K, Brook JD, Hamshere MG. In vivo co-localisation of MBNL protein with DMPK expanded-repeat transcripts. Nucleic Acids Res. 2001;29:2766-71.

40. Fardaei M, Rogers MT, Thorpe HM, Larkin K, Hamshere MG, Harper PS, Brook JD. Three proteins, MBNL, MBLL and MBXL, co-localize in vivo with nuclear foci of expanded-repeat transcripts in DM1 and DM2 cells. Hum Mol Genet. 2002;11:805-14.

41. Mankodi A, Urbinati CR, Yuan QP, Moxley RT, Sansone V, Krym M, et al. Muscleblind localizes to nuclear foci of aberrant RNA in myotonic dystrophy types 1 and 2. Hum Mol Genet. 2001;10:2165-70.

42. Jiang H, Mankodi A, Swanson MS, Moxley RT, Thornton CA. Myotonic dystrophy type 1 is associated with nuclear foci of mutant RNA, sequestration of muscleblind proteins and deregulated alternative splicing in neurons. Hum Mol Genet. 2004;13:3079-88.

43. Black DL. Mechanisms of alternative pre-messenger RNA splicing. Annu Rev Biochem. 2003;72:291-336.

44. Timchenko NA, Cai ZJ, Welm AL, Reddy S, Ashizawa T, Timchenko LT. RNA CUG repeats sequester CUGBP1 and alter protein levels and activity of CUGBP1. J Biol Chem. 2001;276:7820-6.

45. Philips AV, Timchenko LT, Cooper TA. Disruption of splicing regulated by a CUG-binding protein in myotonic dystrophy. Science. 1998;280:737-41.

46. Savkur RS, Philips AV, Cooper TA. Aberrant regulation of insulin receptor alternative splicing is associated with insulin resistance in myotonic dystrophy. Nat Genet. 2001;29:40-7.

47. Dansithong W, Paul S, Comai L, Reddy S. MBNL1 is the primary determinant of focus formation and aberrant insulin receptor splicing in DM1. J Biol Chem. 2005;280:5773-80.

48. Ho TH, Bundman D, Armstrong DL, Cooper TA. Transgenic mice expressing CUG-BP1 reproduce splicing mis-regulation observed in myotonic dystrophy. Hum Mol Genet. 2005;14:1539-47.

49. de Haro M, Al-Ramahi I, De Gouyon B, Ukani L, Rosa A, Faustino NA, et al. MBNL1 and CUG-BP1 modify expanded CUG-induced toxicity in a Drosophila model of myotonic dystrophy type 1. Hum Mol Genet. 2006;15:2138-45.

50. Mankodi A, Teng-Umnuay P, Krym M, Henderson D, Swanson M, Thornton CA. Ribonuclear inclusions in skeletal muscle in myotonic dystrophy types 1 and 2. Ann Neurol. 2003;54:760-8.

51. Kanadia RN, Johnstone KA, Mankodi A, Lungu C, Thornton CA, Esson D, et al. A muscleblind knockout model for myotonic dystrophy. Science. 2003;302:1978-80.

52. Lin X, Miller JW, Mankodi A, Kanadia RN, Yuan Y, Moxley RT, et al. Failure of MBNL1-dependent post-natal splicing transitions in myotonic dystrophy. Hum Mol Genet. 2006;15:2087-97.

53. Kanadia RN, Shin J, Yuan Y, Beattie SG, Wheeler TM, Thornton CA, Swanson MS. Reversal of RNA missplicing and myotonia after muscleblind overexpression in a mouse poly(CUG) model for myotonic dystrophy. Proc Natl Acad Sci U S A. 2006;103:11748-53.

54. Charlet-B N, Savkur RS, Singh G, Philips AV, Grice EA, Cooper TA. Loss of the muscle-specific chloride channel in type 1 myotonic dystrophy due to misregulated alternative splicing. Mol Cell. 2002;10:45-53.

55. Berg J, Jiang H, Thornton CA, Cannon SC. Truncated ClC-1 mRNA in myotonic dystrophy exerts a dominant-negative effect on the Cl current. Neurology. 2004;63:2371-5.

56. Buj-Bello A, Furling D, Tronchère H, Laporte J, Lerouge T, Butler-Browne GS, Mandel JL. Muscle-specific alternative splicing of myotubularin-related 1 gene is impaired in DM1 muscle cells. Hum Mol Genet. 2002;11:2297-307.

57. Kimura T, Takahashi MP, Okuda Y, Kaido M, Fujimura H, Yanagihara T, Sakoda S. The expression of ion channel mRNAs in skeletal muscles from patients with myotonic muscular dystrophy. Neurosci Lett. 2000;295:93-6.

58. Kimura T, Nakamori M, Lueck JD, Pouliquin P, Aoike F, Fujimura H, et al. Altered mRNA splicing of the skeletal muscle ryanodine receptor and sarcoplasmic/endoplasmic reticulum Ca2+-ATPase in myotonic dystrophy type 1. Hum Mol Genet. 2005;14:2189-200.

59. Wansink DG, Wieringa B. Transgenic mouse models for myotonic dystrophy type 1 (DM1). Cytogenet Genome Res. 2003;100:230-42.

60. Jansen G, Groenen PJ, Bächner D, Jap PH, Coerwinkel M, Oerlemans F, et al. Abnormal myotonic dystrophy protein kinase levels produce only mild myopathy in mice. Nat Genet. 1996;13:316-24.

61. Reddy S, Smith DB, Rich MM, Leferovich JM, Reilly P, Davis BM, et al. Mice lacking the myotonic dystrophy protein kinase develop a late onset progressive myopathy. Nat Genet. 1996;13:325-35.

62. Klesert TR, Cho DH, Clark JI, Maylie J, Adelman J, Snider L, et al. Mice deficient in Six5 develop cataracts: implications for myotonic dystrophy. Nat Genet. 2000;25:105-9.

63. Sarkar PS, Appukuttan B, Han J, Ito Y, Ai C, Tsai W, et al. Heterozygous loss of Six5 in mice is sufficient to cause ocular cataracts. Nat Genet. 2000;25:110-4.

64. Fortune MT, Vassilopoulos C, Coolbaugh MI, Siciliano MJ, Monckton DG. Dramatic, expansion-biased, age-dependent, tissue-specific somatic mosaicism in a transgenic mouse model of triplet repeat instability. Hum Mol Genet. 2000;9:439-45.

65. Gourdon G, Radvanyi F, Lia AS, Duros C, Blanche M, Abitbol M, et al. Moderate intergenerational and somatic instability of a 55-CTG repeat in transgenic mice. Nat Genet. 1997;15:190-2.

66. Seznec H, Lia-Baldini AS, Duros C, Fouquet C, Lacroix C, Hofmann-Radvanyi H, et al. Transgenic mice carrying large human genomic sequences with expanded CTG repeat mimic closely the DM CTG repeat intergenerational and somatic instability. Hum Mol Genet. 2000;9:1185-94.

67. Mankodi A, Logigian E, Callahan L, McClain C, White R, Henderson D, et al. Myotonic dystrophy in transgenic mice expressing an expanded CUG repeat. Science. 2000;289:1769-73.

68. van den Broek WJ, Nelen MR, Wansink DG, Coerwinkel MM, te Riele H, Groenen PJ, Wieringa B. Somatic expansion behaviour of the (CTG)n repeat in myotonic dystrophy knock-in mice is differentially affected by Msh3 and Msh6 mismatch-repair proteins. Hum Mol Genet. 2002;11:191-8.

69. Wang GS, Kearney DL, De Biasi M, Taffet G, Cooper TA. Elevation of RNA-binding protein CUGBP1 is an early event in an inducible heart-specific mouse model of myotonic dystrophy. J Clin Invest. 2007;117:2802-11.

70. Orengo JP, Chambon P, Metzger D, Mosier DR, Snipes GJ, Cooper TA. Expanded CTG repeats within the DMPK 3' UTR causes severe skeletal muscle wasting in an inducible mouse model for myotonic dystrophy. Proc Natl Acad Sci U S A. 2008;105:2646-51.

71. Usuki F, Ishiura S, Saitoh N, Sasagawa N, Sorimachi H, Kuzume H, et al. Expanded CTG repeats in myotonin protein kinase suppresses myogenic differentiation. Neuroreport. 1997;8:3749-53.

72. Usuki F, Ishiura S. Expanded CTG repeats in myotonin protein kinase increase susceptibility to oxidative stress. Neuroreport. 1998;9:2291-6.

73. Amack JD, Mahadevan MS. Myogenic defects in myotonic dystrophy. Dev Biol. 2004;265:294-301.

74. Oude Ophuis RJ, Wijers M, Bennink MB, van de Loo FA, Fransen JA, Wieringa B, Wansink DG. A tail-anchored myotonic dystrophy protein kinase isoform induces perinuclear clustering of mitochondria, autophagy, and apoptosis. PLoS One. 2009;4:e8024.

75. Kuyumcu-Martinez NM, Wang GS, Cooper TA. Increased steady-state levels of CUGBP1 in myotonic dystrophy 1 are due to PKC-mediated hyperphosphorylation. Mol Cell. 2007;28:68-78.

76. Jacobs AE, Benders AA, Oosterhof A, Veerkamp JH, van Mier P, Wevers RA, Joosten EM. The calcium homeostasis and the membrane potential of cultured muscle cells from patients with myotonic dystrophy. Biochim Biophys Acta. 1990;1096:14-9.

77. Benders AA, Timmermans JA, Oosterhof A, Ter Laak HJ, van Kuppevelt TH, Wevers RA, Veerkamp JH. Deficiency of Na+/K(+)-ATPase and sarcoplasmic reticulum Ca(2+)-ATPase in skeletal muscle and cultured muscle cells of myotonic dystrophy patients. Biochem J. 1993;293 (Pt 1):269-74.

78. Benders AA, Wevers RA, Veerkamp JH. Ion transport in human skeletal muscle cells: disturbances in myotonic dystrophy and Brody's disease. Acta Physiol Scand. 1996;156:355-67.

79. Cardani R, Baldassa S, Botta A, Rinaldi F, Novelli G, Mancinelli E, Meola G. Ribonuclear inclusions and MBNL1 nuclear sequestration do not affect myoblast differentiation but alter gene splicing in myotonic dystrophy type 2. Neuromuscul Disord. 2009;19:335-43.

80. Furling D, Coiffier L, Mouly V, Barbet JP, St Guily JL, Taneja K, et al. Defective satellite cells in congenital myotonic dystrophy. Hum Mol Genet. 2001;10:2079-87.

81. Furling D, Lemieux D, Taneja K, Puymirat J. Decreased levels of myotonic dystrophy protein kinase (DMPK) and delayed differentiation in human myotonic dystrophy myoblasts. Neuromuscul Disord. 2001;11:728-35.

82. Timchenko NA, Iakova P, Cai ZJ, Smith JR, Timchenko LT. Molecular basis for impaired muscle differentiation in myotonic dystrophy. Mol Cell Biol. 2001;21:6927-38.

83. Kobayashi T, Askanas V, Saito K, Engel WK, Ishikawa K. Abnormalities of aneural and innervated cultured muscle fibers from patients with myotonic atrophy (dystrophy). Arch Neurol. 1990;47:893-6.

84. Shimokawa M, Ishiura S, Kameda N, Yamamoto M, Sasagawa N, Saitoh N, et al. Novel isoform of myotonin protein kinase: gene product of myotonic dystrophy is localized in the sarcoplasmic reticulum of skeletal muscle. Am J Pathol. 1997;150:1285.

85. Kameda N, Ueda H, Ohno S, Shimokawa M, Usuki F, Ishiura S, Kobayashi T. Developmental regulation of myotonic dystrophy protein kinase in human muscle cells in vitro. Neuroscience. 1998;85:311-22.

86. Thornell LE, Lindstöm M, Renault V, Klein A, Mouly V, Ansved T, et al. Satellite cell dysfunction contributes to the progressive muscle atrophy in myotonic dystrophy type 1. Neuropathol Appl Neurobiol. 2009;35:603-13.

87. Amack JD, Paguio AP, Mahadevan MS. Cis and trans effects of the myotonic dystrophy (DM) mutation in a cell culture model. Hum Mol Genet. 1999;8:1975-84.

88. Sabourin LA, Tamai K, Narang MA, Korneluk RG. Overexpression of 3'-untranslated region of the myotonic dystrophy kinase cDNA inhibits myoblast differentiation in vitro. J Biol Chem. 1997;272:29626-35.

89. Amack JD, Mahadevan MS. The myotonic dystrophy expanded CUG repeat tract is necessary but not sufficient to disrupt C2C12 myoblast differentiation. Hum Mol Genet. 2001;10:1879-87.

90. Eberli D, Soker S, Atala A, Yoo JJ. Optimization of human skeletal muscle precursor cell culture and myofiber formation in vitro. Methods. 2009;47:98-103.

91. Amack JD, Reagan SR, Mahadevan MS. Mutant DMPK 3'-UTR transcripts disrupt C2C12 myogenic differentiation by compromising MyoD. J Cell Biol. 2002;159:419-29.

92. Bigot A, Klein AF, Gasnier E, Jacquemin V, Ravassard P, Butler-Browne G, et al. Large CTG repeats trigger p16-dependent premature senescence in myotonic dystrophy type 1 muscle precursor cells. Am J Pathol. 2009;174:1435-42.

93. Borg J, Edström L, Butler-Browne GS, Thornell LE. Muscle fibre type composition, motoneuron firing properties, axonal conduction velocity and refractory period for foot extensor motor units in dystrophia myotonica. J Neurol Neurosurg Psychiatry. 1987;50:1036-44.

94. Wheeler TM. Myotonic dystrophy: therapeutic strategies for the future. Neurotherapeutics. 2008;5:592-600.

95. Warf MB, Nakamori M, Matthys CM, Thornton CA, Berglund JA. Pentamidine reverses the splicing defects associated with myotonic dystrophy. Proc Natl Acad Sci U S A. 2009;106:18551-6.

96. Trip J, Drost G, van Engelen BG, Faber CG. Drug treatment for myotonia. Cochrane Database Syst Rev. 2006:CD004762.

97. Sugino M, Ohsawa N, Ito T, Ishida S, Yamasaki H, Kimura F, Shinoda K. A pilot study of dehydroepiandrosterone sulfate in myotonic dystrophy. Neurology. 1998;51:586-9.

98. Vlachopapadopoulou E, Zachwieja JJ, Gertner JM, Manzione D, Bier DM, Matthews DE, Slonim AE. Metabolic and clinical response to recombinant human insulin-like growth factor I in myotonic dystrophy--a clinical research center study. J Clin Endocrinol Metab. 1995;80:3715-23.

99. Bogdanovich S, Krag TO, Barton ER, Morris LD, Whittemore LA, Ahima RS, Khurana TS. Functional improvement of dystrophic muscle by myostatin blockade. Nature. 2002;420:418-21.

100. Haidet AM, Rizo L, Handy C, Umapathi P, Eagle A, Shilling C, et al. Long-term enhancement of skeletal muscle mass and strength by single gene administration of myostatin inhibitors. Proc Natl Acad Sci U S A. 2008;105:4318-22.

101. Hotchkiss RS, Strasser A, McDunn JE, Swanson PE. Cell death. N Engl J Med. 2009;361:1570-83.

102. Melino G. The Sirens' song. Nature. 2001;412:23.

103. Sheikh MS, Huang Y. Death receptor activation complexes: it takes two to activate TNF receptor 1. Cell Cycle. 2003;2:550-2.

104. Wajant H. The Fas signaling pathway: more than a paradigm. Science. 2002;296:1635-6.

105. Chen G, Goeddel DV. TNF-R1 signaling: a beautiful pathway. Science. 2002;296:1634-5.

106. Susin SA, Lorenzo HK, Zamzami N, Marzo I, Snow BE, Brothers GM, et al. Molecular characterization of mitochondrial apoptosis-inducing factor. Nature. 1999;397:441-6.

107. Brüne B. Nitric oxide: NO apoptosis or turning it ON? Cell Death Differ. 2003;10:864-9.

108. Fesik SW, Shi Y. Structural biology. Controlling the caspases. Science. 2001;294:1477-8.

109. Dejean LM, Martinez-Caballero S, Kinnally KW. Is MAC the knife that cuts cytochrome c from mitochondria during apoptosis? Cell Death Differ. 2006;13:1387-95.

110. Hengartner MO. The biochemistry of apoptosis. Nature. 2000;407:770-6.

111. Li MO, Sarkisian MR, Mehal WZ, Rakic P, Flavell RA. Phosphatidylserine receptor is required for clearance of apoptotic cells. Science. 2003;302:1560-3.

112. Savill J, Gregory C, Haslett C. Cell biology. Eat me or die. Science. 2003;302:1516-7.

113. Scarlatti F, Granata R, Meijer AJ, Codogno P. Does autophagy have a license to kill mammalian cells? Cell Death Differ. 2009;16:12-20.

114. Mizushima N, Levine B, Cuervo AM, Klionsky DJ. Autophagy fights disease through cellular self-digestion. Nature. 2008;451:1069-75.

115. Klionsky DJ. Autophagy: from phenomenology to molecular understanding in less than a decade. Nat Rev Mol Cell Biol. 2007;8:931-7.

116. Schmid D, Münz C. Innate and adaptive immunity through autophagy. Immunity. 2007;27:11-21.

117. Bjørkøy G, Lamark T, Brech A, Outzen H, Perander M, Overvatn A, et al. p62/SQSTM1 forms protein aggregates degraded by autophagy and has a protective effect on huntingtin-induced cell death. J Cell Biol. 2005;171:603-14.

118. Simonsen A, Birkeland HC, Gillooly DJ, Mizushima N, Kuma A, Yoshimori T, et al. Alfy, a novel FYVE-domain-containing protein associated with protein granules and autophagic membranes. J Cell Sci. 2004;117:4239-51.

119. Mizushima N, Klionsky DJ. Protein turnover via autophagy: implications for metabolism. Annu Rev Nutr. 2007;27:19-40.

120. Majeski AE, Dice JF. Mechanisms of chaperone-mediated autophagy. Int J Biochem Cell Biol. 2004;36:2435-44.

121. Arndt V, Dick N, Tawo R, Dreiseidler M, Wenzel D, Hesse M, et al. Chaperone-Assisted Selective Autophagy Is Essential for Muscle Maintenance. Curr Biol. 2010.

122. Jung CH, Ro SH, Cao J, Otto NM, Kim DH. mTOR regulation of autophagy. FEBS Lett. 2010.

123. Chang YY, Juhász G, Goraksha-Hicks P, Arsham AM, Mallin DR, Muller LK, Neufeld TP. Nutrient-dependent regulation of autophagy through the target of rapamycin pathway. Biochem Soc Trans. 2009;37:232-6.

124. Komatsu M, Waguri S, Ueno T, Iwata J, Murata S, Tanida I, et al. Impairment of starvation-induced and constitutive autophagy in Atg7-deficient mice. J Cell Biol. 2005;169:425-34.

125. Masiero E, Agatea L, Mammucari C, Blaauw B, Loro E, Komatsu M, et al. Autophagy is required to maintain muscle mass. Cell Metab. 2009;10:507-15.

126. Huang J, Klionsky DJ. Autophagy and human disease. Cell Cycle. 2007;6:1837-49.

127. Salminen A, Kaarniranta K. Regulation of the aging process by autophagy. Trends Mol Med. 2009;15:217-24.

128. Levine B, Yuan J. Autophagy in cell death: an innocent convict? J Clin Invest. 2005;115:2679-88.

129. Golstein P, Kroemer G. Cell death by necrosis: towards a molecular definition. Trends Biochem Sci. 2007;32:37-43.

130. Zong WX, Thompson CB. Necrotic death as a cell fate. Genes Dev. 2006;20:1-15.

131. Lotze MT, Tracey KJ. High-mobility group box 1 protein (HMGB1): nuclear weapon in the immune arsenal. Nat Rev Immunol. 2005;5:331-42.

132. Maiuri MC, Zalckvar E, Kimchi A, Kroemer G. Self-eating and self-killing: crosstalk between autophagy and apoptosis. Nat Rev Mol Cell Biol. 2007;8:741-52.

133. Galluzzi L, Maiuri MC, Vitale I, Zischka H, Castedo M, Zitvogel L, Kroemer G. Cell death modalities: classification and pathophysiological implications. Cell Death Differ. 2007;14:1237-43.

134. Levine B, Abrams J. p53: The Janus of autophagy? Nat Cell Biol. 2008;10:637-9.

135. Galluzzi L, Aaronson SA, Abrams J, Alnemri ES, Andrews DW, Baehrecke EH, et al. Guidelines for the use and interpretation of assays for monitoring cell death in higher eukaryotes. Cell Death Differ. 2009;16:1093-107.

136. Klionsky DJ, Abeliovich H, Agostinis P, Agrawal DK, Aliev G, Askew DS, et al. Guidelines for the use and interpretation of assays for monitoring autophagy in higher eukaryotes. Autophagy. 2008;4:151-75.

137. Mizushima N, Yoshimori T, Levine B. Methods in Mammalian Autophagy Research. Cell. 2010;140:313-26.

138. Mathieu J, De Braekeleer M, Prévost C, Boily C. Myotonic dystrophy: clinical assessment of muscular disability in an isolated population with presumed homogeneous mutation. Neurology. 1992;42:203-8.

139. Miller SA, Dykes DD, Polesky HF. A simple salting out procedure for extracting DNA from human nucleated cells. Nucleic Acids Res. 1988;16:1215.

140. Bonifazi E, Vallo L, Giardina E, Botta A, Novelli G. A long PCR-based molecular protocol for detecting normal and expanded ZNF9 alleles in myotonic dystrophy type 2. Diagn Mol Pathol. 2004;13:164-6.

141. Sandri M, Sandri C, Gilbert A, Skurk C, Calabria E, Picard A, et al. Foxo transcription factors induce the atrophy-related ubiquitin ligase atrogin-1 and cause skeletal muscle atrophy. Cell. 2004;117:399-412.

142. Adams V, Gielen S, Hambrecht R, Schuler G. Apoptosis in skeletal muscle. Front Biosci. 2001;6:D1-D11.

143. Sarbassov DD, Ali SM, Sabatini DM. Growing roles for the mTOR pathway. Curr Opin Cell Biol. 2005;17:596-603.

144. Cryns V, Yuan J. Proteases to die for. Genes Dev. 1998;12:1551-70.

145. Mammucari C, Milan G, Romanello V, Masiero E, Rudolf R, Del Piccolo P, et al. FoxO3 controls autophagy in skeletal muscle in vivo. Cell Metab. 2007;6:458-71.

146. Zhao J, Brault JJ, Schild A, Cao P, Sandri M, Schiaffino S, et al. FoxO3 coordinately activates protein degradation by the autophagic/lysosomal and proteasomal pathways in atrophying muscle cells. Cell Metab. 2007;6:472-83.

147. Salisbury E, Sakai K, Schoser B, Huichalaf C, Schneider-Gold C, Nguyen H, et al. Ectopic expression of cyclin D3 corrects differentiation of DM1 myoblasts through activation of RNA CUG-binding protein, CUGBP1. Exp Cell Res. 2008;314:2266-78.

148. Cornelison DD. Context matters: in vivo and in vitro influences on muscle satellite cell activity. J Cell Biochem. 2008;105:663-9.

149. Sandri M, Carraro U. Apoptosis of skeletal muscles during development and disease. Int J Biochem Cell Biol. 1999;31:1373-90.

150. Biral D, Jakubiec-Puka A, Ciechomska I, Sandri M, Rossini K, Carraro U, Betto R. Loss of dystrophin and some dystrophin-associated proteins with concomitant signs of apoptosis in rat leg muscle overworked in extension. Acta Neuropathol. 2000;100:618-26.

151. Sandri M, El Meslemani AH, Sandri C, Schjerling P, Vissing K, Andersen JL, et al. Caspase 3 expression correlates with skeletal muscle apoptosis in Duchenne and facioscapulo human muscular

dystrophy. A potential target for pharmacological treatment? J Neuropathol Exp Neurol. 2001;60:302-12.

152. Angelin A, Tiepolo T, Sabatelli P, Grumati P, Bergamin N, Golfieri C, et al. Mitochondrial dysfunction in the pathogenesis of Ullrich congenital muscular dystrophy and prospective therapy with cyclosporins. Proc Natl Acad Sci U S A. 2007;104:991-6.

153. Fanchaouy M, Polakova E, Jung C, Ogrodnik J, Shirokova N, Niggli E. Pathways of abnormal stress-induced Ca2+ influx into dystrophic mdx cardiomyocytes. Cell Calcium. 2009;46:114-21.

154. Berridge MJ, Bootman MD, Roderick HL. Calcium signalling: dynamics, homeostasis and remodelling. Nat Rev Mol Cell Biol. 2003;4:517-29.

155. Cherednichenko G, Hurne AM, Fessenden JD, Lee EH, Allen PD, Beam KG, Pessah IN. Conformational activation of Ca2+ entry by depolarization of skeletal myotubes. Proc Natl Acad Sci U S A. 2004;101:15793-8.

156. MacLennan DH, Rice WJ, Green NM. The mechanism of Ca2+ transport by sarco(endo)plasmic reticulum Ca2+-ATPases. J Biol Chem. 1997;272:28815-8.

157. Futatsugi A, Kuwajima G, Mikoshiba K. Tissue-specific and developmentally regulated alternative splicing in mouse skeletal muscle ryanodine receptor mRNA. Biochem J. 1995;305 (Pt 2):373-8.

158. Kimura T, Lueck JD, Harvey PJ, Pace SM, Ikemoto N, Casarotto MG, et al. Alternative splicing of RyR1 alters the efficacy of skeletal EC coupling. Cell Calcium. 2009;45:264-74.

159. Barreto-Chang OL, Dolmetsch RE. Calcium imaging of cortical neurons using Fura-2 AM. J Vis Exp. 2009.

160. Szappanos H, Cseri J, Deli T, Kovács L, Csernoch L. Determination of depolarisation- and agonist-evoked calcium fluxes on skeletal muscle cells in primary culture. J Biochem Biophys Methods. 2004;59:89-101.

161. Basset O, Boittin FX, Cognard C, Constantin B, Ruegg UT. Bcl-2 overexpression prevents calcium overload and subsequent apoptosis in dystrophic myotubes. Biochem J. 2006;395:267-76.

162. Irwin WA, Bergamin N, Sabatelli P, Reggiani C, Megighian A, Merlini L, et al. Mitochondrial dysfunction and apoptosis in myopathic mice with collagen VI deficiency. Nat Genet. 2003;35:367-71.

163. Aartsma-Rus A, van Ommen GJ. Antisense-mediated exon skipping: a versatile tool with therapeutic and research applications. RNA. 2007;13:1609-24.